PHENOMENOLOGY OF STABILIZING MODULI IN A FRAMEWORK OF G_2 COMPACTIFICATION OF M-THEORY

by

Jing Shao

A dissertation submitted in partial fulfillment
of the requirements for the degree of
Doctor of Philosophy
(Physics)
in The University of Michigan
2009

Doctoral Committee:

Professor Gordon L. Kane, Chair
Professor Daniel M. Burns Jr.
Professor Jianming Qian
Professor James Daniel Wells
Associate Professor James T. Liu

© Jing Shao 2009
All Rights Reserved

TO MY PARENTS AND MY WIFE

ACKNOWLEDGEMENTS

Upon completing this thesis, I would like to express my deepest gratitude to my advisor Professor Gordon Kane for guiding me into the area of string phenomenology and for providing me an enormous range of opportunities for research and collaboration. Without him this thesis would not have been possible. More importantly, his unique flavor and perspective in physics will be invaluable for my future career.

I would also like to thank many other professors – most notably Bobby Acharya, Alexey Petrov, Aaron Pierce, Liantao Wang, James Wells and Cumrun Vafa, for various illuminating discussions and collaborations. I have also learned a lot from many other graduate students and postdocs in the physics department, particularly Konstantin Bobkov, Phill Grajek, Eric Kuflik, Piyush Kumar, Arjun Menon, David Morrissey and Scott Watson. I would like to thank them all.

Finally, and most importantly, I wish to thank my parents and my wife Guodan, for their persistent support and love.

TABLE OF CONTENTS

LIST OF FIGURES

Figure

LIST OF TABLES

Table

LIST OF APPENDICES

Appendix

CHAPTER I

Introduction

The past thirty years have seen the tremendous success of the Standard Model (SM) of particle physics, with predictions being repeatedly tested and confirmed through a variety of experiments. Nevertheless, this paradigm is expected to end with the running of the Large Hadron Collider (LHC) at Geneva, which will open a window into the phenomena at a new energy frontier – TeV scale. There are plenty of reasons both theoretically and experimentally to expect new physics beyond the SM. First of all, the form of the electro-weak symmetry breaking (EWSB) in the SM has not yet been determined by the experiments. Even if the mechanism of the EWSB is correct, the SM cannot explain it. In addition, the SM higgs suffers from large quadratically divergent quantum corrections, which is known as the Hierarchy problem. There are many other issues which in principle cannot be addressed in the SM, for example, the quark mass hierarchy, the CKM matrix, and the strong CP problem. All of these unsatisfactory features strongly suggest modifications of the SM at the TeV scale or some higher scale.

On the cosmological scale, there are also big mysteries awaiting for explanation.

The most notable ones are, for example, "what is the dark matter and dark energy?", "how to explain the inflation and the structure formation?" and "where does the baryon asymmetry in the universe come from?". To address all these questions requires physics at a scale above the electroweak scale or even up to the Planck scale, and need a theory including both the particle physics and gravity.

Given the reasons we have listed so far, we believe that the ongoing experiments shall provide strong evidence for new physics. Among all the possible theories, the low energy supersymmetry (SUSY) is by far the most well motivated one. It does not only stabilize the electroweak scale but also provide a natural candidate for dark matter. If SUSY is discovered in the LHC, confirming it and determining the parameters in the effective lagrangian will be the main subject in the following many years. However, this is not our ultimate goal, since we need a complete theory eventually to explain all the unanswered questions in both particle and cosmological areas. Having a complete theory from the beginning may provide a simple way to organize and address all the present puzzles. So far, such a complete theory could only possibly originate from string theory, which is a consistent quantum theory for both particle and gravity. Working on developing such a complete theory from string theory and study its phenomenology is the main goal of this thesis.

To connect string theory to the real world, one has to first compactify the extra dimensions to a small size, and derive the effective 4D field theory at a high energy scale. Then the effective theory can be evolved down to a low energy scale, where one can compute the relevant physical observables using quantum field theory. A

feature of string compactifications is that there exist many scalar fields, whose vacuum expectation values set the couplings in the 4D effective theory. However, at the perturbative level, there is no superpotential being generated, and these scalar fields can take any possible values, which therefore is a major obstacle for making connections to the observations. In addition, the presence of massless scalar fields is also in consistent with the observations. This is the so called moduli stabilization problem, which must be solved in any realistic string construction. It should be emphasized that people recently realized that the string theory solutions are not likely to be unique, and even after the moduli are stabilized, there could exist an extremely large number of discrete vacua [2–4]. This raises the question whether string theory is predictive at all. Here we take an optimistic point of view, i.e., the fact that there exist a landscape of vacua provides us an opportunity to search for the right vacuum in which we are living, with the help of the experimental observables [5, 6].

Another issue almost of the same importance is how to obtain supersymmetry breaking with TeV scale superpartners. Though there are many possible ways to achieve this, the most natural one in the case of moduli stabilization is through the strong gauge dynamics which breaks the supersymmetry dynamically. In this approach both moduli stabilization and supersymmetry breaking issues can be dealt with simultaneously, and the hierarchy problem can potentially be addressed.

Substantial progress has been made in the past few years towards addressing the dynamical issues of moduli stabilization, supersymmetry breaking and explaining the Hierarchy, within various corners of the entire M-theory moduli space in a reliable

manner [7–10]. The most well-known examples are the KKLT [7] and the Large-Volume [8] type vacua found in the flux compactification [11, 12] of type IIB string theory. The phenomenological consequences of these vacua have been studied in great detail in the literature [13–27].

In this thesis, we focus on a new framework arising from another weakly coupled limit: the eleven dimensional supergravity limit of M-theory. The moduli stabilization issue in such a framework was first discussed in [28] and then investigated in greater detail in [29]. It was shown there that with reasonable assumptions about microscopic structure of the underlying construction, $\mathcal{N}$=1 fluxless compactifications of M-theory on G_2 manifolds can generate the hierarchy between the electroweak and Planck scales and stabilize all the moduli in a de Sitter vacuum. This framework provides a starting point to study the phenomenological consequences if an MSSM sector is assumed to exist. This leads to the interesting phenomenological model – G_2-MSSM. In this thesis, I give a detailed study of the phenomenology of this model, which is mainly based on the two publications [30, 31] and some unpublished results [32]. It should be emphasized that although these papers are written with collaborators, I have made major contributions to all of them and have performed all the essential calculations.

The thesis is organized as follows. In chapter II, after a brief review of some necessary background on string compactification and low energy effective theory, as well as the main results of moduli stabilization in the framework of fluxless G_2 compactification of M-theory [29], the phenomenological model, G_2-MSSM, is motivated and

introduced [30]. In chapter III, we discuss the calculation of the soft terms, renormalization group running, low energy superpartner spectrum and electroweak symmetry breaking (EWSB) [30]. In Chapter IV, we discuss the prospects of G_2-MSSM at the LHC, CP violation and the implications for electric dipole moments [32]. In Chapter V, we discuss the non-thermal production of the dark matter and the cosmological moduli/gravitino problem [31].

CHAPTER II

Theoretical Framework of G_2-MSSM

In order to make our discussion of G_2 phenomenology self-contained, it is helpful to review the essential results for the fluxless M-Theory de Sitter vacua described in [28, 29] and explain our conventions and notation. Compactifications of M-Theory on singular G_2 manifolds are interesting in the sense that they give rise to $\mathcal{N} = 1$ supersymmetry in four dimensions with non-Abelian gauge groups and chiral fermions. The non-Abelian gauge fields are localized along three-dimensional submanifolds of the seven extra dimensions whereas chiral fermions are supported at points at which there is a conical singularity [33–36]. As explained in the introduction, in order to look at phenomenological consequences of these compactifications in a reliable manner, one has to address the dynamical issues of moduli stabilization, supersymmetry breaking and generation of the Hierarchy.

2.1 Compactification, Low Energy Effective Action and Soft Terms

In this section, we provide some basic results of the $\mathcal{N}=1$ 4D supergravity, which typically arises from string/M theory compactifications. For more details, we refer to the textbooks [37, 38] and recent reviews [39, 40]. We also briefly review the soft supersymmetry breaking terms arising from the gravity mediation [41–44].

In the compactifications of string/M theory, we first take the low energy limit of 10D string theory(or 11d M-Theory), which is described by 10D supergravity theory (need to include the effective brane action in cases that they are present), and then perform a Kaluza-Klein dimensional reduce to obtain a 4D effective theory for the massless states. In order for the effective theory to have $\mathcal{N}=1$ supersymmetry, some special geometry for the compact extra dimensions is required, i.e., Calabi-Yau manifold for 10D string theory case and G_2 manifold for M-Theory case.

The $\mathcal{N}=1$ 4D supergravity (up to two derivatives) is specified by two functions which depend on the chiral superfields ϕ^α: the holomorphic gauge kinetic function $f_a(\phi)$ and the real gauge invariant Kähler function $G(\phi,\bar{\phi})$

$$G(\phi,\bar{\phi}) = K(\phi,\bar{\phi}) + \log|W(\phi)|^2. \tag{2.1}$$

Here, $K(\phi,\bar{\phi})$ is the Kähler potential and $W(\phi)$ is the complete holomorphic superpotential. The general Lagrangian can then be written as

$$\begin{aligned}\mathcal{L} &= \frac{1}{2\kappa_4^2}R - K_{\alpha\bar{\beta}}(\phi,\bar{\phi})D_\mu\phi^\alpha D^\mu\phi^{\bar{\beta}} - V(\phi,\bar{\phi}) \\ &\quad -\frac{1}{8}\mathrm{Re}f_{ab}(\phi)F^a_{\mu\nu}F^{b\mu\nu} - \frac{1}{8}\mathrm{Im}f_{ab}(\phi)\epsilon^{\mu\nu\rho\sigma}F^a_{\mu\nu}F^b_{\rho\sigma} + \cdots\end{aligned} \tag{2.2}$$

where $\kappa_4 = \sqrt{8\pi G_N}$ is the 4D gravitional coupling, which can also be expressed in terms of the reduced Planck scale $\kappa_4 = M_P^{-1}$. $F^a_{\mu\nu}$ is the field strength of the gauge fields. The Kähler metric $K_{\alpha\bar{\beta}}$ is given by

$$K_{\alpha\bar{\beta}} = \frac{\partial^2 K(\phi, \bar{\phi})}{\partial\phi^\alpha \partial\phi^{\bar{\beta}}} \tag{2.3}$$

The general form of the scalar potential contains two contributions from F-terms and D-terms,

$$V(\phi, \bar{\phi}) = e^{K/M_P^2}\left(K^{\alpha\bar{\beta}} D_\alpha W D_{\bar{\beta}}\overline{W} - \frac{3}{M_P^2}|W|^2\right) + \frac{1}{2}\left(\mathrm{Re}(f)^{-1}\right)_{ab} D^a D^b \tag{2.4}$$

where M_P is the reduced Planck constant $M_P = M_{\mathrm{Planck}}/\sqrt{8\pi}$. The first term is the F-term scalar potential and the second term is the D-term potential. Here

$$D_\alpha W = \partial_\alpha W + \frac{1}{M_P^2} K_\alpha W = F_\alpha, \tag{2.5}$$

where $K_\alpha \equiv \partial_\alpha K$. For later convenience, we also introduce F^α which is defined as

$$F^\alpha = K^{\alpha\bar{\beta}} D_{\bar{\beta}}\overline{W} \tag{2.6}$$

In the D-term potential, the auxiliary D-fields $D^a(\phi, \bar{\phi})$ satisfy the equation $\partial_\alpha D^\alpha = -iK_{\alpha\bar{\beta}} X^{\alpha\bar{\beta}}$ where $X^{\alpha\bar{\beta}}$ is the holomorphic Killing vectors.

The 4D theory arising from the compactification typically contain scalar fields which are related to the size and shape of the compact dimensions. It is useful to isolate these moduli fields ϕ_m and the matter fields C_α in the Kähler potential and superpotential

$$K \supset \hat{K}(\phi_m, \bar{\phi}_m) + \tilde{K}(\phi_m, \bar{\phi}_m) C^{\alpha\dagger} C^\beta + \frac{1}{2} Z_{\alpha\beta}(\phi_m, \bar{\phi}_m) C^\alpha C^\beta + h.c. \tag{2.7}$$

$$W \supset \hat{W}(\phi_m) + \frac{1}{2}\mu_{\alpha\beta}(\phi_m) C^\alpha C^\beta + \frac{1}{6} Y_{\alpha\beta\gamma}(\phi_m) C^\alpha C^\beta C^\gamma \tag{2.8}$$

It should be noted that the matter fields C^α here do not have the canonical kinetic terms and therefore need to be normalized properly before calculating the physical masses and couplings. From the above equations, one can also notice that the masses and couplings of matter fields are determined by the vacuum expectation values(VEVs) of the moduli.

Now let us discuss the validity of the effective theory. In order for 10D supergravity theory to be valid, the radius of the curvature of gravity background has to be much larger than the characteristic string length $\alpha'^{1/2}$. In the case of compactification, the curvature is related the size of the compact extra dimensions R_c. So the condition is basically

$$R_c > \alpha'^{1/2} \tag{2.9}$$

This implies the compactification scale m_c is much lower than the characteristic string scale $m_s \sim \alpha'^{-1/2}$. Finally, for for 4D theory to be valid, a cutoff should be imposed for the 4D effective supergravity action, i.e.

$$M^{4D}_{\text{cutoff}} \lesssim M_c = \frac{1}{R_c}. \tag{2.10}$$

Below the compactification scale, one can integrated out all the heavy KK states, and the effects can be incorporated into the effective 4D theory. Therefore, one can match the couplings in the effective 4D theory with the 10D theory at a scale $M_{\text{match}} \sim M_c$. Below that scale, all the couplings are then renormalized according to the low energy dynamics within the effective theory. It should be noted that there are uncertainties related to the ambiguity of the matching scale. However, since the

effects typically depend the scale logarithmically, they can be neglected in most of our analysis.

In the Wilsonian effective action, the general non-renormalization theorems apply to the superpotential and gauge kinematic function. It is saying that there are no perturbative quantum corrections to the superpotential at all, and no corrections to the gauge kinetic functions beyond one-loop. The Kähler potential can in principle have corrections at any loop order. Furthermore, all three quantities can have corrections from non-perturbative quantum effects such as instantons. In the type II string theory, there will be string quantum correction in terms of α' and string coupling g_s for the Kähler potential.

Now we are ready to discuss the supersymmetry breaking and soft terms from moduli mediation. As in the rigid supersymmetric theory, the conditions for unbroken supersymmetry are

$$F_\alpha = 0, \quad D^\alpha = 0 \tag{2.11}$$

In the framework of a compactification, one can nicely implement the idea of hidden sector supersymmetry breaking by considering a geometrically separated supersymmetry breaking sector in the extra dimensions. The supersymmetry breaking effects can be mediated through the moduli fields or high dimensional operators to the visible sector. Generally, in the 4D effective action from compacitification, the Kähler potential is parametrized by the moduli fields. Therefore, if the auxiliary components of moduli get VEVs, supersymmetry breaking can be mediated to the visible sector and gives rise to the soft supersymmetry breaking terms, This is the so called

moduli mediation, which is a special form of gravity mediation.

For phenomenological purposes, it is interesting to study the soft terms generated from the supersymmetry breaking in such a compactification framework. The full effective soft lagrangian is typically written as

$$\begin{aligned}\mathcal{L}_{soft} &= \frac{1}{2}(M_a\lambda\lambda + h.c.) - m'^2_{\bar{\alpha}\beta}C^{\bar{\alpha}\dagger}C^{\beta} \\ &\quad -\frac{1}{6}A'_{\alpha\beta\gamma}C^{\alpha}C^{\beta}C^{\gamma} + \frac{1}{2}B'_{\alpha\beta}C^{\alpha}C^{\beta} + h.c.\ . \end{aligned} \tag{2.12}$$

Here C^{α} are the scalar components of the corresponding matter chiral fields, for example, $C^{\alpha} = Q_L, u^c_L, d^c_L, L_L, e^c_L, H_1, H_2$ in the minimal supersymmetry standard Model (MSSM). In the above lagrangian, the soft masses $m'_{\bar{\alpha}\beta}$ and the soft couplings $A'_{\alpha\beta\gamma}$ and $B'_{\alpha\beta}$ are again the un-normalized ones, and must be normalized for physical matter fields.

Given the effective supergravity lagrangian, one can explicitly evaluate the soft terms by taking the scalar and auxiliary fields of moduli to their VEVs, and then decoupling the gravity by taking $M_P \to \infty$ while keeping the gravitino mass $m_{3/2}$ fixed. The soft gaugino masses, un-normalized soft scalar masses, trilinear parameters are given respectively by [44]

$$\begin{aligned} M_a &= \frac{1}{2}(\mathrm{Re}f_a)^{-1}e^{\hat{K}/2}F^m\partial_m f_a \\ m'^2_{\bar{\alpha}\beta} &= (m^2_{3/2} + V_0)\,\tilde{K}_{\bar{\alpha}\beta} - e^{\hat{K}}F^{\bar{m}}(\partial_{\bar{m}}\partial_n\,\tilde{K}_{\bar{\alpha}\beta} - \partial_{\bar{m}}\,\tilde{K}_{\bar{\alpha}\gamma}\,\tilde{K}^{\gamma\bar{\delta}}\partial_n\,\tilde{K}_{\bar{\delta}\beta})F^n \\ A'_{\alpha\beta\gamma} &= e^{\hat{K}}\,F^m\Big[\partial_m Y_{\alpha\beta\gamma} + \hat{K}_m Y_{\alpha\beta\gamma} \\ &\quad -\Big(\tilde{K}^{\delta\bar{\rho}}\,\partial_m\tilde{K}_{\bar{\rho}\alpha}\,Y_{\alpha\beta\gamma} + (\alpha\leftrightarrow\beta) + (\alpha\leftrightarrow\gamma)\Big)\Big] \end{aligned} \tag{2.13}$$

where $Y_{\alpha\beta\gamma}$ are the Yukawa couplings in the original superpotential.

There are also one-loop contributions to the soft terms, which arise from the anomalies of the super-Weyl-Kähler invariance and the sigma-model isometries. In particular, the anomaly mediated gaugino masses are given by [45]

$$M_a^{AMSB} = -\frac{g_a^2}{16\pi^2}\left(b_a\, e^{\hat{K}/2}\overline{W} - b'_a\, e^{\hat{K}/2}F^m\hat{K}_m + 2\sum_i C_a^i e^{\hat{K}/2}F^m\partial_m \ln \tilde{K}_i\right). \quad (2.14)$$

In this expression, $b_a \equiv -(3C_a - \sum_i C_a^i)$ and $b'_a \equiv -(C_a - \sum_i C_a^i)$, where C_a and C_a^i are the Dynkin index of the adjoint representation and of the matter fields respectively with i running over the number of chiral matter fields.

These soft terms should be calculated at the cutoff of the effective theory. Then they are evolved down the low energy scale where the relevant physical masses will be calculated. It should be noted that the evolution of the soft terms are equivalent to the evolution of the corresponding operators in the effective theory. In some case where the hidden sector is strongly coupled, the renormalization of the hidden sector fields should be included and will modify the standard RG running of soft terms. In the case where the supersymmetry is broken by moduli fields whose coupling is suppressed by M_P, the hidden sector effects can be neglected.

2.2 4D Effective Theory from G_2 Compactification of M-Theory

In this section, we briefly review the G_2 compactification in M-theory and the effective 4D theory. More details can be found in the review [36] and the references there. We know that the low energy effective theory of M-Theory is eleven-dimensional supergravity, with corrections in terms of 11D gravitational coupling κ_{11}.

To get $\mathcal{N}=1$ theory, one has to compactify the eleven-dimensional supergravity on a seven-dimensional manifold with G_2-holonomy, which is called G_2 manifold. Moreover, to obtain realistic matter and gauge fields from the compacitification, singular G_2 manifolds are required. The non-Abelian gauge fields are localized along three-dimensional submanifolds of the seven extra dimensions whereas chiral fermions are supported at points at which there is a conical singularity [33–36].

Consider a G_2 manifold X. The complexified moduli space $\mathcal{M}$ of X has $N = b^3(X)$ holomorphic coordinates z^i, defined by

$$z^i = s^i + it^i = \frac{1}{l_{11}^3}\int \varphi + iC, \tag{2.15}$$

where φ is the G_2-invariant 3-form on X and the 11D fundamental length scale l_{11} is given by $1/2k_{11}^2 = 2\pi/l_{11}^9$. The metric on $\mathcal{M}$ is Kähler , derived from the Kähler potential

$$K(z,\bar{z}) = -3\ln\left(4\pi^{1/3}V_X(s)\right) \tag{2.16}$$

where $V_X = \mathrm{Vol}(X)/l_{11}^7$ is a homogeneous function of the s^i of degree 7/3. This classical metric will have quantum corrections, but at large enough volumes such corrections can be argued to be small. For the effective 4D supergravity description to be valid, the size of the compact extra dimensions has to much larger than l_{11}

$$V_X^{1/7} l_{11} > l_{11} \Longrightarrow V_X > 1 \tag{2.17}$$

The most general homogeneous degree 7/3 function is of the form

$$V_X = \prod_{k=1}^{n} s_k^{a_k} f(s_i) \tag{2.18}$$

with a_k such that

$$\sum_{k=1}^{n} a_k = \frac{7}{3} \tag{2.19}$$

and $f(s_i)$ invariant under scaling. For simplicity, in the following analysis in this thesis, we suppose that we are in a region of moduli space where $f(s_i)$ is approximately constant. Then we can take

$$V_X = \prod_{k=1}^{n} s_k^{a_k} \tag{2.20}$$

A more general analysis done recently in [46] shows that the result of moduli stabilization is independent of the choice of $f(s_i)$.

Now let us turn to the gauge kinetic function in the effective 4D theory. The non-Abelian gauge theory arises from the codimension 4 singularity and therefore lives in a seven-dimensional space where three dimensions are wrapped on a three-cycle $\mathcal{Q}$ in the G_2 manifold. Start with the seven-dimensional action

$$S \sim \frac{1}{16\pi(4\pi)^{1/3}\kappa_{11}^{2/3}} \int d^7x\sqrt{g}\sum_a F^a_{\mu\nu}F^{\mu\nu a}. \tag{2.21}$$

After dimension reduction on the three-cycle $\mathcal{Q}$, one should get the standard 4D gauge kinetic term

$$S_{4D} \sim \frac{1}{4g_M^2} \int d^4x\sqrt{g}F^a_{\mu\nu}F^{\mu\nu a} \tag{2.22}$$

where g_M is the 4D gauge coupling. Therefore, the 4D gauge coupling is identified by

$$\begin{aligned} \alpha_M &= \frac{(4\pi)^{1/3}\kappa_{11}^{2/3}}{\mathrm{Vol}(\mathcal{Q})} \\ &= \frac{1}{V_{\mathcal{Q}}}, \end{aligned} \tag{2.23}$$

Here $V_{\mathcal{Q}} = \mathrm{Vol}(\mathcal{Q})/l_{11}^3$ is the (dimensionless) volume of the three-cycle $\mathcal{Q}$. Therefore, the complete gauge kinetic term can be written as

$$\frac{1}{16\pi}\int d^2\theta f_a(z_i)W^\alpha W_\alpha + h.c. \tag{2.24}$$

where $f(z_i)$ is the gauge kinetic function with $\mathrm{Re}f_a(z_i) = 4\pi/g_a^2$. Since the volume of the three-cycle can generically be written as $V_{\mathcal{Q}} = \sum_i N_i s_i$, the gauge kinetic function can be written as $f_a(z_i) = \sum_i N_i z_i$.

2.3 Moduli Stabilization in G_2 Compactification of M-Theory

As explained in [28, 29], one is interested in the zero flux sector since then the moduli superpotential is entirely non-perturbative. This is crucial for both stabilizing the moduli and generating the Hierarchy naturally as we will review. Fluxes generate a large superpotential and, unless there is a mechanism to obtain an exponentially large volume of the extra dimensions, G_2 compactifications with flux will not generate a small mass scale, such as the TeV scale.

We assume that the G_2 manifolds which we consider have singularities giving rise to two non-Abelian, asymptotically free gauge groups. This implies that they undergo strong gauge dynamics at lower energies leading to the generation of a non-perturbative superpotential. At least one of the hidden sectors is assumed to contain light charged matter fields Φ and $\tilde{\Phi}$ (with $N_f < N_c$) as well. There could be other matter fields which are much heavier and decouple well above the corresponding strong coupling scale. Thus in the minimal[1] framework, one has two hidden sectors

[1]More complicated situations are possible, some of them are discussed in [28, 29].

living on three-cycles with gauge group $G_a \times G_b$ undergoing strong gauge dynamics, one of them having a pair of massless charged matter fields transforming in the (anti)fundamental representation of the gauge group. Of course, in addition, it is assumed that there is another three-cycle on which the observable sector gauge theory with the appropriate chiral matter content lives. This will be discussed more in the next subsection. This set of assumptions about the the compactification manifold gives a working definition of the *framework*.

The $\mathcal{N} = 1$ supergravity theory obtained in four dimensions is then characterized by the following hidden sector superpotential:

$$W = M_P^3 \left(A_1 \, \phi^{-(2/P)} \, e^{ib_1 f_1} + A_2 \, e^{ib_2 f_2} \right); \; b_1 = \frac{2\pi}{P}, \, b_2 = \frac{2\pi}{Q} \tag{2.25}$$

Here $\phi \equiv \det(\Phi\tilde{\Phi})^{1/2} = (2\Phi\tilde{\Phi})^{1/2}$ is the effective meson field (for one pair of massless quarks) and P and Q are proportional to one loop beta function coefficients of the two gauge groups which are completely determined by the gauge group and matter representations. For concreteness we can consider the gauge group to be $SU(Q) \times SU(P+1)$ with one vector like family of quarks charged under $SU(P+1)$. The normalization constants A_1 and A_2 are calculable, given a particular G_2-manifold. $f_{1,2}$ are the (tree-level) gauge kinetic functions of the two hidden sectors which in general are different from each other. Schematically, the superpotential of each hidden sector is just equal to the strong coupling scale of the the corresponding gauge theory, i.e. $W \sim \Lambda_1^3 + \Lambda_2^3$. The vacuum structure of the supergravity theory with this superpotential is quite rich, but in general can only be studied numerically. A special

case exists however, when it is possible to study the vacua semi-analytically. This is when the two three-cycles on which the hidden sector gauge fields are localised are in the same homology class, which in terms of gauge kinetic function then implies:

$$f_1 = f_2 \equiv f_{\rm hid} = \sum_{i=1}^{N} N_i \, z_i. \tag{2.26}$$

The supergravity potential is fully specified once the Kähler potential is given. The Kähler potential for matter fields in general is hard to compute from first principles. However, owing to the fact that matter fields are localized at points inside the seven dimensional manifold V_X, it is reasonable to assume that the matter Kähler potential is approximately canonical at leading order. Then, the Kähler potential is given by:

$$K/m_p^2 = -3\ln(4\pi^{1/3}V_X) + \bar{\phi}\phi \tag{2.27}$$

A simple and reasonable ansatz therefore is $V_X = \prod_{i=1}^{N} s_i^{a_i}$ with a_i positive rational numbers subject to the constraint $\sum_{i=1}^{N} a_i = \frac{7}{3}$ [47]. Many qualitative results about moduli stabilization do not seem to rely on this special form of V_X, but this form of V_X is useful since it gives an $N-1$ parameter family of Kähler potentials consistent with G_2-holonomy, which are tractable. In a basis in which the Kähler potential is given by (4.8), the gauge kinetic function is generically a function of all the moduli, i.e. $N_i \neq 0, i = 1, 2.., N$.

In general the scalar potential of the supergravity theory determined by W and K is a reasonably complicated function of all the moduli. Therefore, one expects to find isolated meta-stable minima, which indeed turns out to be the case, as ex-

plained in detail in [29]. The values of the moduli at the minima are completely determined by the "microscopic" constants[2] – $\{a_i, N_i, A_1, A_2, P, Q, N;\ i = 1, 2...N\}$ which characterize the framework. Given a particular G_2-manifold consistent with our assumptions, all of these constants are calculable in principle. Therefore, given a particular G_2-manifold within the framework, one obtains a particular set of microscopic constants and a particular 4D $\mathcal{N} = 1$ supergravity theory.

To find the minima of the moduli potential V explicitly, one first stabilizes the axionic components of the complex moduli and the phase of ϕ. Then one minimizes the potential with respect to s_i and $|\phi|$, which leads to $N + 1$ equations $\partial_{s_i} V = 0$ and $\partial_{|\phi|} V = 0$ (for N moduli). To solve these equations analytically, we consider the class of solutions in which the volume of the hidden sector three-cycle $V_{\mathcal{Q}}$ supporting the hidden sector gauge groups is large. This allows us to reduce the first set of N equations into just two simple equations, which can be solved order by order in a $1/V_{\mathcal{Q}}$ expansion. Physically, this expansion can be understood as an expansion in terms of the small gauge coupling of the hidden sector - $\alpha_0^{\rm hid}$ which is self-consistent since our hidden sectors are assumed to be asymptotically free. The solution corresponding to a metastable minimum with spontaneously broken supersymmetry is given by

$$s_i = \frac{a_i}{N_i}\frac{3}{14\pi}\frac{P_{\rm eff}\, Q}{Q - P} + \mathcal{O}(P_{\rm eff}^{-1}), \tag{2.28}$$

$$|\phi|^2 = 1 - \frac{2}{Q - P} + \sqrt{1 - \frac{2}{Q - P}} + \mathcal{O}(P_{\rm eff}^{-1}), \tag{2.29}$$

where $P_{\rm eff} \equiv P \ln(A_1 Q / A_2 P)$. The natural values of P and Q are expected to lie

[2]These are called "microscopic" because they determine the effective lagrangian at the compactification ($\sim M_{\rm unif}$) scale.

between $\mathcal{O}(1)$ and $\mathcal{O}(10)$. It is easy to see that a large $P_{\rm eff}$ corresponds to small gauge coupling at the cutoff scale $\alpha_0^{\rm hid}$ for the hidden sector from

$$(\alpha_0^{\rm hid})^{-1} = V_{\mathcal{Q}} \approx \frac{Q}{2\pi(Q-P)} P_{\rm eff} \tag{2.30}$$

implying that the expansion is effectively in $P_{\rm eff}^{-1}$. Given the moduli VEVs in Eq. 2.28 and 2.29, it is straightforward to calculate the VEVs for the auxiliary components of z_i and ϕ:

$$F^i/W = -\frac{3P\,a_i}{2\pi\,N_i} + \mathcal{O}\left(\frac{1}{V_{\mathcal{Q}}}\right) \tag{2.31}$$

$$F^\phi/W = -\sqrt{3} + \mathcal{O}\left(\frac{1}{V_{\mathcal{Q}}}\right) \tag{2.32}$$

Typically we can take $a_i \sim 7/3N$. This implies that F^i are much smaller than F^ϕ when N is large. In fact, all the F_i vanish in the large $V_{\mathcal{Q}}$ limit

$$F_i/W = -\frac{49\,N_i}{4\,b_1}\frac{1}{V_{\mathcal{Q}}^2} + \mathcal{O}\left(\frac{1}{V_{\mathcal{Q}}^3}\right) \tag{2.33}$$

As we will see in Chapter II, this hierarchy between F^i and F^ϕ is responsible for the particular pattern of the soft supersymmetry breaking terms in the G_2-MSSM framework.

The ϕ dependence of the potential at the minimum is essentially

$$V_0 \sim m_{3/2}^2 M_P^2 \left[|\phi|^4 + \left(\frac{4}{Q-P} + \frac{14}{P_{\rm eff}} - 3\right)|\phi|^2 + \left(\frac{2}{Q-P} + \frac{7}{P_{\rm eff}}\right)\right] \tag{2.34}$$

Therefore, the vacuum energy vanishes if the discriminant of the above expression vanishes, i.e. if

$$P_{\rm eff} = \frac{28(Q-P)}{3(Q-P)-8}. \tag{2.35}$$

The above condition is satisfied when the contribution from the F-term of the meson field (F_ϕ) to the scalar potential cancels that from the $-3|W|^2$ term. For $Q-P \leq 2$, there is no solution as either s_i or $|\phi|^2$ become negative. The first non-trivial solution occurs when $Q - P = 3$ for which $P_{\text{eff}} = 84$ is required to get a vanishing vacuum energy (to leading order). The appearance of the integer 84 is closely related to the the dimensionality of the G_2 manifold (which is 7) and that of the three-cycle (which is 3). Other choices of $Q - P$ are also possible theoretically, but are not interesting because of the following reasons: a) the corresponding solutions, if they are to remain in the supergravity regime, require the G_2 manifold to have a rather small number of moduli N, since $N < \frac{14Q}{(3(Q-P)-8)\pi}$ [29]. It is unlikely that G_2-manifolds with such few moduli are capable of containing the $MSSM$ spectrum, which has more than a hundred relevant couplings. b) these solutions generically lead to an extremely high susy breaking scale as will be seen in section 3.1.1 on the gravitino mass. So phenomenologically interesting G_2 compactifications arise only for the case $Q-P = 3$ and $P_{\text{eff}} = 84$.

Some comments on the requirement of $P_{\text{eff}} = 84$ are in order. First of all, it is only a leading order result for the potential in $1/V_{\mathcal{Q}}$ expansion. In fact, including higher order $1/V_{\mathcal{Q}}$ corrections leads to the requirement $P_{\text{eff}} \approx 83$ [29]. The potential will also receive higher order corrections in the M-Theory expansion which will change the requirement for P_{eff} (probably by a small amount). One important good feature of the framework is that these higher order corrections to the vacuum energy have little effect on phenomenologically relevant quantities. Therefore, it is sufficient to tune

the vacuum energy to leading order as long as one is interested in phenomenological consequences. From a microscopic point of view, however, there are two issues - a) Is it possible to realize a large value of P_{eff} from explicit constructions? and b) Can the values of P_{eff} scan finely enough such that one can obtain the observed tiny value of the cosmological constant? Regarding a), one notices that P_{eff} depends on the detailed structure of the hidden sector and is completely model dependent. For particular realizations of the hidden sector, P_{eff} can be computed. A detailed discussion about P_{eff} is given in Appendix A.1. However computing P_{eff} in more general cases is difficult because of our limited knowledge of possible three-dimensional submanifolds of G_2 manifolds. In our analysis, we have assumed that three-cycles exist for which it is possible to obtain a large P_{eff}. The situation regarding b) is even less known. This is because very little is known in general about the set of all compact G_2 manifolds. Duality arguments do suggest that the set of compact G_2-manifolds is larger than the space of compact Calabi-Yau threefolds. Unfortunately, there do not currently exist any concrete ideas about that space either! In our work, we have assumed effectively that the space of G_2 manifolds scans P_{eff} finely enough such that vacua exist with values of the cosmological constant as observed.

2.4 Including the Observable Sector – G_2-MSSM

In these compactifications, as mentioned earlier, the observable sector gauge theory resides on a three-cycle different from the one supporting the hidden sector. The observable sector three-cycle is assumed to contain conical singularities at which

which chiral matter is supported. Since two three-manifolds in a dimensional manifold generically do not intersect each other, this implies that the supersymmetry breaking generated by strong gauge dynamics in the hidden sector is generically mediated to the visible sector by the (higher dimensional) gravity multiplet. This gives rise to gravity (moduli) mediation. However, as will be seen later, anomaly mediated contributions will also play an important role for the gaugino masses.

In our analysis henceforth, we will assume a GUT gauge group in the visible sector which is broken to the SM gauge group, with at least an MSSM chiral spectrum, by background gauge fields (Wilson lines). This assumption is well motivated by considering the duality to the $E_8 \times E_8$ heterotic string on a Calabi-Yau threefold. For simplicity, we will present our results for the $SU(5)$ GUT group breaking to the SM group and just an MSSM chiral spectrum, but all our results should hold for other GUT groups breaking in the same way as well.

To summarize, the full low energy $\mathcal{N} = 1$ Supergravity theory of the visible and hidden sectors at the compactification scale ($\sim M_{\rm unif}$) is defined by the following:

$$\begin{aligned} K &= -3M_P^2 \ln(4\pi^{1/3} V_X) + \bar{\phi}\phi + \tilde{K}_{\bar{\alpha}\beta}(s_i)\, \bar{\Phi}_m^{\bar{\alpha}} \Phi_m^{\beta} + Z(s_i)\, H_u H_d + h.c. + ... \\ W &= M_P^3 \left(A_1\, \phi^{-(2/P)}\, e^{ib_1 f_1} + A_2\, e^{ib_2 f_2} \right) + Y_{\alpha\beta\gamma}\, \Phi_m^{\alpha} \Phi_m^{\beta} \Phi_m^{\gamma} \\ & \qquad f_1 = f_2 \equiv f_{\rm hid} = \sum_i N^i z_i; \quad f^0_{vis} = \sum_i N^i_{vis}\, z_i \end{aligned} \tag{2.36}$$

The visible sector is thus characterized by the Kähler metric $\tilde{K}_{\bar{\alpha}\beta}$, un-normalized Yukawa couplings $Y_{\alpha\beta\gamma}$ of the visible sector chiral matter fields Φ_m^{α}, and the (tree-level) gauge kinetic function f^0_{vis} of the visible sector gauge fields. In addition, as is

generically expected in gravity mediation, a non-zero coefficient Z of the Higgs bilinear is assumed. In general there can also be a mass term (μ') in the superpotential W, but as explained in [48], natural discrete symmetries can exist which forbid it, in order to solve the doublet-triplet splitting problem. However, the Giudice-Masiero mechanism in general generates effective μ and $B\mu$ parameters of $\mathcal{O}(m_{3/2})$.

The Kähler metric $\tilde{K}_{\bar{\alpha}\beta}$ will be discussed in section 4.13. The visible sector gauge couplings are determined by the gauge kinetic function f_{vis} which is an integer linear combination of the moduli with the integers determined by the homology class of the three-cycle Q_{vis} which supports the visible gauge group. Because of a GUT-like spectrum, the MSSM gauge couplings are unified at $M_{\rm unif}$ giving rise to the same f^0_{vis}. Since we are assuming an MSSM visible sector below the unification scale, one has to subject N^i_{vis} to the constraint that $f^0_{vis}(M_{\rm unif}) \equiv \alpha^{-1}_{unif}(M_{\rm unif}) \sim \mathcal{O}(25)$. The Yukawa couplings in these vacua arise from membrane instantons which connect singularities where chiral superfields are supported (if some singularities coincide, there could also be $\mathcal{O}(1)$ contributions). They are given by:

$$Y_{\alpha\beta\gamma} = C_{\alpha\beta\gamma}\, e^{i2\pi \sum_i l_i^{\alpha\beta\gamma} z^i} \tag{2.37}$$

where $C_{\alpha\beta\gamma}$ is an $\mathcal{O}(1)$ constant and $l_i^{\alpha\beta\gamma}$ are integers. Factoring out the phases, the magnitude of the Yukawas can be schematically written as:

$$|Y| \sim |C| e^{-2\pi \vec{l}\cdot\vec{s}} \tag{2.38}$$

The normalized Yukawas differ from the above by factors corresponding to field redefinitions. Because of the exponential dependence on the moduli, it is natural

to obtain a hierarchical structure of Yukawa couplings as is observed in nature. However, in general it is very difficult technically to compute the Yukawa couplings quantitatively. Therefore, for our phenomenological analysis, we will assume that the (normalized) Yukawa couplings are the same as those of the Standard Model. This is reasonable as in this work we are primarily interested in studying the effects of supersymmetry breaking and electroweak symmetry breaking.

Since the moduli have been stabilized, the F-terms of the moduli (F_i) and the meson fields (F_ϕ), which are the source of supersymmetry breaking, can be computed explicitly in terms of the microscopic constants. The expressions for F_i and F_ϕ in terms of these microscopic constants have been given explicitly in [29]. Since these F-terms and the quantities in (2.36) together determine the soft supersymmetry breaking parameters, it becomes possible to express all the soft parameters - gaugino masses, scalar masses, trilinears, μ and $B\mu$, in terms of the microscopic constants. Thus, given a particular G_2-manifold one obtains a particular set of microscopic constants and thus a particular point in the MSSM parameter space. The set of microscopic constants consistent with the framework of G_2 compactifications and our assumptions thus defines a subset of the MSSM, which we call the G_2-MSSM. How this works in practice should become clear in the following sections. Formulae (3.3), (3.8), (3.10), (3.19), (3.31) give the soft-breaking parameters at the unification scale, in terms of the microscopic constants.

Before moving on to discussing the phenomenology of the G_2-MSSM vacua in detail, it is worth noting that realistic M-Theory vacua with a visible sector larger

than the MSSM, will give rise to additional, different predictions for low energy phenomenology in general, and LHC signatures in particular. Therefore, the pattern of LHC signatures may help in distinguishing them. We hope to study this issue in the future.

2.4.1 Gauge Coupling Unification

In section 2.4, it was mentioned that in many cases the strong coupling limit of $E_8 \times E_8$ heterotic string theory compactifications on a Calabi-Yau threefold Z is the same as M-Theory compactifications on a singular G_2-holonomy manifold X. Since a GUT-like spectrum is natural in weakly coupled heterotic compactifications, a GUT-like spectrum (breaking down to the MSSM by Wilson-lines) was assumed for G_2 compactifications in our study as well. At a theoretical level, because of an underlying GUT structure, the MSSM gauge couplings are unified at the compactification scale M_{KK} for both heterotic and G_2 compactifications. However, when one tries to impose constraints from the extrapolated values of observed gauge couplings, interesting differences arise between weakly coupled heterotic and G_2 compactifications. Here, we will explain the difference between weakly coupled heterotic compactifications and G_2 compactifications regarding gauge unification and then discuss the procedure used in our analysis to obtain sets of parameters compatible with gauge unification.

In weakly coupled heterotic string compactifications, there is a relation between the Newton's constant G_N, the unified gauge coupling α_{unif}, the string coupling e^{ϕ} and the volume of the internal manifold V_{CY} [49]. Assuming a more or less isotropic

Calabi-Yau, one has $V_{CY} \sim M_{\rm unif}^{-6}$ which gives:

$$G_N \approx \frac{\alpha_{\rm unif}^{4/3}}{4M_{\rm unif}^2}\left(\frac{16\pi}{e^{2\phi}}\right)^{1/3} > \frac{\alpha_{\rm unif}^{4/3}}{4M_{\rm unif}^2} \tag{2.39}$$

since the string coupling is weak by assumption ($e^{2\phi} < 1$). Substituting the values of $\alpha_{\rm unif}$ and $M_{\rm unif}$ obtained by extrapolating the observed gauge couplings in the MSSM, the prediction for G_N turns out to be too large compared to the observed value. Various proposals have been put forward for dealing with this problem within the perturbative heterotic setup, but none of them are obviously compelling.

In G_2 compactifications however, one finds a different relation among the same quantities after doing a similar analysis [50]:

$$G_N \approx \frac{\alpha_{\rm unif}^2}{32\pi^2 M_{\rm unif}^2}\left(\frac{1}{a}\right); \;\; a \equiv \frac{V_X}{V_{\mathcal{Q}_{vis}}^{7/3}} \tag{2.40}$$

Here, a is the dimensionless ratio between the volume of the G_2 manifold V_X and the volume of the three-cycle $\mathcal{Q}_{vis}$ on which the visible sector MSSM gauge group is supported. If one does a more careful analysis and takes into account the threshold corrections to the unified gauge coupling from Kaluza-Klein (KK) modes, one obtains [50]:

$$G_N = \frac{\alpha_{\rm unif}^2}{32\pi^2 M_{\rm unif}^2}\left(\frac{(L(\mathcal{Q}_{vis}))^{2/3}}{a}\right) \tag{2.41}$$

where $L(\mathcal{Q}_{vis})$ is the contribution from the threshold correction. Substituting the values of $\alpha_{\rm unif}$ and $M_{\rm unif}$ obtained by extrapolating the observed gauge couplings in the MSSM and the value of G_N, one finds:

$$\left(\frac{(L(\mathcal{Q}_{vis}))^{2/3}}{a}\right) \approx 15 \tag{2.42}$$

In all examples where duality with heterotic string theory or Type IIA string theory is used to deduce the existence of the G_2 manifold X, "a" is expected to be much less than unity [50]. For G_2-MSSM vacua, with natural values of the microscopic parameters one obtains $V_X = 10 - 100$ [29] while $V_{\mathcal{Q}_{vis}} \sim \alpha_{\text{unif}}^{-1} \sim \mathcal{O}(25)$[3]. Thus, $a \equiv \frac{V_X}{V_{\mathcal{Q}_{vis}}^{7/3}} \ll 1$ is also naturally satisfied for G_2-MSSM vacua. In addition, by expressing V_X and $V_{\mathcal{Q}_{vis}}$ in terms of M_{11} and M_{unif} respectively, $a < 1$ implies $M_{\text{unif}} < M_{11}$ which means that the unification scale constraint stated in section 3.1 can be naturally satisfied. Since $a \ll 1$, from (2.42) one requires:

$$(L(\mathcal{Q}_{vis}))^{2/3} \ll 15 \tag{2.43}$$

The quantity $L(\mathcal{Q}_{vis}))^{2/3}$ depends on certain topological invariants of the three-cycle $\mathcal{Q}_{vis}$ and can be computed for special choices of $\mathcal{Q}_{vis}$. For one such choice - $\mathcal{Q}_{vis} = \mathbf{S^3}/Z_q;\ q \in \mathbf{Z}$, $(L(\mathcal{Q}_{vis}))^{2/3}$ has been computed [50]. It depends on two integers ω, q such that 5ω is not a multiple of q.[4] Figure 2.1 shows the variation of $L^{2/3}$ for $\mathcal{Q}_{vis} = \mathbf{S^3}/Z_q$ as a function of q for different choices of 5ω mod q. One sees that $L^{2/3} \ll 15$ can be obtained in a natural manner for a large range of q. For other choices of $\mathcal{Q}_{vis}$, it is reasonable to expect a similar result. To summarize therefore, G_2-MSSM vacua are naturally compatible with gauge unification in general and the "unification scale constraint" mentioned in section 3.1 in particular.

The value of the unified gauge coupling α_{unif} is also affected by the threshold corrections. The tree-level unified gauge coupling of the visible sector at the com-

[3]The unified coupling constraint will be discussed in Appendix 2.4.2.

[4]It is assumed that an $SU(5)$ GUT group is broken to the MSSM by Wilson lines.

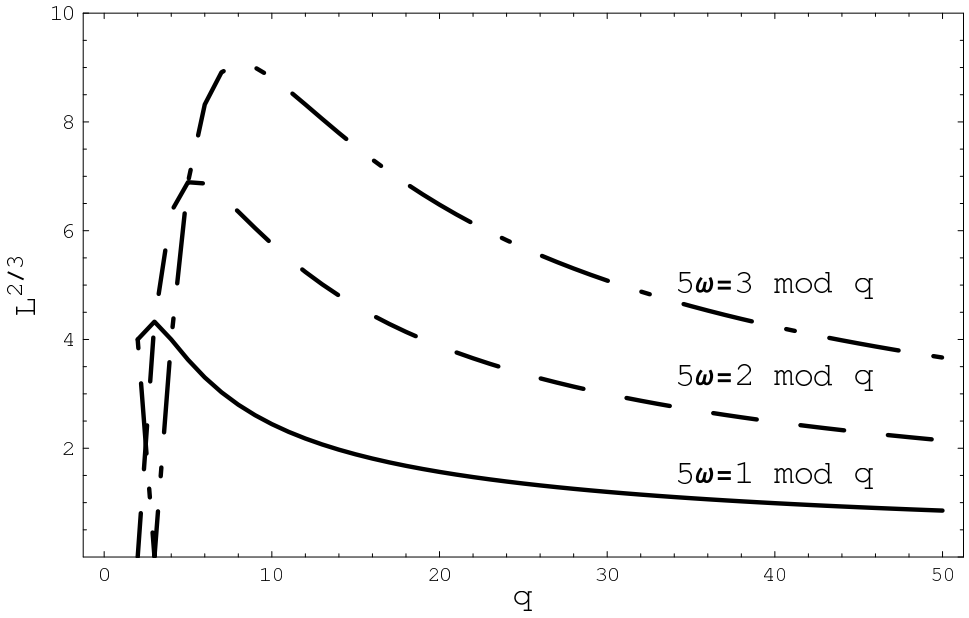

Figure 2.1: Plot of $L^{2/3}$ as a function of integer q from 2 to 50. Different curves correspond to different choices of ω as marked in the plot.

pactification scale is the volume of the visible sector three-cycle $\mathcal{Q}_{vis}$:

$$\alpha_M^{-1} \equiv \mathrm{Re}(f^0_{vis}) = V_{\mathcal{Q}_{vis}} = \sum_{i=1}^{N} N_i^{vis} s_i, \tag{2.44}$$

After taking into account the threshold corrections (at one-loop), one has:

$$\alpha_{\mathrm{unif}}^{-1} \;=\; \alpha_M^{-1} + \delta \tag{2.45}$$

For the one-loop result to be reliable, δ should be small compared to α_M^{-1}. Since for the MSSM $\alpha_{unif}^{-1} \sim 25$ one requires $\alpha_M^{-1} \sim \mathcal{O}(25)$ as well. The conditions under which the microscopic parameters can give rise to the above value of α_M^{-1} is discussed in section 2.4.2. The threshold correction δ can be computed from the topological invariants of the three-cycle $\mathcal{Q}_{vis}$, so it also depends on integers characterizing the topology of $\mathcal{Q}_{vis}$. However, it is in general regularization dependent in contrast to expression (2.41) for the unification scale [50]. Therefore, in our analysis we will

assume δ to be a free parameter varying in a reasonable range such that one-loop results are still reliable.

2.4.2 Constraints on "Microscopic" Parameters

The vacua in realistic G_2 compactifications are characterized by the "microscopic" parameters N_i, N_i^{sm}, a_i, N, P, Q, A_1, A_2 and δ where $i = 1, 2, .., N$. However, only certain parameters such as Q, P, A_2 and δ as well as certain combinations of them, such as V_X, $V_{\mathcal{Q}_{vis}}$ and P_{eff} are responsible for relevant physics quantities. These parameters have to satisfy various constraints such that the effective 4D description and the procedure of moduli stabilization are valid and consistent. In the following, we discuss three important constraints:

- The validity of the supergravity approximation requires $V_X > 1$. We call this the "weak supergravity constraint". In its "strong" form, one could require all geometric moduli s_i to be greater than unity.
- Since it is known that, for an MSSM visible sector $\alpha_{\text{unif}}^{-1} \sim 25$, this implies $V_{\mathcal{Q}_{vis}} \sim 25$. We call this the "unified coupling constraint".
- $M_{11} > M_{\text{unif}} \sim \mathcal{O}(10^{16}\text{ GeV})$, which is required to make intrinsic M-Theory corrections to gauge couplings and other parameters negligible at and below M_{unif}. We call this the "unification scale constraint".

The main question here is that whether all these constraints can be satisfied simultaneously with reasonable choices of the microscopic parameters. Given the large number choices of parameters a_i, N_i, N_i^{sm} with $i = 1, .., N$, in order to make

the analysis tractable, we consider the following two extreme cases:

(a) a_i are roughly equal, $a_i \approx \frac{7}{3N}$.

(b) a_i are maximally asymmetric, for example, $a_1 \approx \frac{7}{3}$ and $a_{i\neq 1} \approx 0$.

Since other choices of the above parameters lie in between the two extremes, presumably so would their implications. For later use, it is useful to rewrite the moduli VEVs as

$$s_i = \frac{a_i}{N_i}\nu, \quad \nu \approx \frac{3P_{\rm eff}Q}{14\pi(Q-P)} \tag{2.46}$$

where $P_{\rm eff} \equiv P \log\left(\frac{A_1 Q}{A_2 P}\right)$.

Let us first consider the weak supergravity constraint for the phenomenologically interesting dS vacua, which reads:

$$V_X = \prod_{i=1}^{N} s_i^{a_i} > 1 \tag{2.47}$$

For case (a), we can rewrite the seven dimensional volume as

$$\begin{aligned} V_X &\approx \left(\frac{7\nu}{3N}\right)^{7/3} \left(\prod_{i=1}^{N} N_i\right)^{-\frac{7}{3N}} \\ &\approx \left(\frac{7\nu}{3N\bar{N}}\right)^{7/3} \end{aligned} \tag{2.48}$$

where $\bar{N}$ is defined to be the geometric mean of the N_i's. One should keep in mind that $\bar{N}$ can be small even if some of the N_i's are large, if N is $\mathcal{O}(10)$ or greater. The supergravity constraint then turns out to be:

$$\frac{7\nu}{3N\bar{N}} > 1 \quad \Longrightarrow \quad \frac{P_{\rm eff}Q}{2\pi N\bar{N}(Q-P)} > 1 \tag{2.49}$$

For the case (b), we have $\left(\frac{a_i}{N_i}\right)^{a_i} \approx 1$ for $i \neq 1$, and so $V_X = \left(\frac{a_1\nu}{N_1}\right)^{7/3}$. Therefore the constraint turns out to be

$$\frac{a_1}{N_1}\nu > 1 \quad \Longrightarrow \quad \frac{P_{\rm eff}Q}{2\pi N_1(Q-P)} > 1 \tag{2.50}$$

A typical set of "reasonable" as well as phenomenologically interesting values is $P_{\rm eff} \sim \mathcal{O}(10-100)$, $Q \sim \mathcal{O}(10)$, $Q-P \sim \mathcal{O}(1)$(but > 3), $\bar{N} \sim \mathcal{O}(1)$ and $N_1 \sim \mathcal{O}(1)$, which easily satisfies the supergravity constraint in case (b). The supergravity constraint for case (a) is also satisfied for many sets of values of the parameters in the above ranges, although not as easily for case (b). For a general case which lies between (a) and (b), we expect a situation in between the two and the constraint should be satisfied for parameters in the above range. The important point is that this constraint can always be satisfied by an asymmetric distribution of a_i.

Now let us consider the unified coupling constraint. The gauge kinetic function for the visible sector is the volume of the visible three-cycle (See Eq.2.44), which obeys the following inequality:

$$V_{\mathcal{Q}_{vis}} > N\left(\prod_{i=1}^{N} N_i^{sm}\right)^{1/N}\left(\prod_{i=1}^{N} s_i\right)^{1/N} \tag{2.51}$$

For case (a), (2.51) can be written as:

$$V_{\mathcal{Q}_{vis}} > N\left(\prod_{i=1}^{N} N_i^{sm}\right)^{1/N}\left(\frac{7\nu}{3N\bar{N}}\right) \tag{2.52}$$

From Eq.(2.49) and assuming $N_i^{sm} > 1$ for all i, we find $V_{\mathcal{Q}_{vis}} > N$. Since for the MSSM $V_{\mathcal{Q}_{vis}} = \alpha_M^{-1} \sim \mathcal{O}(25)$, this implies $N \lesssim \mathcal{O}(25)$. Thus, equal values of a_i require the number of moduli to be relatively small. One way out of this is that

most of the N_i^{sm} are zero, and only $p \lesssim \mathcal{O}(10)$ of them are nonzero. This however, is non-generic. For case (b), one has $\left(\prod_{i=1}^{N} s_i\right)^{1/N} \sim 0$. Therefore, inequality (2.51) can be easily satisfied. Again, case (b) is more easily satisfied than case (a). For a more general situation lying in between (a) and (b), one expects that the constraint can be satisfied for many sets of values of the microscopic parameters.

CHAPTER III

Supersymmetry Breaking in G_2-MSSM

Having introduced the G_2-MSSM framework, we are now ready to examine the associated phenomenology. Since supersymmetry is spontaneously broken, all the supersymmetric partners of the standard model particles get masses. These new particles, if they are light enough, can either be produced in the collider experiments or can participate many different physical processes, and therefore lead to deviations from the Standard Model predictions. In fact, the phenomenology related to the soft supersymmetry breaking sector is quite rich [51]. Before we study the phenomenology in the G_2-MSSM framework, we have to first calculate the soft terms from the 4D effective supergravity setup. These calculations will set the boundary condition for the renormalization group extrapolation of the low energy soft terms. We will then include various threshold corrections and compute the low energy superpartner masses and couplings. In this chapter, we also discuss the electroweak symmetry breaking and the precision gauge coupling unification, which are intimately related to the soft terms.

3.1 Soft Supersymmetry Breaking Terms at $M_{\rm unif}$

3.1.1 Gravitino Mass

The bare gravitino mass in $\mathcal{N}=1$ supergravity can be computed as follows:

$$m_{3/2} \equiv M_P^{-2}\, e^{\frac{K}{2M_P^2}}\, |W| \tag{3.1}$$

This quantity plays an important role in gravity mediated models of supersymmetry breaking and sets the typical mass scale for couplings in the supergravity Lagrangian. It is therefore useful to compute this quantity in detail in the G_2-MSSM.

As explained earlier, $|W|$ is generated by strong gauge dynamics in the two hidden sectors, $W_{1,2} \sim (\Lambda_{1,2})^3$. This implies that the gravitino mass can be schematically expressed as:

$$m_{3/2} \sim \frac{\Lambda^3}{M_P^2} \tag{3.2}$$

up to some factors of volume coming from the Kähler potential in (3.1). More precisely, the gravitino mass is:

$$\begin{aligned} m_{3/2} &= M_P \frac{e^{\phi_0^2/2}}{8\sqrt{\pi} V_X^{3/2}} C_2 \left| P\phi_0^{-\frac{2}{P}} - Q \right| e^{-\frac{P_{\rm eff}}{Q-P}} \\ &\approx M_P \frac{e^{\phi_0^2/2}}{8\sqrt{\pi} V_X^{3/2}} C_2 |Q-P| e^{-\frac{P_{\rm eff}}{Q-P}} \end{aligned} \tag{3.3}$$

where in the last line, $\phi_0 \approx 1$ is used. In the above equation, $C_2 \equiv A_2/Q$ is used for convenience. The exponential part in the equation is roughly Λ_{cond}^3 in units of M_P. As seen from above, the gravitino mass is effectively determined by four parameters: $\{P_{\rm eff}, Q-P, V_X \text{ and } C_2\}$. For $Q-P=3$, the gravitino mass can be well approximated

by

$$m_{3/2} = 708 \text{ TeV} \times C_2 V_X^{-3/2} e^{-(P_{\text{eff}}-83)/3} \tag{3.4}$$

For the case of zero cosmological constant $P_{\text{eff}} = 83$ [1], the exponential is unity and the gravitino mass is bounded from above by 708 TeV. As will be seen later, V_X turns out to be typically in the range 10-100, implying that $m_{3/2}$ naturally lies between 10 and 100 TeV. If one allows a dS minimum with a large cosmological constant, P_{eff} can be smaller than 84 and the gravitino mass can become larger. For larger values of $Q-P$, the P_{eff} required to tune the cosmological constant (see eqn. (2.35)) is smaller. For example, for $Q - P = 4$, $P_{\text{eff}} = 28$ is required. Since the gravitino mass is exponentially sensitive to P_{eff} (as seen from (3.4)), the gravitino mass for $Q - P > 3$ turns out to be much larger then the TeV scale. This is the reason for mainly considering the case $Q - P = 3$.

3.1.2 Scalars and Trilinears at M_{unif}

The general expressions for the un-normalized scalar masses and trilinear parameters are given in Eq. (2.13). In order to determine physical implications, however, one has to canonically normalize the visible matter Kähler potential $K_{visible} = \tilde{K}_{\bar{\alpha}\beta}\Phi^{\bar{\alpha}}\Phi^{\beta} + ...$, which is achieved by introducing a normalization matrix $\mathcal{U}$:

$$\Phi \to \mathcal{U} \cdot \Phi, \quad s.t. \quad \mathcal{U}^{\dagger}\tilde{K}\mathcal{U} = 1. \tag{3.5}$$

[1] The upper limit $P_{\text{eff}} = 84$ obtained in the zeroth order of the $1/V_{\mathcal{Q}_{vis}}$ approximation is modified to $P_{\text{eff}} = 83$ after taking higher order corrections into account.

The $\mathcal{U}s$ are themselves only defined up to a unitary transformation, i.e. $\mathcal{U}' = \mathcal{U} \cdot \mathcal{N}$ is also an allowed normalization matrix if $\mathcal{N}$ is unitary. The normalized scalar masses and trilinears can then be written formally as:

$$\begin{aligned} m^2_{\bar{\alpha}\beta} &= (\mathcal{U}^\dagger \cdot m'^2 \cdot \mathcal{U})_{\bar{\alpha}\beta} \\ \tilde{A}_{\alpha\beta\gamma} &= \mathcal{U}_{\alpha\alpha'}\mathcal{U}_{\beta\beta'}\mathcal{U}_{\gamma\gamma'}A'_{\alpha'\beta'\gamma'} \end{aligned} \tag{3.6}$$

More precisely, the scalar masses can be written as:

$$\begin{aligned} m^2_{\bar{\alpha}\beta} &= (m^2_{3/2} + V_0)\,\delta_{\bar{\alpha}\beta} - \mathcal{U}^\dagger \Gamma_{\bar{\alpha}\beta}\mathcal{U} \\ \Gamma_{\bar{\alpha}\beta} &\equiv e^{\hat{K}} F^{\bar{m}} (\partial_{\bar{m}}\partial_n \tilde{K}_{\bar{\alpha}\beta} - \partial_{\bar{m}} \tilde{K}_{\bar{\alpha}\gamma}\, \tilde{K}^{\gamma\bar{\delta}}\partial_n \tilde{K}_{\bar{\delta}\beta}) F^n \end{aligned} \tag{3.7}$$

Thus, when the cosmological constant has been tuned to be small, the scalar masses generically have a flavor universal and flavor diagonal contribution equal to $m^2_{3/2}$ from the first term in Eq. (3.7) and a flavor non-universal and flavor non-diagonal contribution from the second term in Eq. (3.7). In order to estimate the size of the non-universal and non-diagonal contributions, one has to know about the moduli and meson dependence of the visible sector Kähler metric. This dependence of the matter Kähler metric is notoriously difficult to compute in generic string and M theory vacua, and the vacua under study here are no exception. Therefore, it is only possible to proceed by making reasonable assumptions. Under our assumptions about the meson field kinetic term, the only contribution to the non-universal and non-diagonal terms in Eq. (3.7) comes from the F terms of the moduli F_i. Since $F_i \ll F_\phi$, the non-universal contributions are negligible compared to the universal

and diagonal contribution. Thus,

$$m^2_{\bar{\alpha}\beta} \approx m^2_{3/2}\,\delta_{\bar{\alpha}\beta} \tag{3.8}$$

This implies that flavor changing neutral currents (FCNCs) are adequately suppressed. The fact that the scalar masses are are roughly equal to the gravitino mass can be traced to the non-sequestered nature of the Kähler potential in Eq. (2.36). In the absence of fluxes, the G_2 compactifications considered here do not have any warping, which implies that one generically does not have sequestering in these compactifications [52]. Since the scalars are heavy and also flavor universal at leading order, we expect that no significant signals should occur for observables from loops with sleptons or squarks, in particular for rare flavor violating decays such as $\mu \to e\gamma$, $K \to \pi\nu\bar{\nu}$, $b \to s\gamma$, etc, and also no significant signal for $g_\mu - 2$.

The computation of the trilinears also simplifies under the above assumptions. Again, since the un-normalized Yukawa couplings and the visible sector Kähler metric are not expected to depend on the meson field, the dominant contribution to the trilinears comes from the first term in the expression for trilinears in (2.13). Thus, one has:

$$A'_{\alpha\beta\gamma} \approx e^{\hat{K}}\, F^\phi\, \hat{K}_\phi\, Y'_{\alpha\beta\gamma} \tag{3.9}$$

This implies that the normalized trilinear parameters are:

$$\begin{aligned} \tilde{A}_{\alpha\beta\gamma} &\approx (\mathcal{U}_{\alpha\alpha'}\mathcal{U}_{\beta\beta'}\mathcal{U}_{\gamma\gamma'})\, e^{\hat{K}}\, F^\phi\, \hat{K}_\phi\, Y'_{\alpha'\beta'\gamma'} \\ &\approx e^{\hat{K}/2}\, F^\phi\, \hat{K}_\phi\, Y_{\alpha\beta\gamma} \\ &\approx 1.48\, m_{3/2}\, Y_{\alpha\beta\gamma} \end{aligned} \tag{3.10}$$

Here we have used the fact that the normalized Yukawa couplings are given by $Y_{\alpha\beta\gamma} = e^{\hat{K}/2}(\mathcal{U}_{\alpha\alpha'}\mathcal{U}_{\beta\beta'}\mathcal{U}_{\gamma\gamma'})\, Y'_{\alpha'\beta'\gamma'}$ and that $e^{\hat{K}/2}\, F^{\phi}\, \hat{K}_{\phi} \approx \sqrt{3}\,\phi_0\, m_{3/2} \approx e^{-i\gamma_W}\, 1.48\, m_{3/2}$ [29]. The reduced normalized trilinear parameters have a particularly simple form:

$$A_{\alpha\beta\gamma} \equiv \frac{\tilde{A}_{\alpha\beta\gamma}}{Y_{\alpha\beta\gamma}} \approx 1.48\, m_{3/2} \tag{3.11}$$

Thus, we see that in G_2-MSSM vacua, the scalar masses and trilinears are generically of $\mathcal{O}(m_{3/2})$.

3.1.3 Gaugino Masses at $M_{\rm unif}$

We now turn to gaugino masses. The computation of gaugino masses depends less on our knowledge of the matter Kähler potential, therefore it is possible to obtain quite detailed formulae. In G_2 vacua the tree-level gaugino masses are suppressed relative to the gravitino mass unlike the scalars and trilinears. Therefore, other contributions such as those from anomaly mediation and those from threshold effects arising from integrating out heavy fields can be important. Schematically, one can write

$$M_a(\mu) = M_a^{\rm tree}(\mu) + M_a^{\rm AMSB}(\mu) + M_a^{\rm thres}(\mu) \tag{3.12}$$

In the following we wish to compute each contribution at the unification scale $M_{\rm unif}$. We study the case when the low energy spectrum is that of the MSSM. As mentioned in section 2.4, for concreteness we will assume an $SU(5)$ GUT group broken to the MSSM by a discrete choice of Wilson lines for concreteness. This gives rise to a pair of Higgs triplets whose effects should be properly taken into account. For the case

of a different GUT group breaking to the MSSM by Wilson lines, there would be similar heavy particles whose effects should be taken into account. As we will see, the results obtained will be the same for all GUT groups as long as the low energy spectrum is that of the MSSM.

Tree-level Suppression of Gaugino Masses

The tree-level gaugino masses at the scale μ are given by [44]:

$$M_a^{\rm tree}(\mu) = \frac{g_a^2(\mu)}{8\pi}\left(\sum_{m,n} e^{\hat{K}/2} K^{m\bar{n}} F_{\bar{n}} \partial_m \,{\rm Re} f_a^0\right) \tag{3.13}$$

$$= \frac{g_a^2(\mu)}{8\pi}\sum_{i=1}^{N} e^{\hat{K}/2} K^{i\bar{i}} F_{\bar{i}} N_i^{vis}. \tag{3.14}$$

where f_a^0 is the tree-level gauge kinetic function of the a^{th} gauge group. As explained earlier, the tree-level gauge kinetic function f_a^0 of the three gauge groups in the MSSM are the same ($= f_{vis}^0$) because of the underlying GUT structure. The tree-level gaugino mass at the unification scale can then be computed in terms of microscopic parameters. The details are provided in section VIIIA of [29]. Here, we write down the result:

$$M_a^{\rm tree}(M_{\rm unif}) \approx -\frac{\eta}{P_{\rm eff}}\Big(1+\frac{2}{\phi_0^2(Q-P)}+\mathcal{O}(P_{\rm eff}^{-1})\Big)\, m_{3/2}$$

$$\text{where } \alpha_{\rm unif}^{-1} = {\rm Re}(f_{vis}^0)+\delta;\;\; \eta = 1-\frac{\delta}{\alpha_{\rm unif}^{-1}} \tag{3.15}$$

δ corresponds to threshold corrections to the (unified) gauge coupling and will be discussed more in section 2.4.1. As seen from above, gaugino masses are suppressed by $P_{\rm eff}$ relative to gravitino mass. This property is independent of the details of the Kähler potential for ϕ and the form of V_X.

Because the MSSM is obtained by the breaking of a GUT group by Wilson lines, the gauge couplings of the MSSM gauge groups are unified at the unification scale giving rise to a common $\mathrm{Re}(f^0_{vis})$. This implies that the tree level gaugino masses at $M_{\rm unif}$ are also unified. In particular, for $Q - P = 3$ with a vanishing cosmological constant ($P_{\rm eff} = 83$) and the Kähler potential given by (4.8), one has an explicit expression for the gaugino mass:

$$\begin{aligned} M_a^{\rm tree}(M_{\rm unif}) &\approx -\frac{1}{83}\eta\left(1+\frac{2}{3\phi_0^2}+\frac{7}{83\phi_0^2}\right)\times m_{3/2} \\ &\approx \eta\, 0.024\, m_{3/2} \end{aligned} \tag{3.16}$$

Here we have used the fact that for $Q - P = 3$, $\phi_0^2 \approx 0.73$. As explained in section 2.3, a large $P_{\rm eff}$ is required for the validity of our solutions. Therefore, the parametric dependence on $P_{\rm eff}^{-1}$ in Eq.(3.15) indicates a large suppression in gaugino masses. The precise numerical value of the suppression may change if one considers a more general form of the matter Kähler potential since then the numerical factor multiplying $P_{\rm eff}^{-1}$ in (3.15) may change in general. However as long as the couplings for higher order terms in the matter Kähler potential such as $(\bar{\phi}\phi)^2$ are sufficiently small, a large numerical suppression is generic. In our analysis henceforth, we will assume that to be the case.

From a physical point of view, the suppression of gaugino masses is directly related to the fact that the F-terms of moduli F_i (in Planck units) are suppressed compared to $m_{3/2}$ and that the gauge kinetic function f_a^0 in (3.13) only depends on the moduli s_i. This implies that the F-term of the meson field does not contribute in (3.15). It

is also useful to compare the above result for the tree-level suppression of gaugino masses in G_2 dS vacua with that of Type IIB dS vacua. In KKLT and large volume type IIB compactifications, the moduli F terms also vanish in the leading order leading to a suppression of tree-level gaugino masses, although for a different reason - the flux contribution to the moduli F terms cancels the contribution coming from the non-perturbative superpotential [23]. Another difference is that the subleading contributions in those Type IIB vacua are suppressed by the inverse power of the volume of the compactification manifold. Note that a large associative three-cycle on a G_2 manifold ($V_{\mathcal{Q}_{vis}}$) does not translate into a large volume compactification manifold. So, it is possible for G_2 vacua to have a large $V_{\mathcal{Q}_{vis}}$ while still having a high compactification scale.

Anomaly Mediated Contributions

Since the tree-level gaugino mass is suppressed, the anomaly mediated contributions become important and should be included. In our framework they are not suppressed. The general expression for the anomaly contribution to gaugino masses at scale μ is written as [45]:

where i runs over all the MSSM chiral fields. Again, since the Kähler metric for visible sector matter fields is expected to be independent of the meson field, the third term in (4.12) is much smaller than the first two. Thus, the anomaly mediated

contribution can be simplified:

$$\begin{aligned} \frac{M_a^{AMSB}(M_{\rm unif})}{g_a^2} &\approx -\frac{1}{16\pi^2}\left[b_a - b'_a\phi_0^2\left(1+\frac{2}{(Q-P)\,\phi_0^2}\right)\right] m_{3/2} \qquad (3.17) \\ b_a &\equiv -(3C_a - \sum_i C_a^i);\;\; b'_a \equiv -(C_a - \sum_i C_a^i) \end{aligned}$$

As seen from (3.17), the anomaly mediated contributions are not universal. Since the anomaly mediated contributions are numerically comparable to the tree-level contributions, the gaugino masses will be non-universal at the unification scale. That the tree-level and anomaly mediated contributions are similar in size seems to be accidental – one is suppressed by $1/P_{\rm eff} = 1/83$, the other by the loop factor $1/16\pi^2$, and these factors are within a factor of two of each other.

The Complete Gaugino Masses

In principle, there can also be threshold corrections to gaugino masses from high scale physics and it is important to take them into account. In general, a threshold correction to the gaugino masses at a scale M_{th} is induced by a threshold correction to gauge couplings by the following expression [53]:

$$\Delta M_a = g_a^2(M_{th})\, F^I \partial_I \left(\Delta\, f_a^{thresh}\right) \qquad (3.18)$$

In these M-theory compactifications, possible threshold corrections at scales $\leq M_{\rm unif}$ can arise from the following:

- Generic heavy M-theory excitations Ψ of $\mathcal{O}(M_{11})$ - $\Delta f_a^{M\,theory}$.
- 4D particles in the GUT multiplet with mass $\approx M_{\rm unif}$ - $\Delta f_a^{T,\tilde{T}}$.

- Kaluza-Klein (KK) excitations of $\mathcal{O}(M_{\rm unif})$ - Δf_a^{KK}.

It turns out that threshold corrections to the gauge couplings from KK modes are constants [50]. Therefore, from (3.18), they will not give rise to any threshold correction to the gaugino masses. In addition, the corrections from generic heavy M-theory states T with mass $\sim M_{11}$ as well as from 4D heavy GUT particles with mass ($\sim M_{\rm unif}$) (such as Higgs triplets in $SU(5)$), to the gaugino masses are also negligible. So, the complete gaugino mass can be approximately written as:

$$\frac{M_a(M_{\rm unif})}{g^2_{GUT}} \approx -\frac{1}{16\pi^2}\left\{b_a + \left(\frac{4\pi\,{\rm Re}(f^0)}{P_{\rm eff}} - b'_a\phi_0^2\right)\left(1+\frac{2}{\phi_0^2(Q-P)}\right)\right\} m_{3/2} \quad (3.19)$$

$$\text{where} \quad b_1 = 33/5, \quad b_2 = 1.0, \quad b_3 = -3.0, \quad b'_1 = -\frac{33}{5}, \quad b'_2 = -5.0, \quad b'_3 = -3.$$

The above analytical expression for gaugino masses is true up to the first subleading order in the $1/V_{\mathcal{Q}}$ expansion. In general, the full gaugino mass at the unification scale (3.19) depends on the parameters $\{{\rm Re}(f^0),\, Q-P,\, \delta,\, V_X,\, P_{\rm eff}$ and $C_2\}$. For the phenomenologically interesting case with $Q-P=3$ and $P_{\rm eff}=83$, there are effectively only four parameters: $\{{\rm Re}(f^0), \delta, V_X, C_2\}$. As seen from (3.4), $m_{3/2}$ is determined from the last two parameters - V_X and C_2. Therefore, the ratio of the gaugino masses to the gravitino mass for the phenomenologically interesting case of $Q-P=3, P_{\rm eff}=83$ just depends on the parameters ${\rm Re}(f^0)$ and δ which are subject to the constraint $\alpha_{\rm unif}^{-1} = {\rm Re}(f^0)+\delta \approx \mathcal{O}(25)$ (see section 2.4). The gaugino masses are plotted as a function of δ in Figure 3.1 for $m_{3/2}=20$ TeV. Notice that M_2 and M_3 are smaller than M_1 by a factor of few at the unification scale. However, as will be seen promptly, the gluino will still turn out to be the heaviest gaugino because of

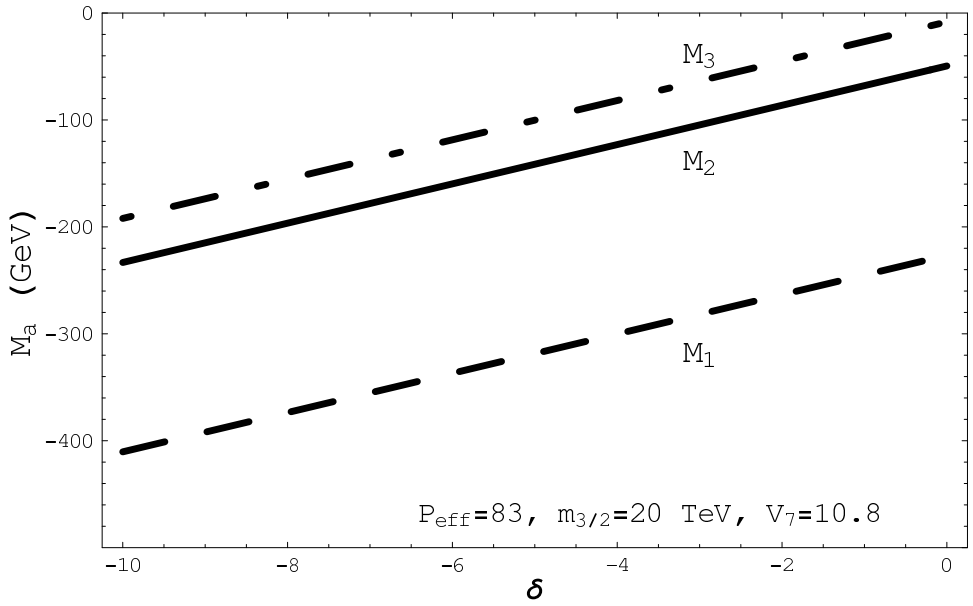

Figure 3.1: The gaugino masses at the unification scale are plotted as functions of threshold correction to the gauge kinetic function δ for $Q - P = 3$, $P_{\rm eff} = 83$, $m_{3/2} = 20$ TeV and $\alpha_{unif}^{-1} = 26.5$.

RG effects.

3.2 Superpartner Spectrum at M_{EW} and Electroweak Symmetry Breaking

As seen in previous section, the scalar and Higgsino masses at $M_{\rm unif}$ are close to that of the gravitino. This has to be larger than $\gtrsim 10$ TeV in order to evade the LEP II chargino bound because of the large suppression of the gaugino masses relative to the gravitino. In addition, a gravitino mass of $\gtrsim 10$ TeV is also required to mitigate the moduli and gravitino problems.

In order to connect to low-energy physics, one has to RG evolve the soft supersymmetry breaking parameters from $M_{\rm unif}$ to the electroweak scale. It turns out that RG evolution increases the masses of the first and second generation squarks

and sleptons. However, since the increase is mostly proportional to the gaugino masses [54] which are much smaller than the high-scale sfermion mass, the masses of the first and second generations squarks and sleptons are still of $\mathcal{O}(m_{3/2})$. The masses of the third generation squarks and sleptons - stops, sbottoms and staus are also affected non-trivially by the trilinear parameters (again of $\mathcal{O}(m_{3/2})$) because of their larger Yukawa couplings [54]. In particular, the lightest stop ($\tilde{t}_1$) becomes much lighter than the other sfermions (even though still considerably heavier than the gauginos). Finally, the μ parameter, which determines the masses of the higgsinos, does not change much during RG evolution because of the non-renormalization theorem. So, the μ parameter at the electroweak scale is also of $\mathcal{O}(m_{3/2})$.

Because of the large hierarchy in the spectrum, it is convenient to work in an effective theory with the heavy fields (scalars and Higgsinos) integrated out at their characteristic scale ($M_s \sim 10 - 100$ TeV). The low energy effective theory below M_s only contains the light gauginos and the SM particles. Therefore it is very important to compute the masses of gauginos as these are the only light new states predicted by the theory[2]. To take into account the threshold effects of these heavy states on the gaugino masses, we follow the "match and run" procedure which is a good approximation when $M_a \ll M_s$. In this paper, we use a one-loop two-stage RGE running with a tree-level matching at the scale M_s. All other thresholds are calculated using the exact one-loop results.

[2]The lightest stop could also be light in some cases.

3.2.1 Gaugino Masses at M_{EW}

The weak scale gaugino mass parameters at one-loop can be related to those at unification scale by a RG evolution factor K_a as follows:

$$M_a(M_{\rm weak}) \;=\; K_a\, M_a(M_{\rm unif}) \tag{3.20}$$

The RG evolution factors K_a are given by:

$$K_a = \left(\frac{\alpha_a^s}{\alpha_{unif}}\right)\left(\frac{\alpha_a^{EW}}{\alpha_a^s}\right)^{\tilde{b}_a^{SM}/b_a^{SM}} \tag{3.21}$$

where $\tilde{b}_a$'s and b_a's are the β function coefficients of the gaugino masses and gauge couplings respectively:

$$\begin{aligned} \tilde{b}_1^{SM} &= 0, \quad \tilde{b}_2^{SM} = -6, \quad \tilde{b}_3^{SM} = -9 \\ b_1^{SM} &= \frac{41}{10}, \quad b_2^{SM} = -\frac{11}{6}, \quad b_3^{SM} = -5. \end{aligned} \tag{3.22}$$

α_a^s and α_a^{EW} are the gauge couplings at the decoupling scale M_s and the electro-weak scale $M_{\rm EW}$ respectively, which can be expressed as

$$\begin{aligned} (\alpha_a^s)^{-1} &= \alpha_{unif}^{-1} + \frac{b_a}{2\pi}\ln\left(\frac{M_{\rm unif}}{M_s}\right) \\ (\alpha_a^{EW})^{-1} &= (\alpha_a^s)^{-1} + \frac{b_a^{SM}}{2\pi}\ln\left(\frac{M_s}{M_{EW}}\right) \end{aligned} \tag{3.23}$$

As an example, for $\alpha_{unif} = 1/26.5$, for M_s varying from 10 TeV to 100 TeV, the corresponding RG factors are

$$K_1 \approx 0.47 - 0.49, \quad K_2 \approx 0.99 - 1.08, \quad K_3 \approx 3.7 - 4.6. \tag{3.24}$$

Notice that the RG evolution factor K_3 is quite large for a large M_s. This prevents the gluino becoming the LSP even though the gluino mass M_3 is typically small at the unification scale.

Once the running masses of the gauginos at the low scale are calculated, their pole mass can be obtained by adding weak scale threshold corrections. For general MSSM parameters, they are given in [55]. In our 'match and run' procedure, the threshold corrections of heavy scalars and Higgsinos are automatically included except some finite terms which are usually small and negligible. However, since in our case the Higgsino mass μ is of order $m_{3/2}$, the finite threshold correction cannot be neglected and is given by [55–57]:

$$\begin{aligned} \Delta M_{1,2}^{\text{finite}} &\approx -\frac{\alpha_{1,2}}{4\pi}\frac{\mu \sin(2\beta)}{(1-\frac{\mu^2}{m_A^2})}\ln(\frac{\mu^2}{m_A^2}) \\ &\approx \frac{\alpha_{1,2}}{4\pi}\mu = \frac{\alpha_{1,2}}{4\pi} z_{\text{eff}}\, m_{3/2} \end{aligned} \tag{3.25}$$

In the second line, we have used the fact that $\frac{\mu^2}{m_A^2} \sim 1$ so that the logarithm can be expanded. In addition, since μ does not change much in the RG evolution, it is a good approximation to use its high scale value $\mu \equiv z_{\text{eff}}\, m_{3/2}$. It should be noted that this correction is actually proportional to $\mu(B\mu)^*$ and in general has the same phase as the moduli and anomaly mediated gaugino masses (see Section 4.2.1 for details). Therefore, it leads to a decrease in both bino (M_1) and wino (M_2) masses. Since $\alpha_2 > \alpha_1$, this correction will most significantly affect M_2. Therefore it could potentially affect the identity of the LSP. For the case with gravitino mass $m_{3/2} \sim 30$ TeV, this finite correction to M_2 is roughly 100 GeV, which may even dominate over the tree-level mass. This large correction to $M_{1,2}$ is not surprising since the low energy effective theory is non-supersymmetric and there is no symmetry to protect the gaugino masses from finite radiative corrections. This leads to gaugino

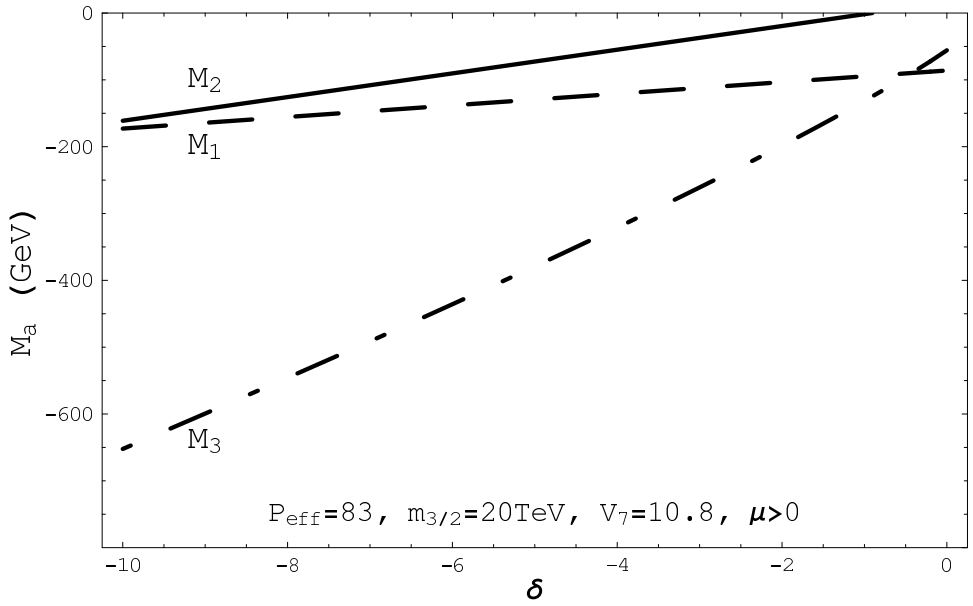

Figure 3.2: Gaugino Masses at low scales (including the correction in Eq. (3.25)) as a function of δ for the case with cosmological constant tuned to zero ($P_{\rm eff} = 83$), $Q - P = 3$, $V_X = 10.8$, $C_2 = 1$ and $\alpha_{unif}^{-1} = 26.5$.

mass at low scale as shown in Figure 3.2.

Of course, one also has to include weak scale threshold corrections from gaugino-gauge-boson loops. These are especially important for the gluino mass:

$$\Delta M_3^{\rm rad} = \frac{3g_3^2}{16\pi^2}\left(3\ln\left(\frac{M_{\rm EW}^2}{M_3^2}\right)+5\right)M_3 \tag{3.26}$$

For M_3 not much heavier than $M_{\rm EW}$, there is a substantial correction of at least $3\alpha_3 M_3$.

We calculated the gaugino mass at the Weak scale, with all these corrections taken into account. As mentioned before, the hierarchy of gaugino masses is most sensitive to δ and $P_{\rm eff}$. In order to obtain realistic phenomenology, we choose $Q - P = 3$ and tune the cosmological constant to obtain $P_{\rm eff} = 83$. Then, the hierarchy of gaugino masses mainly depends on δ - the threshold corrections to the unified gauge coupling.

The dependence of gaugino masses on δ is shown in Figure 3.2. From the figures, we the wino tends to be the LSP ($|M_2| < |M_1|$) in the region with small δ. Also, $|M_3|$ is significantly larger than $|M_1|, |M_2|$ for values of $|\delta| \gtrsim 3$. As will be seen in section 2.4.1, $|\delta| \gtrsim 3$ is favored by precision gauge unification.

3.2.2 Electroweak Symmetry Breaking

Since the scalars in the G_2-MSSM are generically very heavy, there are large logarithmic corrections to the Higgs potential. To analyze EWSB in such a theory, it is better to work in the low energy effective field theory in which all heavy fields are decoupled. Then, the large logarithmic corrections are automatically resummed when the Higgs parameters are RG evolved to the low scale. After decoupling all the heavy fields, the low energy effective theory is simply the standard model plus light gauginos. It is well known that in order to have electroweak symmetry breaking, there must exist a light Higgs doublet below the decoupling scale with negative mass parameter. It was pointed out in [58] that generically it is very hard to get EWSB predominantly from radiative effects below the decoupling scale, more so if the decoupling scale is not too high (as in our case). Therefore, if electroweak symmetry breaking happens in the effective theory at low scale, it should also happen in the MSSM theory at the decoupling scale. This means that we only need to check the existence of EWSB at the decoupling scale in the MSSM framework.

In order to do that, we have to first diagonalize the mass matrix of (h_u, h_d^*):

$$\begin{pmatrix} m_{H_u}^2 + \mu^2 & -b \\ -b & m_{H_d}^2 + \mu^2 \end{pmatrix} \tag{3.27}$$

The eigenvalues are

$$\zeta_{1,2} = \frac{1}{2}\Big[(m_u^2 + m_d^2) \pm \sqrt{(m_u^2 - m_d^2)^2 + 4b^2}\Big], \tag{3.28}$$

where $m_u^2 = m_{H_u}^2 + \mu^2$ and $m_d^2 = m_{H_d}^2 + \mu^2$. The light Higgs doublet h is a superposition of h_u and h_d

$$h = \sin\beta h_u + \cos\beta h_d^* \tag{3.29}$$

where β is determined by the diagonalization of the matrix. In a complete high scale theory, the mass matrix Eq. (3.27) is completely determined by the high scale boundary condition. The existence of EWSB depends on whether there is one negative eigenvalue.

In the G_2-MSSM, the effective μ and $B\mu$ terms in the low-energy lagrangian can arise from the non-zero Higgs bilinear coupling Z, if the μ term in the original superpotential is forbidden by some discrete symmetry[3] as in [48]. In such a case, they are given by [44]:

$$\begin{aligned} \mu &= \Big(m_{3/2}Z - e^{\hat{K}/2}F^{\bar{m}}\partial_{\bar{m}}Z\Big)(\tilde{K}_{H_u}\tilde{K}_{H_d})^{-1/2} \\ B\mu &= \Big\{(2m_{3/2}^2 + V_0)Z - m_{3/2}e^{\hat{K}/2}F^{\bar{m}}\partial_{\bar{m}}Z + m_{3/2}e^{\hat{K}/2}F^m[\partial_m Z - Z\partial_m \ln(\tilde{K}_{H_u}\tilde{K}_{H_d})] \\ &- e^{\hat{K}}F^{\bar{m}}F^n[\partial_{\bar{m}}\partial_n Z - \partial_{\bar{m}}Z\partial_n \ln(\tilde{K}_{H_u}\tilde{K}_{H_d})]\Big\}(\tilde{K}_{H_u}\tilde{K}_{H_d})^{-1/2} \end{aligned} \tag{3.30}$$

[3]This is favored by the motivation of the solution to the doublet-triplet splitting problem

where Z is the Higgs bilinear coefficient and $\tilde{K}$ is the Kähler metric for the Higgs fields. Z is a complex-valued function of all hidden sector chiral fields in general. However, with the reasonable assumption that the visible sector Kähler metric and the Higgs bilinear coefficient Z are independent of the meson field ϕ, one can make simplifications. Combining the above with the fact that $F^i \ll F^\phi$, one has the following approximation:

$$\begin{aligned} \mu &\approx m_{3/2} Z \, (\tilde{K}_{H_u} \tilde{K}_{H_d})^{-1/2} \\ B\mu &\approx (2m_{3/2}^2 + V_0) Z \, (\tilde{K}_{H_u} \tilde{K}_{H_d})^{-1/2} \end{aligned} \tag{3.31}$$

Therefore, we impose the following boundary conditions

$$\mu(M_{\text{unif}}) \approx z_{\text{eff}} m_{3/2}, \quad B\mu(M_{\text{unif}}) \approx 2 z_{\text{eff}} m_{3/2}^2 \tag{3.32}$$

Using the above relation and RG evolving them to the decoupling scale, one can obtain a Higgs mass matrix which is parameterized by z_{eff}. One then finds that for $z_{\text{eff}} < z_{\text{eff}}^* \sim \mathcal{O}(1)$ there will always be a negative eigenvalue and so electroweak symmetry is broken. This condition for the existence of EWSB is naturally satisfied if $z_{\text{eff}} \sim \mathcal{O}(1)$. Since all elements in the mass matrix (3.27) are $\mathcal{O}(m_{3/2})$, the mixing coefficients ($\sin\beta$ and $\cos\beta$) of h_u and h_d^* are of the same order. Thus, $\tan\beta$ is naturally predicted to be of $\mathcal{O}(1)$. This is in contrast to usual approaches to high-scale model-building where μ and $B\mu$ are completely unknown from theory and are only determined after fixing M_Z and choosing $\tan(\beta)$. In the G_2-MSSM, $\tan\beta$ is not a free parameter and is determined by the relation between μ and $B\mu$ predicted from the theory.

Since all the elements in the mass matrix (3.27) are $\mathcal{O}(m_{3/2})$, the Higgs mass eigenvalues should also be $m_{3/2}$ which is around 100 times larger than the EW scale. This implies a fine-tuning if there is no magic cancellation. So, even though the existence of EWSB is generic, getting the correct Z mass is not. As will be discussed below, the requirement of obtaining the correct Z-boson mass fixes the precise value of $z_{\rm eff}$. This requires a fine-tuning of $z_{\rm eff}$.

In the following we describe the precise procedure used for obtaining EWSB with the correct Z mass. The heavy scalars are decoupled at M_s and the couplings of the low energy effective theory (consisting of the SM particles and the MSSM gauginos) are matched with those of the complete MSSM. Most importantly, the matching condition for the quartic coupling of the Higgs is given by:

$$\lambda(m_s) = \frac{\frac{3}{5}g_1^2 + g_2^2}{8}\cos^2 2\beta \tag{3.33}$$

It turns out that at energies below the decoupling scale M_s, the *one-loop* RG evolution of m (the SM Higgs mass parameter), λ and the Yukawa couplings is the same as that of the Standard Model:

$$\begin{aligned}
16\pi^2\frac{d\lambda}{dt} &= 24\lambda^2 - 6y_t^4 + 12\lambda y_t^2 + \frac{27}{200}g_1^4 + \frac{9}{20}g_1^2g_2^2 + \frac{9}{8}g_2^4 - \frac{9}{5}\lambda g_1^2 - 9\lambda g_2^2 \\
16\pi^2\frac{dm^2}{dt} &= m^2(6\lambda + 6y_t^2 - \frac{9}{10}g_1^2 - \frac{9}{2}g_2^2) \\
16\pi^2\frac{dy_t}{dt} &= y_t\Big[(\frac{9}{2}y_t^2 + \frac{3}{2}y_b^2 + y_\tau^2) - (\frac{17}{20}g_1^2 + \frac{9}{4}g_2^2 + 8g_3^2)\Big] \\
16\pi^2\frac{dy_b}{dt} &= y_t\Big[(\frac{3}{2}y_t^2 + \frac{9}{2}y_b^2 + y_\tau^2) - (\frac{1}{4}g_1^2 + \frac{9}{4}g_2^2 + 8g_3^2)\Big] \\
16\pi^2\frac{dy_\tau}{dt} &= y_\tau\Big[(3y_t^2 + 3y_b^2 + \frac{5}{2}y_\tau^2) - (\frac{9}{4}g_1^2 + \frac{9}{4}g_2^2)\Big]
\end{aligned} \tag{3.34}$$

It is important to mention that the above equations are different from the corre-

sponding ones for split-supersymmetry because Higgsinos in the G_2-MSSM are also very heavy (of $\mathcal{O}(m_{3/2})$) unlike that in split-supersymmetry [59]. Therefore, for the G_2-MSSM, the Higgsinos also decouple below M_s forbidding additional terms which appear in the one-loop RG equations for split-supersymmetry. From above, the quartic coupling λ will get a large correction from RG evolution because of the large top Yukawa coupling. The gaugino masses M_a on the other hand will only receive one-loop corrections from gauge boson exchange. The corresponding RGE equations at one-loop are as follows:

$$16\pi^2 \frac{dM_1}{dt} = 0 \tag{3.35}$$

$$16\pi^2 \frac{dM_2}{dt} = -12 b_2^2 M_2 \tag{3.36}$$

$$16\pi^2 \frac{dM_3}{dt} = -18 b_3^2 M_3 \tag{3.37}$$

Given the boundary conditions for soft parameters for realistic M-theory vacua as in section 3.1, one finds that EWSB occurs if z_{eff} is of $\mathcal{O}(1)$. But the generic value of M_Z is around $m_{3/2}$, which can be seen from the fact that all the Higgs parameters are of the order of $m_{3/2}$. In order to get $M_Z = 91$ GeV, one has to tune z_{eff} so that μ and $B\mu$ take values such that the lightest Higgs mass parameter comes out to be around M_{EW}. This fine-tuning is a manifestation of the little hierarchy problem - an unexplained hierarchy between the electroweak (SM-like Higgs) and superpartner (scalar) scales. Our current understanding of the theory does not yet allow us to explain the little hierarchy problem by a dynamical mechanism.

In the low energy effective theory the ratio of the Higgs mass to the Z mass turns

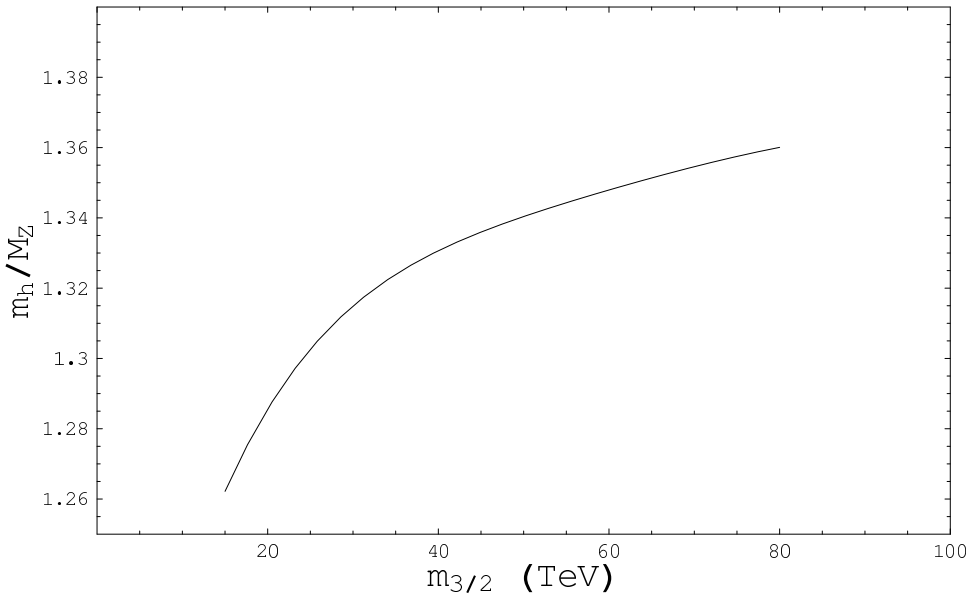

Figure 3.3: Plot of the ratio of the Higgs mass and the Z mass as a function of the gravitino mass.

out to be quite robust[4]. The ratio is given by:

$$\frac{m_h}{m_Z} = \frac{2\sqrt{\lambda}(M_{EW})}{(\frac{3}{5}g_1^2 + g_2^2)(M_{EW})} \tag{3.38}$$

λ is determined by the gauge couplings, Yukawa couplings and $\tan\beta$. One has to use the boundary condition for λ at M_s as in Eq. (3.33) and then RG evolve it to the electroweak scale using the first equation in Eq. (3.34). The gauge couplings at the electroweak scale can also be determined by their RGEs. Thus, one can obtain the ratio m_h/m_Z as a function of $m_{3/2}$ as shown in Figure 3.3. It is worth noting that this ratio only mildly depends on $m_{3/2}$. If M_Z is tuned to its experimental value, we can use λ obtained from the RG equation or from Figure 3.3 to predict the Higgs boson mass for any given value of $m_{3/2}$. Once one finds the Higgs VEV v, the Higgs

[4]even when one does not tune z_{eff} to obtain the correct Z mass as explained in the previous paragraph.

mass is simply $m_h^2 = 2\lambda v^2$ just as in the Standard Model since all heavy scalars and Higgsinos have already been decoupled. The Higgs boson mass thus computed turns out to be of $\mathcal{O}(120)$ GeV for a range of interesting values of $m_{3/2}$ as it only mildly depends on it. Since all susy-breaking large logarithms have already been taken into account in the 'Match and Run' procedure, only some finite term contributions could have been missed in this analysis. One could take those effects into account as well in a more detailed analysis, but that would not change the Higgs mass significantly. The origin of the above value of the Higgs mass can be understood as follows. If one did not decouple the scalars and Higgsinos at M_s, then the Higgs mass receives very large radiative corrections, making the Higgs mass heavy as required. However, because of the hierarchy between the scalars and gauginos, these radiative corrections are hard to compute in a controlled manner. In the spirit of effective field theory therefore, it makes sense to integrate out the scalars and Higgsinos at M_s. In this picture, all the radiative corrections to the Higgs mass can be incorporated in the running of the quartic coupling λ. λ gets renormalized from M_s to M_{EW} giving rise to a heavy Higgs.

3.3 Precision Gauge Coupling Unification

As seen in section 2.4.1, G_2-MSSM vacua naturally incorporate gauge coupling unification from a top-down point of view. We will now examine the issue of precision gauge coupling unification including the low scale threshold corrections. There are two aspects to this issue:

- Is there a unification of gauge couplings at a high scale $\mathcal{O}((1-3)\times 10^{16})$ GeV by continuing the gauge couplings up in energy from the laboratory scale including all the low-scale thresholds?

- Whether the unified gauge coupling and the unification scale obtained are consistent with the theoretical prediction in terms of "microscopic" parameters.

As we will see, it turns out that the G_2-MSSM is compatible with precision gauge coupling unification in the sense that there exists a relatively large set of reasonable microscopic parameters which gives rise to precise gauge coupling unification.

Before going into details, it is important to notice the following general fact – gaugino masses at the unification scale and hence the low scale depend on the value of α_{unif}^{-1}. However, the value of α_{unif}^{-1} itself depends on corrections to the gauge couplings from superpartner thresholds at low scale. This means that there is a feedback between the spectrum of superpartner masses and the value of α_{unif}^{-1}. Therefore, one has to remember to take into account the effects of this feedback in general.

Since the squarks and sleptons come in complete GUT multiplets, they do not affect gauge unification. The Higgs doublets, Higgsinos and gauginos do affect gauge unification since they do not form complete GUT multiplets. Since the Higgsino mass (μ) in these vacua are heavy ($\mathcal{O}(m_{3/2})$) and is robustly determined by the gravitino mass once the EWSB breaking constraint is imposed, for a fixed gravitino mass gauge coupling unification will mostly depend on the light gaugino masses,

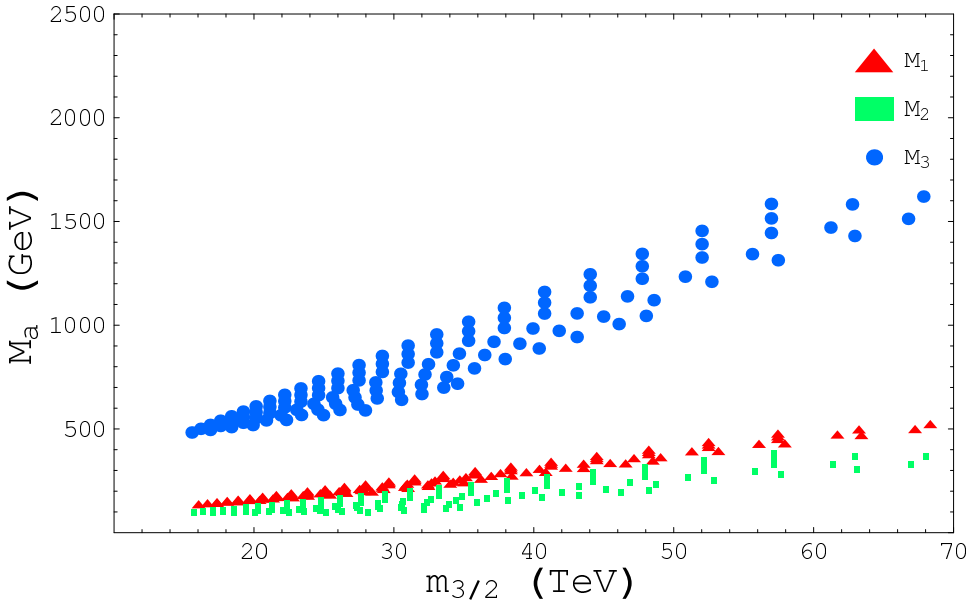

Figure 3.4: Gaugino Mass spectra vs $m_{3/2}$ compatible with gauge unification for $P_{\text{eff}} = 83$, $C_2 = 5$. The red, green and blue lines correspond to gaugino mass M_1, M_2 and M_3 respectively.

the gaugino mass ratio $|M_3|/|M_2|$ in particular because it contributes the most to the threshold corrections to the gauge couplings. We find that in order to have precise unification, this ratio has to be greater than around $3-4$. This sensitivity to $|M_3|/|M_2|$ is much greater here than in split-SUSY where both the Higgsinos and gauginos are light. Finally, if there are particles in the GUT multiplet in addition to the MSSM (the Higgs triplets in the $SU(5)$ case for example) that are lighter than M_{unif}, then one should also take their threshold contributions to the gauge couplings into account. However one finds that their threshold contribution causes α_3^{-1} and α_1^{-1} to move away from each other. Therefore, the requirement of precision gauge unification forces us to assume that such particles (like the triplets) are at least as heavy as the unification scale. It seems possible to arrange that in many models.

Based on the above arguments, we performed a complete scan over the parameter space on which the gaugino masses depend – $\{\delta,\, V_X,\, C_2,\, \alpha_{vis}^{-1}\}$, assuming $Q - P = 3, P_{\text{eff}} = 83$. As negative δ is necessary to obtain the right unification scale, we take a range $-10 \leq \delta \leq 0$. C_2 is taken to be $\mathcal{O}(1)$. $\alpha_{vis}^{-1} \equiv \text{Re}(f^0)$ is taken to be of $\mathcal{O}(25)$. The lower and upper bounds on V_X are given by [5]:

$$\begin{aligned} V_X^{min} &= 1; \text{ weak supergravity constraint (section 2.4.2)} \\ V_X^{max} &= V_{\mathcal{Q}_{vis}}^{7/3} \approx (\alpha_{unif}^{-1} - \delta)^{7/3}; \text{ corresponding to } a \equiv \frac{V_X}{V_{\mathcal{Q}_{vis}}^{7/3}} = 1 \end{aligned} \tag{3.39}$$

In addition, we consider a gravitino mass below 100 TeV so that the spectrum is light enough to be potentially be seen at the LHC, as well as satisfy all our constraints. From the previous discussion, we know that $|M_3|$ is typically a few times larger than $|M_2|$, and it turns out that gauge couplings unify very well around some unification scale. The gaugino mass spectra compatible with precision gauge unification and all bounds on superpartner masses are shown in Figure 3.4. The most stringent bound among superpartner mass bounds is that of the lightest chargino from LEP II. For the bino LSP case, the bound is $M_{\tilde{C}_1} \geq 104$ GeV. However for a wino LSP, which turns out to be relevant for us, the bound depends on the mass splitting $\Delta M \equiv M_{\tilde{\chi}_1^\pm} - M_{\tilde{\chi}_1^0}$; for simplicity we take $M_{\tilde{C}_1} \geq 80$ GeV [60].

The procedural details used are as follows. For a choice of δ, C_2, V_X and α_{unif}^{-1} in the above range as well as for a set of initial values of Yukawa couplings and z_{eff} at $M_{\text{unif}} \sim \mathcal{O}(10^{16})$ GeV, the MSSM spectrum was computed at low scales using the

[5] The upper bound is determined from the fact that in both heterotic and type IIA duals of these vacua, the parameter $a \equiv \frac{V_X}{V_Q^{7/3}}$ is always less than unity [50].

analysis in sections 3.1.3 and 3.2.1. The experimental values of the gauge couplings (both their max. and min. values taking the uncertainty into account) were then RG evolved backwards to the high scale using two-loop RGEs which depend on the superpartner thresholds. The unified gauge coupling and the unification scale were determined by the requirement $\alpha_1(M_{\text{unif}}) = \alpha_2(M_{\text{unif}})$. The Yukawa couplings were evolved to the high scale at the same time. The original parameters were scanned within their respective ranges and only those values for which the initial assumed α_{unif} was equal to the value of the computed α_{unif} up to experimental uncertainties, were recorded. M_Z was checked to be approximately 91 GeV. The condition for gauge coupling unification, i.e. $\alpha_{3,min}(M_{\text{unif}}) < \alpha_{1,2}(M_{\text{unif}}) < \alpha_{3,max}(M_{\text{unif}})$, was checked and only sets of parameters which satisfied the above condition as well as other constraints on superpartner masses, were recorded. In the above condition, $\alpha_{3,min}(M_{\text{unif}})$ and $\alpha_{3,max}(M_{\text{unif}})$ are the lower and upper values of α_3 at the unification scale, determined by RG evolving the low scale experimental value of α_3 taking the uncertainties into account. The low scale gaugino mass spectra consistent with precise gauge coupling unification are plotted in Figure 3.4. One sees from Figure 3.4 that only discrete values of gaugino masses are possible since it is not possible to satisfy precision gauge unification constraints for continuous sets of parameters.

3.4 What is the LSP?

From Figure 3.4, the lightest supersymmetric particle (assuming R-parity conservation) turns out to be predominantly wino-like. The Higgsinos are of $\mathcal{O}(m_{3/2})$ and

are much heavier than the gauginos. Here, as usual we have assumed that $Q - P = 3$ and $P_{\text{eff}} = 83$.

It is worthwhile to compare and contrast the results obtained for the G_2-MSSM for the nature of the LSP with those for the Type IIB vacua corresponding to the "mirage mediation" framework mentioned in the introduction. There one always gets bino LSPs. In mirage mediation, the gaugino mass contribution is dominated by the tree-level and conformal anomaly contribution (the first term in Eq. (4.12)) which are of the same order [53]. The second and third term in Eq. (4.12) are negligible because of the assumption of sequestering. On the other hand, for the G_2-MSSM, the Konishi anomaly contribution coming from the second and third term in Eq. (4.12) is also important as one does not expect sequestering in general. The second important difference is that the μ parameter is very large for the G_2-MSSM (of $\mathcal{O}(10)$ TeV) compared to that for mirage mediation. This implies that the finite contribution to M_1 and M_2 from Eq. (3.25) in the G_2-MSSM is quite important in contrast to that in mirage mediation. Therefore, due to all the above reasons, the nature of the LSP obtained for the G_2-MSSM is different from that for mirage mediation.

3.5 Summary and Benchmark Spectra

To summarize, the G_2-MSSM models have a distinctive spectrum. One finds that, at the compactification scale ($\sim M_{\text{unif}}$), the gauginos are light ($\lesssim 1$ TeV) and are suppressed compared to the trilinears, scalar and Higgsino masses which are roughly equal to the gravitino mass ($\sim 30 - 100$ TeV). At the electroweak scale, the lightest

top squark turns out to be significantly lighter than the other squarks ($\sim 1-10$ TeV) because of RGE running. In addition, there are significant finite threshold corrections to bino and wino masses from the large Higgsino mass. Radiative electroweak symmetry breaking is generic and $\tan\beta$ is naturally predicted from the structure of the high scale theory to be of $\mathcal{O}(1)$[6]. The value of m_Z is fine-tuned, however, implying the existence of the Little-hierarchy problem, which, because of the larger scalar masses is worse than the usual little hierarchy.

For concreteness, we generate four benchmark G_2-MSSM models with $Q - P = 3$, $P_{\text{eff}} = 83$. The "microscopic" input parameters and corresponding low-scale mass spectra are shown in Table 3.5. These models are consistent with the precision gauge coupling unification.

[6]Theoretical predictions of $\tan\beta$ are fairly rare

parameter	BM-1	BM-2	BM-3	BM-4
δ	-4	-6	-8	-10
$m_{3/2}$	67558	35252	34295	17091
V_X	14	21.6	22	35
α_{unif}^{-1}	26.7	26.4	26.5	26.0
$Z_{\rm eff}$	1.58	1.65	1.65	1.77
$\tan\beta$	1.44	1.45	1.45	1.45
μ	87013	45572	44164	22309
$m_{\tilde{g}}$	994.7	732.5	900.4	573.5
$m_{\tilde{\chi}_1^0}$	116.6	110.9	173.1	107.1
$m_{\tilde{\chi}_2^0}$	390.0	228.3	253.5	137.1
$m_{\tilde{\chi}_1^\pm}$	116.7	111.0	173.2	107.3
$m_{\tilde{u}_L}$	67600	35254	34298	17094
$m_{\tilde{u}_R}$	67559	35264	34298	17093
$m_{\tilde{t}_1}$	18848	9010	8700	3850
$m_{\tilde{t}_2}$	49554	25707	24998	12378
$m_{\tilde{b}_1}$	49554	25707	24998	12378
$m_{\tilde{b}_2}$	67497	35220	34265	17076
$m_{\tilde{e}_L}$	67558	35253	34296	17091
$m_{\tilde{e}_R}$	67559	35253	34296	17091
$m_{\tilde{\tau}_1}$	67527	35237	34280	17084
$m_{\tilde{\tau}_2}$	67543	35245	34288	17088
m_h	123.6	120.8	120.3	118.1
m_A	1.3×10^5	7.0×10^4	6.8×10^4	3.4×10^4
A_t	1.8×10^4	7.8×10^3	7.4×10^3	2.9×10^3
A_b	1.6×10^5	8.3×10^4	8.1×10^4	4.0×10^4
A_τ	1.8×10^5	9.5×10^4	9.3×10^4	4.5×10^4

Table 3.1: "Microscopic" parameters and low scale spectra for four benchmark G_2-MSSM models. All masses are in GeV. The top mass is taken to be 174.3 GeV in our calculation. For all the above points, $Q - P = 3$ and $P_{\rm eff} = 83$ are taken as discussed in the text. The gravitino mass depends mainly on the combination $C_2 V_X^{-3/2}$ as in Eq. (3.4). So the spectra are largely determined by two parameters δ and $m_{3/2}$. All the above spectra are consistent with current observations. Scalar masses are lighter for benchmark 4, so flavor changing effects need to be explicitly checked later.

CHAPTER IV

LHC Prospects and CP Violation

Having discussed the supersymmetry breaking and calculated the soft terms as well as the sparticle mass spectra at low energy, it is ready to discuss various aspects of low energy phenomenology of this framework. In this Chapter, we first study the superpartner production and decay at the LHC as well as the prospects for detection. Then, in the rest of chapter, we study the CP violation in the soft supersymmetry breaking section and the prediction for electric dipole moments.

4.1 LHC Prospects of G_2-MSSM

This section is devoted to studying the phenomenological consequences of the G_2-MSSM at the LHC.

The pattern of sparticle spectra at low scales crucially determines the pattern of signatures at a hadronic collider. As discussed in Chapter III, it is clear that the G_2-MSSM spectrum is characterized by heavy, multi-TeV scalars and higgsinos, sub-TeV gauginos, and an SM-like Higgs field[1]. Thus, the arrangement of the sub-TeV

[1]The parameter $\tan\beta$ is of $\mathcal{O}(1)$

fields crucially determines the pattern of observable signatures at the LHC.

In the G_2-MSSM, the LSP is predominantly a neutral Wino. For the models examined, the following hierarchy between the sub-TeV particles was observed:

$$m_{\tilde{g}} > m_{\tilde{\chi}_2^0} > m_{\tilde{\chi}_1^\pm} > m_{\tilde{\chi}_1^0} \tag{4.1}$$

The $\tilde{\chi}_1^0$ is nearly degenerate with the $\tilde{\chi}_1^\pm$ ($m_{\tilde{\chi}_1^\pm} - m_{\tilde{\chi}_1^0} < 200$ MeV). Variation of high-scale input parameters P_{eff}, V_X, and δ simply shift the overall mass scale and relative mass splitting of the fields, but do not modify this hierarchy. This feature significantly constrains the possible decay modes observable at the LHC.

4.1.1 Production Cross Sections

Given the fact that the only light superpartners in the G_2-MSSM framework are gauginos, their productions dominate the superpartner productions. The primary production modes for the G_2-MSSM models are neutralino-chargino associate production ($\tilde{\chi}_1^0\,\tilde{\chi}_1^\pm$), chargino pair production ($\tilde{\chi}_1^+\,\tilde{\chi}_1^-$) and gluino pair production ($\tilde{g}\,\tilde{g}$). Table 4.1 shows the production cross sections for the four G_2-MSSM benchmark models. The cross sections were obtained using PYTHIA [61]. Associated production of $\tilde{g}\tilde{\chi}_1^\pm$ or $\tilde{g}\tilde{\chi}_1^0$, and other modes that proceed through a t- or u-channel squark exchange are heavily suppressed. The $\tilde{\chi}_1^0\tilde{\chi}_1^\pm$ and $\tilde{\chi}_1^+\tilde{\chi}_1^-$ modes can proceed through an s-channel $W^\pm$ or Z boson, respectively, which drives the large cross section despite this suppression. Production of $\tilde{\chi}_1^\pm\tilde{\chi}_2^0$ pairs is suppressed because of the tiny Wino component in $\tilde{\chi}_2^0$. Production of $\tilde{\chi}_i^0\tilde{\chi}_j^0$ pairs is suppressed because the higgsino component of $\tilde{\chi}_i^0$ is negligible.

Channel	BM-1	BM-2	BM-3	BM-4
$pp \to \tilde{g}\,\tilde{g}$	0.25 pb	1.9 pb	0.49 pb	8.6 pb
$pp \to \tilde{\chi}_1^0\,\tilde{\chi}_1^\pm$	6.4 pb	8.1 pb	1.6 pb	8.4 pb
$pp \to \tilde{\chi}_1^+\,\tilde{\chi}_1^-$	2.2 pb	2.7 pb	0.5 pb	2.8 pb

Table 4.1: Cross sections of dominant production modes for four G_2-MSSM benchmark models at the LHC.

4.1.2 Decay of Superpartners

Having discussed the production channels and the associated cross sections, we now turn to the decay of the produced superpartners. The second lightest neutralino $\tilde{\chi}_2^0$ dominantly decays into chargino plus W, i.e. $\tilde{\chi}_2^0 \to \tilde{\chi}_1^\pm W^\mp$ as long as $m_{\tilde{\chi}_2^0} > m_{\tilde{\chi}_1^\pm}$. Otherwise, it decays through an off-shell W. The lightest chargino $\tilde{\chi}_1^\pm$ is almost in degenerate in mass with the LSP. Its decay is different from that of the usual Bino LSP models, and will be discussed in the next section. In the following, we shall only focus on the gluino decay.

Since $m_{\tilde{q}} > m_{\tilde{g}}$, the produced gluinos proceed through a three-body decay into two quarks and either a $\tilde{\chi}_2^0$, $\tilde{\chi}_1^0$, or a $\tilde{\chi}_1^\pm$. The decay channels and the associated branching ratios for the four benchmark models can be found in Table 4.2.

Channel	BM-1	BM-2	BM-3	BM-4
$\widetilde{g} \to \widetilde{\chi}_{1,2}^0 t^\mp t^\pm$	37%	39%	62%	36%
$\widetilde{g} \to \widetilde{\chi}_1^\pm t^\mp b^\pm$	25%	21%	14%	16%
$\widetilde{g} \to \widetilde{\chi}_{1,2}^0 b^\mp b^\pm$	8%	9%	5%	10%
$\widetilde{g} \to \widetilde{\chi}_1^\pm q^\mp q'^\pm$	18%	19%	11%	21%
$\widetilde{g} \to \widetilde{\chi}_{1,2}^0 q^\mp q^\pm$	11%	12%	7%	15%

Table 4.2: Decay channels and branching ratios of gluino for the four G_2-MSSM benchmark models. The branching ratios are calculated using SUSY-HIT [1].

For a three-body decay of gluino, the decay width is proportional to $m_{\tilde{q}}^{-4}$. Therefore, the decay through $\tilde{t}_1$ is favored because it is much lighter than all other squarks. In addition, since $\tilde{t}_1$ is mostly right-handed, it preferably decay to top and Bino-like $\tilde{\chi}_2^0$. This indicates that the dominant decay of gluino is via $\tilde{g}\tilde{g} \to \tilde{t}_1^* \bar{t} \to \tilde{\chi}_2^0 t\bar{t}$. The other possible final states of gluino decay are either suppressed by the larger intermediate squark mass or the small stop mixing angle. In order to have a more realistic analysis, we also have to take into account the phase space factors, which affect the decay widths and so the branching ratios. For the channel $\tilde{\chi}_2^0 t\bar{t}$, the allowed phase space is typically smaller than those of other channels. In cases where the gluino mass is below TeV scale, this effect is significant and leads to additional suppression in the decay width. Therefore, the branching ratio of $\tilde{\chi}_2^0 t\bar{t}$ channel is not so much greater than those of the rest of the channels, as we can see from Table 4.2.

In addition to the dominant three-body decay modes described above, the gluino can also have a two-body decay mode to the gluon (g) and the second neutralino $\tilde{N}_2$. This mode mostly proceeds through a $\tilde{t}_1 \approx \tilde{t}_R$ since it is lightest squark. Thus, for the wino-LSP cases considered, $BR(\tilde{g} \to \tilde{\chi}_2^0 g) > BR(\tilde{g} \to \tilde{\chi}_1^0 g)$ due of the much greater bino content of the $\tilde{\chi}_2^0$. The overall suppression is still high however, and $BR(\tilde{g} \to \tilde{\chi}_2^0 g) \lesssim 0.02$ with the maximum fraction occurring only for models with a very high spectrum.

4.1.3 Signatures at the LHC

As we have seen in Section 4.1.1, the dominant production for G_2-MSSM is the direct production of electro-weakinos $\tilde{\chi}_1^+\tilde{\chi}_1^-$ and $\tilde{\chi}_1^0\tilde{\chi}_1^\pm$. The first channel gives rise to events with two LSPs plus some very soft particles from chargino decay, which have very small missing E_T because it is the vector sum of P_Ts of the visible objects. The second channel can gives rise to additional Ws, but again the missing E_T is small because of the same reason. Therefore, events from both channels are difficult to trigger on since there is no hard jets or a large missing E_T [2].

Now consider the gluino pair production. For reasons mentioned in section 4.1.2, the majority of gluino decay modes include a pair of either top or bottom quarks, or a combination of both. The top quark decays exclusively as: $t \to W + b$, which results in at least two b-jets per decay, and four b-jets for a $\tilde{g}\,\tilde{g}$ event for these modes. Therefore, a typical signature for the G_2-MSSM models is multi-bjets plus missing E_T.

There are also a fair number of leptonic events. The leptonic events have two sources - firstly, the tops decay to Ws which could decay semi-leptonically. Secondly, the $\tilde{\chi}_2^0$ produced from $\tilde{g} \to t\,\bar{t}\,\tilde{\chi}_2^0$ decays predominantly as: $\tilde{\chi}_2^0 \to \tilde{\chi}_1^\pm\,W$, which could again decay semi-leptonically. Therefore, one has an observable fraction of multi-lepton events. An important point to notice is that since all leptons come from W bosons, one expects no flavor correlation in opposite-sign dilepton events. Finally,

[2]There could be leptons from Ws, but it suffer from the huge Standard Model background

since gluino pair production is the dominant mechanism leading to observable lepton events, the single lepton and dilepton charge asymmetry is expected to be very small.

Long-lived Gluino?

In models with light gauginos and super-heavy squarks, such as in split-supersymmetry [62–64], the decay width of the gluino is suppressed by the super-heavy masses of the squarks, leading to a long life-time of the gluino. This leads to a distinctive signature of gluinos being detected directly by detectors at the LHC [62]. In the G_2-MSSM models, the squarks are much less heavier than in split-supersymmetry although still considerably heavier than the gauginos. Therefore, it becomes interesting to find out if the lifetime of the gluino is long enough such that it could be detected directly.

For a gluino which decay via a three-body process, the lifetime is given by

$$\begin{aligned} \tau_{\tilde{g}} &\sim \frac{96\pi}{\alpha_s\,\alpha_1}\frac{m_{\tilde{q}}^4}{M_{\tilde{g}}^5} \\ &\approx 8\times 10^{-16}\ \text{sec}\times\left(\frac{\mathrm{m_{\tilde{q}}}}{20\ \text{TeV}}\right)^4\left(\frac{500\ \text{GeV}}{\mathrm{M_{\tilde{g}}}}\right)^5. \end{aligned} \tag{4.2}$$

where $m_{\tilde{q}}$ is the average mass of squarks. The above result serves as a basic estimation of the gluino lifetime in the G_2-MSSM models. Let us now make some more detailed discussion. Given the fact that the right-handed stop is the lightest squark, which is 3-5 times smaller than first two generation squarks, the lifetime would be at least two orders of magnitude smaller if $m_{\tilde{t}_1}$ is used in Eq. 4.2. However, the decay to the $\tilde{\chi}_2^0 t\bar{t}$ final state generally suffers from the phase space suppression, while the one to the $\tilde{\chi}_1^- t\bar{b}$(or $\tilde{\chi}_1^+ b\bar{t}$) final state is suppressed by the small left- and right-handed stop mixing. An estimate based on this analysis again gives a gluino lifetime $\sim$

10^{-16} sec for typical gluino and squark masses. Therefore, Eq.4.2 does give the correct estimation of gluino lifetime in G_2-MSSM.

Since both gluino and squark masses are proportional to the gravitino mass, we can see from Eq.4.2 that the lifetime of gluino decreases as the gravitino mass increases. In addition, for a heavy gluino($\gtrsim 1$ TeV), the decay to $\tilde{\chi}_2^0 t\bar{t}$ final state will have negligible phase space suppression and so the gluino lifetime will be smaller than the one calculated from Eq.4.2. Therefore, the gluino lives longer in a case with light superpartners. Let us now take $\tau_{\tilde{g}} = 5 \times 10^{-16}$ sec as the standard lifetime of gluino for a light G_2-MSSM mass spectrum. This corresponds to a distance of 0.15 μm before the gluino decay, which is much smaller than the resolution for a displaced vertex, for example $\gtrsim 10\mu m$ in ATLAS detector. Therefore, the gluino does not live long enough such that it can be detected through a displaced vertex. However, the lifetime of a very light gluino could have a large relativistic enhancement with a factor $\gamma \sim 3$ TeV$/m_{\tilde{g}}$. In such a case, there could be a few events with displaced vertex at the LHC with a few 100 fb^{-1} integrated luminosity.

Detecting Wino LSP at the LHC

A characteristic feature of models with a $\widetilde{W}$ LSP is the near degeneracy between $\tilde{\chi}_1^\pm$ and $\tilde{\chi}_1^0$. At tree-level $\Delta M = m_{\tilde{\chi}_1^\pm} - m_{\tilde{\chi}_1^0}$ is zero at leading order. However, inclusion of higher order corrections at tree level as well as loop corrections splits the degeneracy enough so that the $\tilde{\chi}_1^\pm$ decays to either soft hadronic, or leptonic states; the former resulting in the emission of one or more soft $\pi^\pm$ depending on the size of

the mass difference. In general, detection of such decays is difficult because the soft decay products are swamped by excessive backgrounds. Detection possibilities for such decays were considered previously in [65] for AMSB models with positive results. The techniques are general, however, and can be applied to the G_2-MSSM as well. The sensitivity to detection depends on the level of ΔM. This mass difference can be split into three regimes: $\Delta M < m_{\pi^\pm}$, $m_{\pi^\pm} < \Delta M \lesssim 200$ MeV and 200 MeV $\lesssim \Delta M \lesssim$ few GeV, each having unique signatures and requiring different detection strategies.

In the G_2-MSSM, the dominant contribution to the splitting ΔM arises at loop-level. For small chargino and neutralino mixing (true for the G_2-MSSM) and keeping only gauge boson contributions, we can derive the following approximate formula for the one-loop correction to ΔM [66]

$$\begin{aligned}\Delta M &= \frac{g^2}{8\pi^2} M_2 \Big[2c_W^2 B_0(M_2, M_2, M_Z) + 2s_W^2 (M_2, M_2, 0) - 2B_0(M_2, M_2, M_W) \\ &- c_W^2 B_1(M_2, M_2, M_Z) - s_W^2 B_1(M_2, M_2, 0) + B_1(M_2, M_2, M_W) \Big] \end{aligned} \tag{4.3}$$

where B_0 and B_1 are the Passarino-Veltman functions. The mass splitting is independent of the masses of heavy fields which have been integrated out in the effective theory. After numerically evaluating this correction, the mass splitting turns out to be larger than the charged pion mass(139.6 MeV) when $M_2 \gtrsim 70$ GeV[3]. This can be seen from Figure 4.1.

Here the mass gap is large enough to produce either soft pions or leptonic decay

[3]The LEP II lower bound for a wino LSP in degenerate with the lightest chargino at leading order is ~ 88 GeV [60]

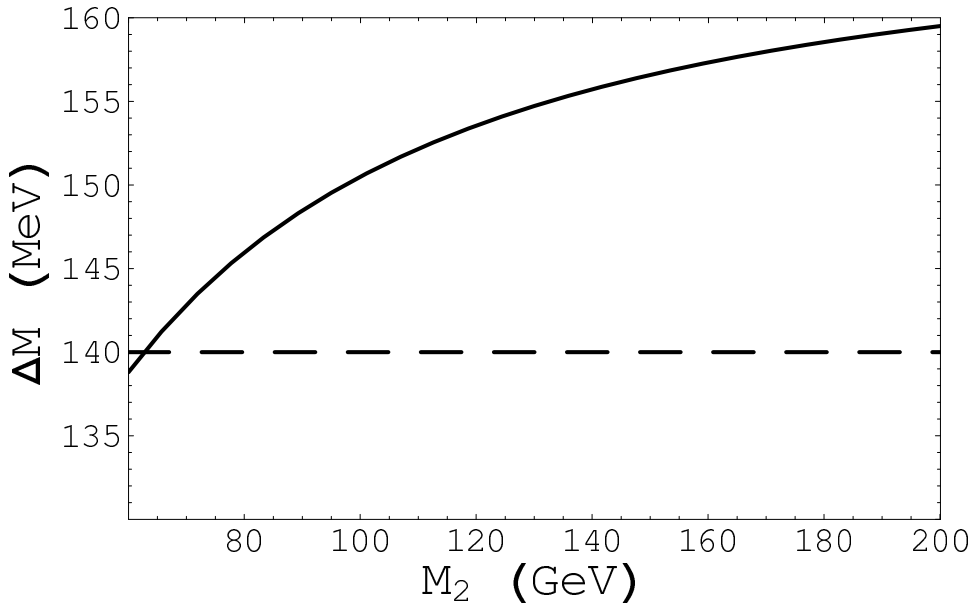

Figure 4.1: The chargino and Wino LSP mass difference as a function of Wino mass M_2 as shown as the solid line. The dash line in the plot corresponds to the charged pion mass 139.6 MeV.

products. It will decay before the muon chambers but still a significant distance inside of the inner tracking system. The dominant signature in this regime is significant missing energy, combined with a charged track that "kinks" when the $\tilde{\chi}_1^{\pm}$ decays to very soft hadrons or leptons. Also possible is a "track-stub"; a clear, charged track that appears to vanish when the soft decay products are not detected. This latter scenario requires dedicated off-line analysis to resolve.

4.2 CP Violation and EDMs

The null measurements of the electric dipole moments (EDMs) of the neutron [67], and recently, heavy atoms like Thallium (^{205}Tl) [68,69] and Mercury (^{199}Hg) [70,71], have put very strong constraints on the amount of CP violation from new physics

beyond the Standard Model (SM). The precision of these measurements is expected to significantly improve in a few years. If an excess above the SM prediction is observed, it requires the presence of new physics beyond the SM. However, since the EDMs, even if observed, are already "small", this strongly suggests that the new physics must be such that it has an underlying mechanism to naturally suppress EDMs.

In general versions of supersymmetric extensions of the Standard Model, new sources of CP violation can arise from complex phases of the soft supersymmetry breaking parameters. These phases are therefore tightly constrained to be small [72, 73](or to have cancellation [74–77]) for TeV scale superpartners. Thus, from a theoretical perspective, the existence of such small phases has to be explained by some underlying mechanism. Many studies of supersymmetric models from a low-energy phenomenological perspective focus on the mediation mechanism and only parameterize the supersymmetry breaking. Explaining small soft CP-violating phases, which requires a dynamical understanding of supersymmetry breaking, is especially challenging as this is not available in such a framework. Without a specification of the supersymmetry breaking mechanism, this problem exists in both gravity and gauge-mediated models of supersymmetry breaking in general.

Put differently, whenever supersymmetry is treated as a general TeV-scale effective theory both the values and phases of the soft-breaking masses are treated as arbitrary, and EDMs are typically much larger than experimental values. Many people have argued that such large EDMs are implied or required from supersymmetry,

and that this is a problem for supersymmetry. Such arguments ignore the fact that any underlying theory will predict and relate phases. This implies that the underlying theory of which low energy supersymmetry is a lower limit has a structure that suppresses or relates the low scale phases.

In this section, we study the CP violating phases in the soft supersymmetry breaking sector in the G_2-MSSM framework. In principle, CP violating phases can be generated when supersymmetry is broken. However, we find that they are naturally small in the G_2-MSSM framework, providing an excellent starting point to explain the non-observation of EDMs. The mechanism is a non-trivial generalization of an old idea [78](and more recently [79]), and may also apply to other string compactification scenarios where moduli are stabilized in a de Sitter vacuum.

Although the CP-violating phases from supersymmetry breaking are small at leading order, there could be additional significant contributions to the CP violation. First, in the M-theory framework, the trilinear matrices are typically not proportional to the Yukawa matrices after moduli are stabilized, which in general leads to non-trivial CP-violating phases in the trilinear A-terms in the physical quark basis and therefore generates non-zero EDMs [73, 80]. That allows upper bounds for EDMs to be calculated in the M-theory framework, contrary to what would happen in other SUSY models. The estimated upper bounds of EDMs are all within the current experimental limits. For some values of parameters, some upper bounds on the EDM can be close to the experimental limit. Second, off-diagonal contributions to Kähler potential may contribute CP-violating effects which could be significant. These will

be studied in detail in the following sections.

4.2.1 Small CP-violating Phases from SUSY breaking Superpotential and Kähler Potential

For the convenience of the discussion, let us start with the effective Kähler potential and superpotential in the G_2-MSSM framework. First, the superpotential can be separated into two parts:

$$W = \hat{W} + Y'_{\alpha\beta\gamma} C^\alpha C^\beta C^\gamma \tag{4.4}$$

where $\hat{W}$ depends only on the moduli $z_i = s_i + it_i$ and the meson ϕ. Here C_α are the matter fields in the minimal supersymmetric standard model (MSSM) with α being higgs, quark or lepton chiral superfields. $Y'_{\alpha\beta\gamma}$ denote the superpotential Yukawa couplings. The effective Yukawa couplings (still not fully normalized) in the MSSM are given by $Y_{\alpha\beta\gamma} = e^{K/2} Y'_{\alpha\beta\gamma}$. The connection to the usual convention in MSSM can be made by taking the first index to be the Higgs fields, the second to be the quark doublets, and the third to be the quark singlets, for example, $Y_{H_u Q_i u_j} \equiv Y^u_{ij}$. In the M-theory framework, an elegant way to generate Yukawa couplings is from membrane instantons which generically take the form [34]

$$Y'_{\alpha\beta\gamma} = c_{\alpha\beta\gamma}\, e^{i\, 2\pi \sum_i l_i^{\alpha\beta\gamma} z^i} \tag{4.5}$$

with $c_{\alpha\beta\gamma} = \mathcal{O}(1)$ and $l_i^{\alpha\beta\gamma}$ being integers determined by the homology class of the three-manifold which the instanton wraps.

The first term $\hat{W}$ is the moduli superpotential, and is generated non-perturbatively

from gaugino condensation [81]

$$\hat{W}/m_p^3 = A_1 \left(\det(\phi^2)\right)^a e^{-b_1 f_{\rm hid}} + A_2 e^{-b_2 f_{\rm hid}} \tag{4.6}$$

Here $b_{1,2}$ are the beta function coefficients of the two hidden sector gauge groups and $f_{\rm hid}$ are the corresponding gauge kinetic functions given by $f_{\rm hid} = \sum_{i=1}^{N} N_i z_i$. In the first term in the superpotential, we have included the meson field $\phi = (\tilde{\mathcal{Q}}\mathcal{Q}^T)^{1/2}$. The parameter a in the superpotential is a constant depending on N_c and N_f, and is not important for our discussion.

The Kähler potential can be written as

$$K = \hat{K} + \tilde{K}_{\alpha\beta} C^{\alpha\dagger} C^{\beta} + \left(Z_{\alpha\beta} C^{\alpha} C^{\beta} + h.c.\right) \tag{4.7}$$

Here $\hat{K}$ is the moduli Kähler potential and $\tilde{K}_{\alpha\beta}$ is the Kähler metric of matter fields C^{α}. $Z_{\alpha\beta}$ is expected to be non-zero only for Higgs field $H_{u,d}$, which is needed to generate μ and B terms. In these compactifications, matter fields with different flavors are localized at different singularities [50]. Therefore, the Kähler metric is expected to be nearly flavor diagonal $\tilde{K}_{\alpha\beta} \approx \tilde{K}_{\alpha}\delta_{\alpha\beta}$. As argued in [46], the Kähler metric for localized matter fields C_α in the 11D frame is canonical, i.e. $C_\alpha^\dagger C_\alpha$ due to the absence of local moduli. Going to the Einstein frame implies that there is an overall dependence on the internal volume V_X, which still preserves the diagonality. Of course, there could be non-perturbative corrections which leads to non-diagonal Kähler metric, for example from instantons wrapping a three-manifold connecting the two singularities. However, these corrections are typically exponentially small.

The Kähler potential for moduli fields contains two pieces

$$\hat{K}/m_p^2 = -3\ln(V_X) + \frac{2}{V_X}\mathrm{Tr}\left(\phi^\dagger\phi\right) \tag{4.8}$$

Here V_X is the volume of the G_2 manifold in units of the eleven-dimensional length scale l_{11}. The second term originates from the Kähler potential for vector-like matter fields $\mathcal{Q}$ and $\tilde{\mathcal{Q}}$ in the hidden sector, which generally takes the form [46]

$$\hat{K} = \frac{1}{V_X}\left(\mathcal{Q}^\dagger\mathcal{Q} + \tilde{\mathcal{Q}}^\dagger\tilde{\mathcal{Q}}\right) \tag{4.9}$$

By using the D-term equations $\mathcal{Q}^\dagger\mathcal{Q} = \tilde{\mathcal{Q}}^T\tilde{\mathcal{Q}}^*$ and the definition of the meson field ϕ, it can be rewritten in terms of ϕ as given in second term in Eq. (4.8). Of course, there could be additional (higher order) corrections, these will be discussed in Section A.13. Now for the simple case $N_f = 1$, we can replace $\det(\phi^2)$ by ϕ^2 and $\mathrm{Tr}(\phi^\dagger\phi)$ by $\overline{\phi}\phi$ in Eq. (4.6) and (4.8) respectively.

After supersymmetry is spontaneously broken by the strong gauge dynamics, soft supersymmetry breaking terms in the visible sector are generated which take the following form

$$\begin{aligned}\mathcal{L}_{soft} &= \frac{1}{2}(M_a\lambda\lambda + h.c.) - m^2_{\bar{\alpha}\beta}\hat{C}^{\bar{\alpha}\dagger}\hat{C}^\beta \\ &- \frac{1}{6}\hat{A}_{\alpha\beta\gamma}\hat{C}^\alpha\hat{C}^\beta\hat{C}^\gamma + \frac{1}{2}\left(B_{\alpha\beta}\hat{C}^\alpha\hat{C}^\beta + h.c.\right)\end{aligned} \tag{4.10}$$

where $\hat{C}^\alpha$ are the canonically normalized chiral matter fields. The trilinear $\hat{A}_{\alpha\beta\gamma}$ can often be factorized as $A_{\alpha\beta\gamma}Y_{\alpha\beta\gamma}$. In the following, we will be careful in distinguishing between trilinears $\hat{A}$ and A.

CP-violating Phases

Now we turn to the CP-violating phases in the soft Lagrangian. In order to study the dependence of the soft parameters on complex phases, it is crucial to understand the structure of the superpotential in the relevant supersymmetry breaking vacuum. In the superpotential W in (4.6), A_1, A_2, z_i and ϕ are complex variables in general. However, (see Appendix B.1) the relative phase between the first and second terms in W is fixed by the minimization of axions in the vacuum [78, 82]. This leaves just one overall phase in the superpotential, $e^{i\gamma_W}$. This argument can be generalized to extend to a large class of superpotentials, as explained in Appendix B.1. Since it is possible to do a global phase transformation of the superpotential without affecting physical observables, this overall phase γ_W is not physical and can be rotated away. From now on, we will take $\gamma_W = 0$. The Kähler potential, K, as seen from (4.8), only depends on real fields s_i which determine V_X and the combination $\bar{\phi}\phi$, so does not contain any explicit phases.

The structure of the F-terms $F^I = \hat{K}^{I\bar{J}} F_{\bar{J}} \equiv \hat{K}^{I\bar{J}}(\partial_{\bar{J}}\overline{W} + (\partial_{\bar{J}}K)\overline{W})$ where I, J run over both z_i and ϕ in general, can be computed as follows. For J corresponding to M-theory geometric moduli z_i, it is easy to see $\partial_{\bar{J}}K$ is real and $F_{\bar{J}} =$ real. For J corresponding to meson moduli ϕ, $(\partial_{\bar{J}}K)\overline{W} =$ real $\times\, e^{i\gamma_\phi}$, where γ_ϕ is the phase of ϕ. Also, since W depends holomorphically on $\{z_i, \phi\}$ as in the first line in (4.6), one again finds $\partial_{\bar{J}}\bar{W} = \overline{W}/\overline{\phi} =$ real $\times\, e^{i\gamma_\phi}$. Therefore, we have $F_{\bar{J}} =$ real $\times\, e^{i\gamma_\phi}$ for J corresponding to meson moduli ϕ. Based on these observations, it is not

difficult to find that F^I = real or F^I = real $\times\, e^{i\gamma_\phi}$ depending on I equals to z_i or ϕ respectively. This leads to interesting implications for the soft supersymmetry breaking parameters.

First, the tree-level gaugino masses are given by:

$$M_a^{\rm tree}(\mu) \;=\; \frac{g_a^2(\mu)}{8\pi}\left(\sum_I e^{\hat{K}/2}F^I\partial_I\, f_a^{vis}\right) \tag{4.11}$$

Since f_a^{vis} only depends on the geometric moduli z_i with integer coefficient, and as we have found, the auxiliary component F^I of z_i are real, there are no phases generated for the tree-level gaugino masses. In the M-theory framework, the tree-level gaugino masses are suppressed relative to the gravitino mass [28]- [46], and the one-loop anomaly mediated contribution has to be included, which is given by [45]

$$\begin{aligned} M_a^{AMSB} \;&=\; -\frac{g_a^2}{16\pi^2}\Big(b_a\, e^{\hat{K}/2}\overline{W} - b'_a\, e^{\hat{K}/2}F^I\hat{K}_I \\ &+\; 2\sum_i C_a^i e^{\hat{K}/2}F^I\partial_I \ln\tilde{K}_i\Big). \end{aligned} \tag{4.12}$$

This contribution includes terms proportional to either $\overline{W}$ or $F^I\partial_I\hat{K}$ or $F^I\partial_I\tilde{K}_i$. Since the Kähler potential is a real function of z_i, $\partial_{z_i}\hat{K}$ and $\partial_{z_i}\tilde{K}$ are real. In addition, the Kähler potential only depends on $\bar{\phi}\phi$, which implies that the derivative with respective to ϕ are proportional to $\bar{\phi} \sim e^{-i\gamma_\phi}$. Therefore, all these terms are real, which gives rise to real anomaly mediated gaugino masses. Hence, the gaugino masses have no observable phase in the above framework.

The trilinear A-terms (with the Yukawa couplings factored out) are given in general by [44]:

$$A_{\alpha\beta\gamma} \;=\; e^{\hat{K}/2}F^I\partial_I\left[\ln\left(e^{\hat{K}}Y'_{\alpha\beta\gamma}/\tilde{K}_\alpha\tilde{K}_\beta\tilde{K}_\gamma\right)\right] \tag{4.13}$$

where I, J run over both z_i and ϕ. It should be noted that in order to be able to factor out the Yukawa matrices the matter Kähler metric has to be diagonal. This is a good approximation in the M-theory framework as we have discussed. Since the moduli Kähler potential $\hat{K}$ and the visible sector Kähler metric $\tilde{K}$ are real function of $z_i + \bar{z}_i$ and $\bar{\phi}\phi$ and superpotential takes the form in Eq. (4.5), it is straightforward to check that the contractions $F^I \partial_I \hat{K}$, $F^I \, \partial_I \tilde{K}$ and $F^I \partial_I \ln \hat{Y}'$ are all real, implying that no CP phases are generated in the trilinear A-terms through supersymmetry breaking. However, it should be mentioned that there could be phases in the full trilinear couplings $\hat{A}$ coming from the Yukawa couplings, as we shall discuss in the next section.

Finally, we move on to the μ and B terms. We focus on the case where the superpotential contribution to the overall high scale μ parameter vanishes. This can be easily guaranteed by a symmetry [34]. In this case, μ and B parameters of $\mathcal{O}(m_{3/2})$ can be generated by the Giudice-Masiero mechanism [83] via the parameter $Z_{\alpha\beta}$ in Eq. (4.8). The general result for μ and B can be written in terms of Z, $F^I \partial_I \hat{K}$, $F^I \, \partial_I \tilde{K}$ and $F^I \, \partial_I Z$ [44], all of which have the same phase γ_Z from $Z_{\alpha\beta}$ (complex in general). Therefore, both μ and B can have a phase e^{γ_Z}. However, this phase is not physical since it can be eliminated by a $U(1)_{PQ}$ rotation [51].

4.2.2 CP-violating Phases from Yukawa

Although the CP-violating phases from supersymmetry breaking are small as found above, there is an additional contribution to CP violation if the trilinear $\hat{A}$

parameters are not aligned with the Yukawas. This can be easily seen as follows. Since the Yukawa matrix generically contains $\mathcal{O}(1)$ phases in order to explain the observed CKM phase, the unitary matrices needed to go to the super-CKM basis (in which the Yukawa matrices are real and diagonal) also contain some phases. Therefore, the rotation by itself can induce CP-violating phases even if the A or $\hat{A}$ matrices are initially completely real as long as $\hat{A}$'s are not proportional to Yukawas in the flavor basis (or equivalently A's are flavor non-universal and non-diagonal). This implies in particular that the diagonal components of trilinear $\hat{A}$ will contain CP phases in the super-CKM basis, giving rise to possibly important contributions for EDMs.

In the M-theory framework, as we can see from Eq. (4.5), the Yukawa couplings generally depend on the geometric moduli z_i which get non-zero F-term vevs. Hence, from (4.13) we find that the second term in the expression for trilinears gives rise to an $\mathcal{O}(1)$ misalignment between the Yukawas and the trilinears. If the Yukawa couplings depend on moduli or other hidden sector fields which do not break supersymmetry, then the trilinears can be naturally aligned with the Yukawas [79]. However, within M-theory, this does not seem to be a generic situation; hence we will consider the conservative case in which the trilinears are misaligned with the Yukawas.

In the remainder of this section, we will estimate the diagonal CP phases in the trilinear $\hat{A}$ in the super-CKM basis since they are directly related to the EDM observables. We consider flavor non-universal and non-diagonal trilinear A-matrices (in the gauge eigenstate basis) at the GUT scale with real $\mathcal{O}(1)$ matrix elements. To

set the convention, we write down the soft trilinear terms explicitly

$$\begin{aligned}\mathcal{L}_{soft} &\sim A^u_{ij}\, Y^u_{ij}\, \bar{Q}_{Li} H_u u_{Rj} + A^d_{ij}\, Y^d_{ij}\, \bar{Q}_{Li} H_d d_{Rj} \\ &+ A^e_{ij}\, Y^e_{ij}\, \bar{L}_{Li} H_d e_{Rj} \end{aligned} \tag{4.14}$$

where $A^{u,d,e}$ are the trilinear matrices in the gauge eigenstate basis of matter fields.

For the M-theory framework, chiral matter fields are localized on singular points inside the compact G_2 manifold [34, 35, 84, 85]. From the phenomenological point of view, the Yukawas in this framework can be described by a hierarchical Yukawa texture (see Eq. (4.5))

$$Y^u_{ij} \sim \epsilon^q_i \epsilon^u_i, \quad Y^d_{ij} \sim \epsilon^q_i \epsilon^d_j, \quad Y^e_{ij} \sim \epsilon^l_i \epsilon^e_j, \tag{4.15}$$

This kind of texture can also be realized by the localization of matter fields in extra dimensional models [86–89] or by a spontaneously broken flavor symmetry (Froggatt-Nielson mechanism) [90]. Then, the fermion mass hierarchy is given by:

$$\begin{aligned} & m^u_i/m^u_j \sim |\epsilon^q_i \epsilon^u_i|/|\epsilon^q_j \epsilon^u_j|, \quad m^d_i/m^d_j \sim |\epsilon^q_i \epsilon^d_i|/|\epsilon^q_j \epsilon^d_j|, \\ & m^e_i/m^e_j \sim |\epsilon^l_i \epsilon^e_i|/|\epsilon^l_j \epsilon^e_j| \end{aligned} \tag{4.16}$$

It is straightforward to check that the observed fermion mass hierarchy can be accommodated by a set of properly chosen ϵ_i with the hierarchy $|\epsilon_1| \lesssim |\epsilon_2| \lesssim |\epsilon_3|$. The above Yukawa couplings can have $\mathcal{O}(1)$ phases in order to explain the CP phase in the CKM matrix. To simplify the discussion, we eliminate the phases in the diagonal elements by redefinition of the quark and lepton fields. Therefore, the diagonal elements $(\hat{A}^\psi)_{11,22,33}$ with $\psi = u, d, e$ are all real at the GUT scale.

First, we point out that the renormalization group (RG) corrections to the trilinear couplings typically mix the phases between different flavors. This will lead to phases in the diagonal elements of the trilinear matrices. It can be understood from the RG equation for Yukawa couplings and trilinear couplings, e.g. for Y^u and $\hat{A}^u$, which are given by

$$\begin{aligned}
\frac{dY^u}{dt} &\sim \frac{1}{16\pi^2} Y^u \left[3\mathrm{Tr}(Y^u Y^{u\dagger}) + 3Y^{u\dagger}Y^u + Y^{d\dagger}Y^d\right] \\
\frac{d\hat{A}^u}{dt} &\sim \frac{1}{16\pi^2} \hat{A}^u \left[3\mathrm{Tr}(Y^u Y^{u\dagger}) + 5Y^{u\dagger}Y^u + Y^{d\dagger}Y^d\right] \\
&+ \frac{Y^u}{16\pi^2}\left[6\mathrm{Tr}(\hat{A}^u Y^{u\dagger}) + 4Y^{u\dagger}\hat{A}^u + 2Y^{d\dagger}\hat{A}^d\right] \qquad (4.17)
\end{aligned}$$

where only terms involving Yukawas are explicitly shown. From the above equations, we notice that the phases in $\hat{A}^u$ evolve during the RG running. To illustrate this, one can examine the following term which contributes to the running of $\hat{A}^u_{11}$:

$$\frac{d\hat{A}^u_{11}}{dt} \sim \frac{5}{16\pi^2}\hat{A}^u_{13}Y^{u\dagger}_{33}Y^u_{31} + \frac{4}{16\pi^2}Y^u_{13}Y^{u\dagger}_{33}\hat{A}^u_{31} \qquad (4.18)$$

From the equation, one can see that the phases of Y^u_{31}, Y^u_{13}, $\hat{A}^u_{13}$ and $\hat{A}^u_{31}$ can enter $\hat{A}^u_{11}$, which is real at the high scale, through the RG evolution. The magnitude of this correction is typically large since the magnitude of the right-hand side of the above equation is proportional to $\frac{1}{16\pi^2}|Y^u_{33}|^2$ given the factorizable Yukawa matrices as in Eq. (4.15). This indicates that the RG correction to $\hat{A}^u_{11}$ is large and involve an $\mathcal{O}(1)$ phase. This is also true for other elements in the trilinear matrices and Yukawa matrices. The only exception is for the third generation Y^u_{33} and $\hat{A}^u_{33}$, for which the largest RG corrections come from the terms involving only Y^u_{33} and $\hat{A}^u_{33}$ with additional flavor mixing terms typically suppressed by $\epsilon_2^2/\epsilon_3^2$. Since $\hat{A}^u_{33}$ has

the same phase as Y^u_{33}, the corresponding A-term $A^u_{33} = \hat{A}^u_{33}/Y^u_{33}$ remains real up to corrections of the order $(\epsilon_2/\epsilon_3)^2$.

Starting from the Yukawa matrices $Y^{u,d,e}_{ij}$ defined in the gauge eigenstate basis, the super-CKM basis can be achieved by unitary rotations of the matter fields so that the Yukawa matrices are real and diagonal. In the super-CKM basis, the trilinear couplings become

$$(\hat{A}^\psi_{\rm SCKM})_{ij} = (V^{\psi\dagger}_L)_{il}\, A^\psi_{lk}\, Y^\psi_{lk}\, (V^\psi_R)_{kj} \tag{4.19}$$

where $\psi = u, d, e$. Given the hierarchical Yukawa matrices in Eq. (4.15), the unitary transformation matrices are given by

$$\begin{aligned} (V^u_L)_{ij} &\sim (V^u_L)_{ji} \sim \epsilon^q_i/\epsilon^q_j, \text{ for } i < j \\ (V^u_R)_{ij} &\sim (V^u_R)_{ji} \sim \epsilon^u_i/\epsilon^u_j, \text{ for } i < j \end{aligned} \tag{4.20}$$

One can now perform the same transformation for the trilinear terms to get the diagonal elements in the super-CKM basis, which can be schematically written as

$$(\hat{A}^u_{\rm SCKM})_{11} \approx \epsilon^q_1\epsilon^u_1 \sum_{i,j=1,2,3} \xi_{ij} A^u_{ij}, \tag{4.21}$$

$$(\hat{A}^u_{\rm SCKM})_{22} \approx \epsilon^q_2\epsilon^u_2 \sum_{i,j=2,3} \eta_{ij} A^u_{ij}, \tag{4.22}$$

$$(\hat{A}^u_{\rm SCKM})_{33} \approx Y^u_{33}A^u_{33} \sim \epsilon^q_3\epsilon^u_3 A^u_{33} \tag{4.23}$$

where ξ_{ij} and η_{ij} are $\mathcal{O}(1)$ coefficients arising from the Yukawa matrices, and are complex in general. In the above equations, we have neglected subleading terms suppressed by the fermion mass hierarchy. Since the off-diagonal components in A_{ij} are $\mathcal{O}(1)$ within our framework, the summations in Eq. (4.21) and (4.22) are expected

to be of $\mathcal{O}(1)$ in magnitude with $\mathcal{O}(1)$ phases. The $(\hat{A})_{33}$ component, however, does not mix with other components and is proportional to Y^u_{33}, so no phase is generated at leading order for $\hat{A}^u_{33}$.

Therefore, we conclude that the first two diagonal components of the complete trilinear coupling in the super-CKM base can contain order one phases, while the third diagonal component is real up to a small correction, i.e.

$$\begin{aligned} \mathrm{Im}(\hat{A}^u_{\mathrm{SCKM}})_{11} &\sim A_0 Y^u_{11}, \\ \mathrm{Im}(\hat{A}^u_{\mathrm{SCKM}})_{22} &\sim A_0 Y^u_{22}, \\ \mathrm{Im}(\hat{A}^u_{\mathrm{SCKM}})_{33} &\sim A_0 \left(\frac{\epsilon_2}{\epsilon_3}\right)^2 Y^u_{33} \end{aligned} \tag{4.24}$$

where A_0 is the characteristic magnitude of the trilinear A-terms. Here we do not distinguish between q, u, d and use ϵ_i for the average value. For later purposes, it is convenient to take $\epsilon_2/\epsilon_3 \sim 0.1$, which provides a right order of magnitude estimate and is also compatible with the quark mass hierarchy. This result has important implications for EDM predictions, which we compute in section 4.2.4.

4.2.3 Electric Dipole Moments and The Experimental Limits

Before starting our calculation of EDMs, we briefly summarize some general results relevant for the calculation of EDMs. In the minimal supersymmetric standard

models, the important CP-odd terms in the Lagrangian are:

$$\begin{aligned}\delta\mathcal{L} = \quad & -\sum_{q=u,d,s} m_q\bar{q}(1+i\theta_q\gamma_5)q + \theta_G\frac{\alpha_s}{8\pi}G\tilde{G} \\ & -\frac{i}{2}\sum_{f=u,d,s}(d_q^E\bar{q}F_{\mu\nu}\sigma_{\mu\nu}\gamma_5 q + \tilde{d}_q^C\bar{q}g_s t^a G^a_{\mu\nu}\sigma_{\mu\nu}\gamma_5 q) \\ & -\frac{1}{6}d_q^G f_{\alpha\beta\gamma}G_{\alpha\mu\rho}G^{\rho}_{\beta\nu}G_{\gamma\lambda\sigma}\epsilon^{\mu\nu\lambda\sigma}, \end{aligned} \tag{4.25}$$

where θ_G is the QCD θ angle, The terms in the second line in (4.25) are dimension five operators, which are generated by CP violation in the supersymmetry breaking sector and evolved down to $\sim$ 1 GeV. The coefficients $d_q^{E,C}$ correspond to quark electric dipole moment and chromo-electric dipole moment(CEDM) respectively. The last line in (4.25) contains the gluonic dimension six Weinberg operator. The CP-odd four-fermion interactions are not important here, and so have not been included above.

Now let us briefly summarize the EDM results for electrons, neutrons and mercury in terms of the coefficients of these operators. The electron EDM in minimal supersymmetric models is given by:

$$d_e^E = d_e^{\chi^+} + d_e^{\chi^0} + d_e^{\mathrm{BZ}}$$

where $d_e^{\chi^\pm}$ and $d_e^{\chi^0}$ are one-loop contributions from the neutralino and chargino while d_e^{BZ} is the two-loop Barr-Zee type contribution [91–99]. It should be noted that what is actually measured is the atomic EDM d_{Tl}, which receives contributions mainly from the electron EDM and the CP-odd electron-nucleon couplings [100]:

$$d_{Tl} \;=\; -585\times d_e^E - 8.5\times 10^{-19} e\,\mathrm{cm}(C_S\,\mathrm{TeV}^2) + \cdots$$

where C_S is the coefficient of the operator $\bar{e}i\gamma_5 e\bar{N}N$. The C_S coefficient could be generated from a new scalar particle coupled to quarks and leptons through a CP-odd higgs like coupling [100]. However, this is independent of CP-odd interactions originating from the soft terms. Given the current experimental limit $|d_{Tl}| < 9 \times 10^{-25} e\,\mathrm{cm}$, we obtain an upper limit on electron EDM

$$|d_e^E| < 2 \times 10^{-27} e\,\mathrm{cm}$$

For the neutron, there exist several different approaches to compute the corresponding EDM. In the following discussion, we shall follow a simple approach, i.e., the naive dimensional analysis (NDA) [101–103]. The neutron EDM can be calculated as:

$$d_n = \frac{4}{3} d_d - \frac{1}{3} d_u. \tag{4.26}$$

In this expression, the quark EDMs can be estimated via NDA as:

$$d_q = \eta^E d_q^E + \eta^C \frac{e}{4\pi} d_q^C + \eta^G \frac{e\Lambda}{4\pi} d^G$$

with $d_q^{E,C} = d_q^{\tilde{g}(E,C)} + d_q^{\tilde{\chi}^+(E,C)} + d_q^{\tilde{\chi}^0(E,C)}$. The QCD correction factors are given by $\eta^E = 1.53$, $\eta^C \sim \eta^G \sim 3.4$ [75], and $\Lambda \sim 1.19$ GeV is the chiral symmetry breaking scale. The current experimental limit on neutron EDM is given by

$$|d_n| < 3 \times 10^{-26} e\,\mathrm{cm}$$

The current theoretical estimate for the mercury EDM induced by dimension 5 operators is given by [104]:

$$d_{H_g} = -7.0 \times 10^{-3}\, e\, (d_d^C - d_u^C - 0.012 d_s^C) + 10^{-2} \times d_e$$

where we have included the contribution from the strange quark CEDM [105]. The recent experimental result on Mercury EDM [71] significantly tightens the bound

$$|d_{Hg}| < 3.1 \times 10^{-29}\, e\,\mathrm{cm}$$

The QCD θ-term in (4.25) also contributes to EDMs of the neutron, deuteron and the mercury atom [106]:

$$\begin{aligned} d_n &\sim 3 \times 10^{-16}\theta \quad e\,\mathrm{cm} \\ d_D &\sim -1 \times 10^{-16}\theta \quad e\,\mathrm{cm} \\ |d_{Hg}| &\sim \mathcal{O}(10^{-18} - 10^{-19})\,\theta \quad e\,\mathrm{cm} \end{aligned}$$

These formulae together with suppressed leptonic EDMs provide a correlation pattern for the θ-induced electric dipole moments. The current upper bound on the neutron EDM implies $\theta < \mathcal{O}(10^{-10})$, which leads to the strong CP problem. Once EDMs are observed for n, Hg and Tl it will be essential to separate the strong and weak contributions, by combining data on different nuclei and d_e^E.

4.2.4 Predictions for EDMs

For an explicit computation of the EDMs, it is important to specify the general structure of supersymmetry breaking parameters, in particular the structure of the trilinear parameters (especially the imaginary part of the diagonal components), as well as that of the scalar and gaugino masses, since all of these appear in the final expression for the EDMs. This is the subject of this section.

Within the M-theory framework, the general structure of supersymmetry break-

ing parameters is as follows. For the choice of microscopic parameters with a vanishingly small positive cosmological constant, the gravitino mass naturally turns out to be in the range 10-100 TeV [29]. The gravitino mass is essentially $\sim F_\phi/m_p$. However, as mentioned earlier, the F-terms of the moduli are suppressed compared to F_ϕ. Since the gauge kinetic function for the visible sector depends only on the moduli, from (4.11) it is easy to check that the gaugino masses are suppressed relative to that of the gravitino. However, this suppression does not hold for the scalar masses, trilinears, μ and $B\mu$ parameters unless the visible sector is sequestered from the supersymmetry breaking sector. Since sequestering is not generic in M-theory, the scalar masses, trilinears, μ and $B\mu$ parameters typically turn out to be of $\mathcal{O}(m_{3/2}) \sim \mathcal{O}(10)$ TeV. The third generation squarks, however, could be significantly lighter because of the RG effects.

As we have discussed in Section 4.2.1, within the M-theory framework it is natural to expect that the Kähler metric for visible matter fields is approximately diagonal in the flavor indices. Then, the scalar mass matrix turns out to be roughly diagonal with suppressed off-diagonal contributions. The estimates for the EDMs then depend on the overall scale of the squark masses. So, for concreteness we consider gauginos with masses $\lesssim 600$ GeV, non-universal but flavor-diagonal scalar mass matrices with masses ~ 20 TeV, and $\mu, B\mu$ and trilinear parameters of the same order as scalar masses. Some contributions to EDMs depend primarily on third generation sfermion masses, so we also mention the situation when third generation scalars are much lighter, i.e. $\mathcal{O}(1)$ TeV.

We now estimate the contribution to the EDMs of the electron, neutron and mercury from dimension 5 and 6 operators (Eq. (4.25)) in the M-theory framework. As we have seen in the Section III, the CP-violating phases appear only in the trilinear $\hat{A}$ parameters. After renormalization group evolution and the super-CKM rotation of the trilinear matrices, these phases appear in the off-diagonal elements in the squark mass matrices, leading to imaginary parts of mass-insertion parameters as follows:

$$(\delta_q^{ii})_{LR} = \frac{v_q((\hat{A}^q_{SCKM})_{ii} - \mu^* Y^q_{ii} R_q)}{(m^2_{\tilde{q}})_{ii}} \tag{4.27}$$

where $R_{u(d)} = \cot\beta\ (\tan\beta)$ and $v_{u(d)} = v\sin\beta\ (v\cos\beta)$. As explained above, $\hat{A}_{SCKM}$ is in general a 3×3 matrix in the Super-CKM basis and its diagonal components contain CP-violating phases. Thus, these insertion parameters contribute to EDMs through the dimension 5 and 6 operators in (4.25).

Leading Contributions

The dimension five electric and chromo-electric couplings can be generated at leading order [72, 74, 75] at one-loop through the vertices $f\tilde{f}\tilde{\chi}^0_i$, $f\tilde{f}'\tilde{\chi}^\pm_i$ and $q\tilde{q}\tilde{g}$ as can be seen in Fig. 4.2.

In general, the squark mass matrix may not be aligned with the quark mass matrix, which could lead to dangerous flavor changing neutral currents. Nevertheless, in the case with super-heavy scalars ($\gtrsim 10$ TeV), the flavor constraints could be satisfied even with large flavor non-universality. In the following, let us first consider the simple situation where the flavor mixing in the squark mass eigenstates is negligible.

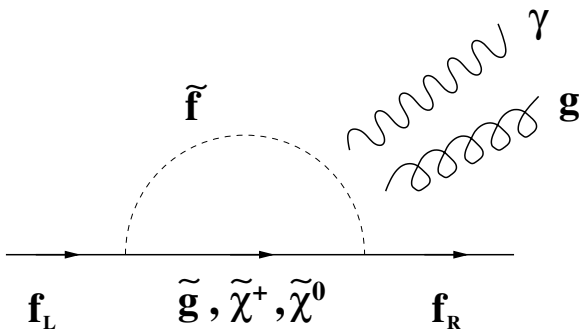

Figure 4.2: One-loop diagrams contributing to the dimension 5 operators

This allows us to treat the mass matrix of each flavor separately. We will return to the case of large flavor mixing at the end.

First consider the quark CEDM which contributes to both the mercury and neutron EDMs. Since there exists a hierarchy between gauginos and squarks in the M-theory framework [28, 29], one can expand using the small ratio $r \equiv m_i^2/m_{\tilde{q}}^2$, where m_i is the corresponding neutralino, chargino or gluino masses in the diagram. One then obtains the following result

$$d_q^C \sim \frac{g_s \alpha}{4\pi} \frac{m_q}{m_i^3} \mathrm{Im}(A_q^{\mathrm{SCKM}}) r^2 G(r) \tag{4.28}$$

where A_q is the diagonal element of the corresponding trilinear matrix (without Yukawa coupling) in the super-CKM bases. In the expression, the function $G(r) = C(r) + rC'(r)$ for gluinos and $G(r) = B(r) + rB'(r)$ for charginos and neutralinos. The function $B(r)$ and $C(r)$ are loop functions defined in the Appendix 4.2.1. One can see that d_q^C decreases rapidly as $m_{\tilde{q}}^{-4}$ when the squark masses increase. However, the function $G(r)$ behaves differently for different particles $(\tilde{g}, \tilde{\chi}^{\pm}, \tilde{\chi}^0)$ in the loop. Due the gaugino and squark mass hierachy, r is small. From Fig. 4.3, we can see that $C(r) + rC'(r)$ is enhanced in the small r region compared to other functions which

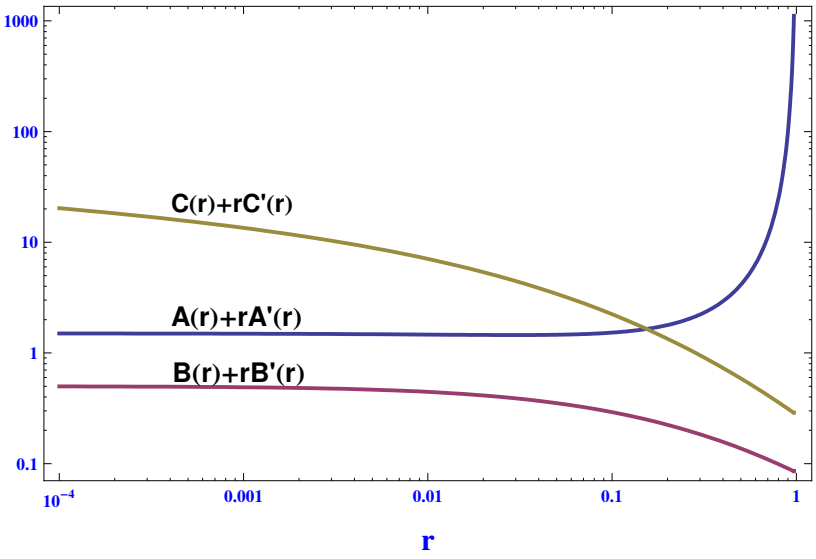

Figure 4.3: Comparison of the one-loop functions $A(r)$, $B(r)$ and $C(r)$. The x coordinate is the ratio $r \equiv m_i^2/m_{\tilde{q}}^2$.

remain small. Therefore, the gluino contribution dominates the quark CEDM. For the quark EDM, it is given by a similar expression as (4.28) but now the quantity $G(r)$ is determined only by $A(r)$ and $B(r)$. In particular, $G(r)$ is determined solely by $B(r)$ for $\tilde{g}$ and $\tilde{\chi}^0$ in the loop, and by a combination of $A(r)$ and $B(r)$ for $\tilde{\chi}^\pm$ in the loop. Since $B(r)$ and $A(r)$ are much smaller than $C(r)$ as seen from Figure 4.2, the quark EDM contributions to the neutron EDM are negligible compared to that of the quark CEDM contributions. Therefore, we only need to calculate the quark CEDM, for which the gluino diagram gives the dominant contribution as explained above. Since $A_q \sim m_{\tilde{q}}$ in the M-theory framework, one obtains:

$$d_q^C \sim 10^{-28} \cdot \left(\frac{m_q}{1\text{MeV}}\right)\left(\frac{m_{\tilde{g}}}{600\text{GeV}}\right)\left(\frac{20\text{TeV}}{m_{\tilde{u}}}\right)^3 e\,\text{cm} \tag{4.29}$$

Based on the quark EDM and CEDM, the neutron EDM can be computed from

(4.26):

$$d_n^{NDA} \sim 3 \times 10^{-28} \cdot \left(\frac{m_{\tilde{g}}}{600\text{GeV}}\right) \left(\frac{20\text{TeV}}{m_{\tilde{u}}}\right)^3 e\,\text{cm} \tag{4.30}$$

Similarly, the mercury EDM is

$$|d_{H_g}| \sim 10^{-30} \cdot \left(\frac{m_{\tilde{g}}}{600\text{GeV}}\right) \left(\frac{20\text{TeV}}{m_{\tilde{u}}}\right)^3 e\,\text{cm} \tag{4.31}$$

Moving on to the electron EDM, it can be computed at leading order from the one-loop neutralino and chargino diagrams. However, as shown in section 4.2.1, there are no CP-violating phases in the gaugino sector. This implies that the chargino diagram does not contribute as seen from Eq. (B.13). The neutralino contribution, on the other hand, gives rise to a non-zero contribution because of a dependence on the selectron mixing parameters (which contains CP-violating phases) in its couplings. Given the fact that the higgsino coupling to electron and selectron is suppressed by the small Yukawa coupling, and the wino does not couple the RH fermion and sfermion, the dominant contribution is from the diagram with $\tilde{\chi}_2^0$(almost pure bino in the M-theory framework), which can be calculated using Eq. (B.17) in the Appendix. Thus, the electron EDM is given by:

$$d_e^E \sim \left(\frac{m_{\tilde{\chi}_2^0}}{200\text{GeV}}\right) \left(\frac{20\text{TeV}}{m_{\tilde{e}}}\right)^3 \times 10^{-31}\, e\,\text{cm} \tag{4.32}$$

Two-loop Contributions

So far, we have considered the one-loop contribution to quark and electron EDMs (and/or CEDMs). In addition, there are two-loop Barr-Zee type contributions [91–99] such as the one in Fig. 4.4. In general, the Barr-Zee type diagrams can involve

either squarks or charginos in the inner loop, and higgs bosons (neutral or charged) and gauge bosons in the outer loop [4]. Since only the trilinear couplings contain CP-violating phases in our framework, we consider those diagrams with third generation squarks running in the inner loop as seen in Figure 4.4. When the mass splitting between the two third generation squarks is not particularly large, the diagram to the quark CEDM can be estimated as (see Appendix B.3):

$$\begin{aligned} d_f^{C\,\mathrm{BZ}} &\approx \frac{g_s \alpha_s}{64\pi^3} \frac{m_f R_f \mu}{M_A^4} \sum_{q=\tilde{t},\tilde{b}} y_q^2 \,\mathrm{Im}(A_q^{\mathrm{SCKM}}) F'(r_q) \\ &\sim 10^{-32} \cdot R_f \left(\frac{m_f}{1\mathrm{MeV}}\right) \left(\frac{20\mathrm{TeV}}{m_{\tilde{u}}}\right)^2 e\,\mathrm{cm} \end{aligned} \tag{4.33}$$

where $R_f = \cot\beta(\tan\beta)$ for $I_3 = 1/2(-1/2)$, $r_q \equiv m_{\tilde{q}}^2/M_A^2$ with $m_{\tilde{q}}$ third generation squark mass and M_A the pseudoscalar mass of A_0. For simplicity, in the above estimation, we take $\mu \sim M_A \sim m_{\tilde{t},\tilde{b}} \sim m_{\tilde{u}}$. It can be seen that the result of the Barr-Zee diagram to quark CEDM (similar for EDM) is negligibly small. One of the reasons is that CP violation in the third generation is suppressed by about two orders of magnitude as in (4.24). Similarly, for the electron EDM the result is:

$$d_e^{E\,\mathrm{BZ}} \sim 10^{-33} \cdot \left(\frac{20\mathrm{TeV}}{m_{\tilde{u}_3}}\right)^2 \tan\beta \;\; e\,\mathrm{cm} \tag{4.34}$$

which is again quite suppressed. This contribution may be enhanced for large $\tan\beta$ as seen from above. The M-theory framework, however, predicts $\tan\beta = \mathcal{O}(1)$ [46].

The neutron EDM could also get a contribution from the dimension six pure gluonic operator (Weinberg operator), which can be generated from the two loop

[4]The two-loop diagram considered in split supersymmetry are not relevant here, since there the CP violation is not from trilinear couplings, but instead from the chargino sector.

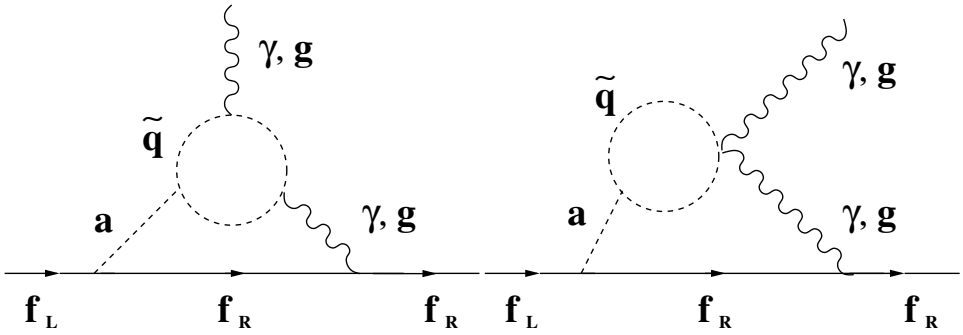

Figure 4.4: Two-loop Barr-Zee type diagrams contributing to the dimension 5 operators.

gluino-top-stop and gluino-bottom-sbottom diagrams. For the case where CP violation only comes from the soft trilinear couplings, the result can be estimated by [107]

$$d^G \approx -3\alpha_s \left(\frac{g_s}{4\pi}\right)^3 \frac{1}{m_{\tilde{g}}^3} \sum_{q=t,b} \mathrm{Im}(A_q^{\mathrm{SCKM}}) z_q H(z_1, z_2, z_q) \tag{4.35}$$

where $z_i = m_{\tilde{q}_i}^2/m_{\tilde{g}}^2$ for $i = 1, 2$, and $z_q = m_q^2/m_{\tilde{g}}^2$ for $q = t, b$. The two-loop function $H(z_1, z_2, z_t)$ is given in [107]. This gives a contribution to the neutron EDM $d_n^G \sim 10^{-30}\, e\,\mathrm{cm}$ for $m_{\tilde{t},\tilde{b}} \approx 20$ TeV, $m_{\tilde{g}} = 600$ GeV and $A_q = 20$ TeV. Thus the neutron EDM from the Weinberg operator is smaller than the one-loop CEDM contribution. However, when the masses of the third generation squarks and trilinears are around 1 TeV, the contribution to the neutron EDM can be significantly larger, and be comparable to the one-loop result.

In general, imaginary parts of the off-diagonal components of squark mass matrix, e.g. non-zero $\mathrm{Im}(m_{\tilde{q}\,23}^2)_{LR}$ could also generate quark and electron EDMs. However, these contributions require more than a single insertion, therefore they are usually not as large as the one-loop contribution we have discussed.

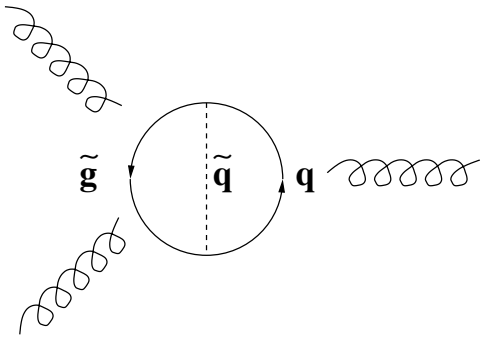

Figure 4.5: Feynman diagram contributing to the Weinberg operator

To summarize our results, we have calculated the EDMs arising from the CP-violating phases in the trilinear terms in a general framework with light gauginos and heavy scalars, and the results are within current experimental bounds. We find that the one-loop diagram is typically the dominant contribution to EDMs. However, in contrast to the situation in which gauginos and scalars have masses of the same order, the one-loop diagram with gluinos gives the largest contribution to the quark CEDM due to the enhanced loop factor at small r. This leads to a larger ratio between neutron EDM and electron EDM of $\mathcal{O}(10^3)$. In typical supersymmetric models with gauginos and scalars of the same order, this ratio is $\lesssim 10^2$ [106]. Finally, it is easy to see that the mercury EDM provides the most stringent limit on the squark masses. For squark masses around 10 TeV, the mercury EDM will increase to $\sim 10^{-29}\, e\,\mathrm{cm}$, which could be tested in the near future with better experimental precision. Basically, we have found that the CP-violating phases in the trilinear couplings, which arise from the Yukawa couplings when supersymmetry is broken, and the suppression from M-theory giving heavy scalar masses are combined to give upper bounds on the EDMs in the M-theory framework.

4.2.5 Higher-Order Corrections and Generalizations

In Section 4.2.1, we found that there are no CP-violating phases from supersymmetry breaking at leading order in the framework of M-theory compactifications considered. It is therefore important to check if corrections to the Kähler potential and superpotential lead to further contributions to CP-violating phases in the soft parameters and in turn to the EDMs. Although the detailed form of possible corrections is not known in M-theory, some general arguments can neverthless be made, which strongly suggest that higher order corrections still naturally suppress CP-violating phases.

The corrections to the soft parameters may arise in general from corrections in the superpotential and the Kähler potential. In the zero flux sector, which we have considered, the superpotential may receive additional non-perturbative corrections from strong gauge dynamics or from membrane instantons. These corrections can be naturally suppressed compared to the existing terms if the arguments in the corresponding exponentials are just $\mathcal{O}(1)$ larger than that in the existing terms. Even if they are comparable, the mechanism of dynamically alignment of the phases can still be applied and leads to no additional phases. More importantly, large corrections could arise in the Kähler potential for the hidden sector comprising the moduli and hidden matter fields, such as terms with higher powers of ϕ. However, the field ϕ is composed of elementary quark fields $\mathcal{Q}, \tilde{\mathcal{Q}}$ which are charged under the hidden gauge group. Therefore, higher order corrections must be functions of $\mathcal{Q}^\dagger \mathcal{Q}$

or $\tilde{\mathcal{Q}}^\dagger\tilde{\mathcal{Q}}$ in order to be gauge invariant. When written in terms of ϕ, these corrections are always functions of $\phi^\dagger\phi$. This structure is important for our claim of small CP-violating phases since it does not introduce any new phases in the soft parameters. In addition, the crucial fact that the Kähler potential is a real function of $z_i + \bar{z}_i$ is also expected to be true under the perturbative corrections. The dependence on $z_i + \bar{z}_i$ is a reflection of the shift symmetry of the axion $t_i \to t_i + \delta$, which is only broken by non-perturbative effects. Thus, although it is very hard in general to compute the form of corrections in M-theory, the above result should be quite robust as it only relies on symmetries.

One could try to generalize the results obtained within the M-theory framework so that they could be applied to other string compactifications as well. Consider an $\mathcal{N} = 1$ string compactification to four dimensions which can be described by $\mathcal{N} = 1$ supergravity at energies lower than the compactification scale. The nature of the hidden sector dynamics is such that there are gauge-singlet scalar fields X_i and moduli fields T_j, both of which break supersymmetry in general. These additional scalar fields X_i could arise from matter fields for example. The following conditions, if satisfied, would lead to no CP-violating phases in the soft supersymmetry breaking parameters:

- The moduli superpotential is a polynomial in X_i and exponential in T_j of the form:

$$\hat{W} = \hat{W}_0 + \sum_{n=1}^{N_W} \hat{W}_n, \quad \hat{W}_n = d_n(X_i)\exp(b_n^j T_j), \tag{4.36}$$

where $\hat{W}_0$ is a constant and d_n are polynomial function of X_i, and b_n^j are real.

- The Kähler potential is a real function of $T_j + \overline{T}_j$ and $\bar{X}_i X_i$

$$K = K(T_i + \bar{T}_i, \bar{X}_i X_i) \tag{4.37}$$

- The gauge kinetic functions are given by $f_a = k_a^j T_j$ with real constants k_a^j.

- The holomorphic (unnormalized) Yukawa couplings have the following structure:

$$Y'_{\alpha\beta\gamma} = y(X_i)\, e^{\sum_j c_j^{\alpha\beta\gamma} T_j}\, h_{\alpha\beta\gamma} \tag{4.38}$$

where $y(x_i)$ is a polynomial function of X_i and $c^{\alpha\beta\gamma}$ are real. These parameters could also vanish in specific cases. In addition, the Kähler potential and superpotential can also depend the other scalar fields which do not break supersymmetry, which we do not included explicitly here.

The dynamical alignment of the phases among different terms in the superpotential is expected to hold as explained in Section 4.2.1 and Appendix B.1. Thus, the structure of W guarantees that F^{T_i}'s remain real. The requirement that the kähler potential be a function of $\bar{X}_i X_i$ and that the superpotential and holomorphic (unnormalized) Yukawas be a polynomial function of X_i makes sure that the contractions $F^{X_i}\partial_{X_i} K$ and $F^{X_i}\partial_{X_i} Y$ to be real. Therefore, both gaugino masses and trilinear couplings are real up to an overall phase which can be rotated away. The phases of μ and B can also be rotated away if they are generated from the Giudice-Masiero mechanism. The conditions listed above can be seen as a non-trivial generalization of the ones

discussed in [78,79]. They can be naturally satisfied in a general moduli stabilization framework in which additional matter fields provide a dynamical F-term uplifting mechanism for the vacuum energy.

4.2.6 Summary

In this section, we have discussed CP violation in theories arising from fluxless M-theory compactifications with low energy supersymmetry and all moduli stabilized. We have found that CP-violating phases only arise from the Yukawas of the quark and lepton not from soft supersymmetry breaking, at the leading order. However, trilinear couplings can pick up CP-violating phases from the Yukawa couplings when the trilinear matrices are not proportional to the Yukawa matrices. Given a model of Yukawas, one can estimate the effects of these phases of Yukawas on the trilinear couplings, and therefore on the EDMs.

We have estimated the contribution of CP phases in the trilinear couplings to the electron, neutron and mercury electric dipole moments, and found that the estimated upper bounds of the EDMs are all within the current experimental limits. The estimated upper bound for mercury EDM is near the current experimental limit and could be probed in the near future. On the other hand, we found a large splitting between the neutron EDM and the electron EDM resulting from the mass hierarchy between gauginos and scalars as predicted by the M-theory framework. This provides an additional means to test the framework. It should be emphasized that our results of EDMs are based on the fact that the CP-violating phases are entirely from the

Yukawas, and therefore, any experimental result which indicates other source of phases would contradict with and rule out this approach.

We also discuss effects of possible corrections to the Kähler potential and superpotential, and the generalization to other string compactifications. Note that our results are largely independent of a full solution to flavor problems. It has been effectively assumed that a solution of the flavor problems exists, but the precise mechanism has been left unspecified.

The quark Yukawas give the CKM phases, and the lepton Yukawas the PNMS phases. The latter can provide the phases needed for baryogenesis via leptogenesis consistent with the above framework, as described in [108]. So even with no phases from the soft supersymmetry breaking this framework can give a complete description of all known CP violation.

CHAPTER V

Solving Moduli/Gravitino Problem and Non-thermal Dark Matter

5.1 Introduction

The existence of Dark Matter seems to require physics beyond the Standard Model. If this physics arises from a string/M-theory vacuum, one is faced with various problems associated with the moduli fields, which are gauge-singlet scalar fields that arise when compactifying string/M-theory to four dimensions. In particular, moduli fields can give rise to disastrous cosmological effects.

For example, the moduli have to be stabilized, or made massive, in accord with cosmological observations. Even if these moduli are made massive, there could be a large amount of energy stored in them leading to the formation of scalar condensates. In most cases, this condensate will scale like ordinary matter and will quickly come to dominate the energy density. The moduli are unstable to decays to photons, and when this occurs, the resulting entropy can often spoil the successes of big-bang nucleosynthesis (BBN). This is the cosmological moduli problem [109–113]. In supersymmetric extensions of the standard model, the overproduction of gravitinos

can cause similar problems and have been a source of much investigation [114–118, 118–120, 120–125].

In addition, the "standard" picture in which Dark Matter (DM) particles are produced during a phase of thermal equilibrium can be significantly altered in the presence of moduli. The moduli, which scale like non-relativistic matter, typically dominate the energy density of the Universe making it matter dominated. Therefore, the dominant mechanism for production of DM particles is non-thermal production via the direct decay of moduli[1]. However, this can lead to further problems since it is easy to produce too much dark matter compared with what we observe today.

In the G_2-MSSM framework, all moduli are stabilized by dynamically generated non-perturbative superpotential. It is also attractive in the sense that they provide a mechanism for supersymmetry breaking at low scales ($\sim$ TeV), thus accommodating the hierarchy between the Electroweak and Planck scales (see [11, 129, 130] for reviews). Since one can concretely study the couplings between moduli and matter fields, we have an opportunity to address many issues in particle physics and cosmology from an underlying microscopic viewpoint.

In this Chapter we focus on the Dark Matter and moduli/gravitino problems. We will show that the moduli, gravitino and dark matter problems are all naturally solved within this framework. Because of the presence of moduli, the Universe is matter-dominated from the end of inflation to the beginning of BBN. The LSPs

[1]For other phenomenologically based approaches to non-thermal dark matter and the related issue of baryon asymmetry in the presence of scalar decay see [126–128].

are mostly produced non-thermally via moduli decays. The final result for the relic density only depends on the masses and couplings of the lightest of the moduli (which decay last) and the mass of the LSP. This is related to the fact that the LSP is a Wino in the G_2-MSSM and that there is a fairly model independent critical LSP density at freeze out. For natural/reasonable choices of microscopic parameters defining the G_2 framework, one finds that it is possible to obtain a relic density of the right order of magnitude (up to factors of $\mathcal{O}(1)$). With a more sophisticated understanding of the microscopic theory, one might obtain a more precise result. The qualitative features which are crucial in solving the above problems may also be present in other realistic string/M-theory frameworks.

Moduli which decay into Wino LSPs have been considered previously in the context of Anomaly Mediated Supersymmetry Breaking Models (AMSB) by Moroi and Randall [131]. The moduli and gaugino masses they consider are qualitatively similar to those of the G_2-MSSM. There are some important differences however. In particular, the MSSM scalar masses in the [131] are much lower than the G_2-MSSM, leading to much fewer LSPs produced per modulus decay compared to the G_2 models. Furthermore, unlike in AMSB, in the G_2 case one is able to calculate all the moduli masses and couplings explicitly which leads to a more detailed understanding. In essence, though, many of the important ideas in our work are already present in [131]. The G_2-MSSM models can be thought of as a concrete microscopic realization of the relevant qualitative features of the AMSB models.

Interestingly, our actual result for the relic density (equation 5.53) is a few times

larger than the WMAP value if we use central values for the microscopic constants, which should probably be regarded as a success. It is also worth remarking that, contrary to common views, it is not at all possible to get any value one wants – we can barely accommodate the actual observed value in the G_2 framework.

The Chapter is organized as follows. In Section 5.2 we briefly summarize early universe cosmology in the presence of moduli, and address many of the issues associated with their stabilization and decay. In Section 5.3 we give a non-technical overview of the main results. This is largely because much of this paper involves technical calculations. In section 5.4 we present a brief review of the G_2-MSSM, a model which arises after considering moduli stabilization within the framework of M-theory compactifications. A basic discussion of decay rates and branching ratios for the moduli and gravitinos in this model follows, with a detailed calculation left for Appendix C.2. Then in section 5.5, we consider again the cosmology of moduli presented in section 5.2) for the case of the G_2-MSSM. In section 5.6, after a review of dark matter production in both the thermal and non-thermal cases, we consider the dark matter abundance arising from the non-thermal decay of the G_2-MSSM moduli. This section is a more technical overview of the salient features of dark matter production, leaving an even more detailed treatment for Appendix C.1. In this section we present our main result, which is that the G_2-MSSM naturally predicts a relic density of Wino-like neutralinos of about the right magnitude in agreement with observation. This is followed by a detailed discussion of the results obtained and how it depends on the qualitative (and quantitative) features of the underlying

physics. We then conclude with considerations for the future.

5.2 Early Universe Cosmology in the Presence of Moduli

Before considering the particular case of moduli in the G_2-MSSM, we first briefly review the early universe evolution of moduli and the associated cosmological issues that can result. This section will also serve to set our conventions.

Currently, the only convincing model leading to a smooth, large, and nearly isotropic Universe as well as providing a mechanism for generating density perturbations for structure formation is cosmological inflation. At present we have very little understanding of how the "inflationary era" might arise within the M-theory framework. In what follows,therefore, we will assume that adequate inflation and (p)reheating have taken place and focus on the post-reheating epoch. We will also conservatively take the inflationary reheat temperature to be near the unification scale $10^{14} - 10^{15}$ GeV, so that possibilities for high-scale baryogenesis exist. We will comment more on this issue at the end.

During inflation, the moduli fields are generically displaced from their minima by an amount of $\mathcal{O}(M_P)$ [132]. This can be seen by looking at the following generic potential experienced by the moduli:

$$V(\psi) \sim \frac{1}{2}m_{soft}^2(\psi - \psi_0)^2 - H_{inf}^2(\psi - \psi_0)^2 + \frac{1}{M_P^{2n}}(\psi - \psi_0)^{4+2n} \tag{5.1}$$

where ψ_0 is the true vacuum-expectation-value (vev) of the field, i.e. in the present Universe. Only the first term in (5.1) comes from zero-temperature supersymmetry breaking, the other two highlight the importance of high-scale corrections and the

mass-squared parameter ($\sim -H_{inf}^2$) which results from the finite energy density associated with cosmological inflation [132]. As argued earlier, the potential (5.1) is dominated by the last two terms during inflation since $H_{inf} \gg m_{soft} \sim m_{3/2}$. Thus, a minimum of the potential will occur near:

$$\langle \psi \rangle_{inf} \sim \psi_0 + M_P \left(\frac{H_{inf}}{M_P} \right)^{1/(n+1)} \qquad H \gg m_{soft}. \tag{5.2}$$

Here, for simplicity, we have implicitly assumed that the induced mass-squared parameter for ψ during inflation is negative and of $\mathcal{O}(H_{inf}^2)$. This is possible for a non-minimal coupling between the inflationary fields and the moduli, a generic possibility within string theory. A large displacement of moduli fields is also possible when the induced mass-squared parameter during inflation is positive, but much smaller than $|H_{inf}^2|$. In this case, large dS fluctuations can drive the moduli fields to large values during inflation. Therefore, independent of details, the assumption we make is that gauge singlet scalar fields like moduli (and meson fields in the G_2-MSSM) will be displaced from their present minimum by large values.

After the end of inflation and subsequent cosmological evolution, when $H \lesssim m_{3/2}$, the soft mass term in the potential will dominate and we have:

$$\langle \psi \rangle_{present} \sim \psi_0 \qquad H \lesssim m_{soft}. \tag{5.3}$$

ψ_0 is also typically of order M_P. In Section 5.4, we will present the soft masses and decay rates for the moduli arising from soft SUSY breaking in the G_2-MSSM low-energy effective theory relevant in the present Universe. Thus, we see that by considering moduli in the early universe with high-scale inflation, it is a rather generic conse-

quence to expect moduli to be displaced from their low-energy (present) minimum by an amount:

$$|\Delta\psi| \equiv |\langle\psi\rangle_{inf} - \langle\psi\rangle_{present}| \approx M_P \left(\frac{H_{inf}}{M_P}\right)^{1/(n+1)} \lesssim M_P \tag{5.4}$$

5.2.1 Addressing the "Overshoot Problem"

The evolution of moduli after the end of inflation is governed by the following equation:

$$\ddot{\psi} + (3H + \Gamma_\psi)\dot{\psi} + \frac{\partial V}{\partial \psi} = 0. \tag{5.5}$$

where the modulus decay rate $\psi \to XX$ is given by:

$$\Gamma_\psi = D_\psi \frac{m_\psi^3}{M_P^2}, \tag{5.6}$$

which reflects the fact that the modulus is gravitationally coupled ($\Gamma_\psi \sim G_N \sim M_P^{-2}$) and D_ψ is a model dependent constant that is typically order unity. After the end of inflation, the Universe is dominated by coherent oscillations of the inflaton field and $H \sim \frac{2}{3t}$. After the decay of the inflaton and subsequent reheating at temperature T_r, the Universe is radiation dominated and $H \sim \frac{1}{2t}$. In both these phases, the evolution of the moduli can be written as:

$$\ddot{\psi} + \mathcal{O}(1)\frac{1}{t}\dot{\psi} + \frac{\partial V}{\partial \psi} = 0. \tag{5.7}$$

where we have neglected Γ_ψ as it is planck suppressed. The minimum of the potential now is *time-dependent* due to the time dependence of the Hubble parameter. The evolution of the moduli in the presence of matter and/or radiation as in the case above, has been studied in [133–142]. In this case, as the modulus begins to roll

down the potential, it was shown in [133, 136, 137, 140]) that the presence of matter/radiation has a slowing effect on the evolution of the field. This can naturally allow for the relaxation of moduli into coherent oscillations about the time-dependent minimum[2]. This 'environmental relaxation' can then slowly guide the modulus to the time-dependent minimum.

Another possibility arises if the minimum of the potential is located at a point of enhanced symmetry where additional light degrees of freedom become important. This naturally arises in SUGRA theories that are derived from string theories, where an underlying knowledge of the UV physics is known [138, 139, 143, 144]. If the modulus initially has a large kinetic energy, as it evolves close to the point of enhanced symmetry, new light degrees of freedom will be produced and then backreact to pull the modulus back to the special point of enhanced symmetry. This simple example of 'moduli trapping' is present in a large number of examples in string theory with points of enhanced symmetry [138, 139, 141, 142].

The above effects lead to a natural solution of the so-called 'overshoot problem' [145] (see also [146]), as argued below. As the universe expands and cools, the Hubble parameter (H) decreases until it eventually drops below the mass of the modulus m_ψ ($\sim m_{3/2}$). Thus, from Eq. (5.1), we see that the first term in the potential now becomes of the same order as the other two terms and can no longer be neglected. At this time the modulus field becomes under-damped and begins to oscillate freely about the true minimum ψ_0 with amplitude $f_\psi \sim (M_P^n\, m_\psi)^{1/(n+1)}$. As an example, for

[2]We thank Joe Conlon and Nemanja Kaloper for discussions on this approach.

$n = 1$, f_ψ is $(M_P\, m_\psi)^{1/2}$ leading to a potential value $V \sim m_\psi^2 f_\psi^2 \sim m_\psi^3 M_P$ which is much smaller than the overall height of the potential barrier at this time ($\sim m_\psi^2 M_P^2$, as in any soft susy breaking potential). Thus, there is no overshoot problem.

The modulus will now quickly settle into coherent oscillations at a time roughly given by $t_{osc} = 2H^{-1} \sim 2m_\psi^{-1}$. After coherence is achieved, the scalar condensate will then evolve as pressure-less matter[3], i.e. $\rho_m(t_{osc}) = \frac{1}{2} m_\psi^2 f_\psi^2$. Because the condensate scales as pressure-less matter $\rho_m \sim 1/a^3$, its contribution relative to the background radiation $\rho_r \sim 1/a^4$ will grow with the cosmological expansion as $a(t) \sim 1/T$. Thus, if enough energy is stored initially in the scalar condensate it will quickly grow to dominate the total energy density.

5.3 Overview of Results

This section summarizes the our main results without technical details.

As explained above, the moduli start oscillating when the Hubble parameter drops below their respective masses. Then they eventually dominate the energy density of the Universe before decaying. Within the context of G_2-MSSM models, the relevant field content is that of the MSSM and $N+1$ real scalars. N of these are the moduli, X_K, of the G_2-manifold and the remaining one is a scalar field, ϕ, called the meson field, which arises in the hidden sector dominating the supersymmetry breaking. A reasonable choice for N would be $\mathcal{O}(50)$ - $\mathcal{O}(100)$.

[3]If there are additional terms that contribute to the potential (besides the soft mass), then a coherently oscillating scalar does not necessarily scale as pressure-less matter.

The masses are roughly as follows. The lightest particles beyond the Standard Model particles are the gauginos. In terms of the gravitino mass, $m_{3/2}$, their masses are of order $\kappa\, m_{3/2}$, suppressed by a small number κ. κ is determined by a combination of tree level and one-loop contributions which turn out to be comparable. The tree-level contribution is suppressed essentially because ϕ dominates the supersymmetry breaking, and to leading order, the gauge couplings are independent of ϕ. The precise spectrum of gaugino masses is qualitatively similar, but numerically different, to AMSB models. The LSP is a Wino in the G_2-MSSM, similar to AMSB models. The current experimental limits on gauginos require that the gravitino mass is at least 10 TeV or so. In the G_2 framework, gravitinos naturally come out to be of $\mathcal{O}(10-100)$ TeV [29]. 50 TeV is a typical mass that we consider in this paper. The MSSM sfermions and higgsinos have masses of order $m_{3/2}$, except the right handed stop which is a factor of few lighter due to RG running. Of the N moduli, one, X_N is much heavier than the rest, X_i. The heavy modulus mass is about 600 $m_{3/2}$, while the $(N-1)$ light moduli are essentially degenerate with masses $\sim 2m_{3/2}$. Finally the meson mass is also about $2m_{3/2}$. The decays of the moduli and meson into gravitinos will therefore be dominated by the heavy modulus X_N.

The decays can be parameterized by the decay width as,

$$\Gamma_X = D_X \frac{m_X^3}{M_P^2} \tag{5.8}$$

reflecting the fact that the decays are gravitationally suppressed. D_X is a constant which we calculate to be order one for the moduli but order 700 for ϕ. So, the light

moduli have decay widths of order 10^{-13}eV, corresponding to a lifetime of order 10^{-3} s. The heavier scalars have shorter lifetimes, 10^{-5} s for ϕ and 10^{-10} for X_N, see tables 1 and 2. So, as the Universe cools further and H reaches a value of order Γ_{X_N}, the heavy modulus decays. When this happens, the Universe is reheated to a temperature, roughly of order $T_r \sim (\Gamma_{X_N}^2 M_P^2)^{1/4} \sim 40$ GeV. The entropy is increased in this phase, by a factor of about 10^{10}. This greatly dilutes the thermal abundance of gravitinos and MSSM particles produced during reheating (by the inflaton). The abundance of the light moduli and meson are also diluted. Then, when H reaches order Γ_ϕ the meson decays. This reheats the Universe to a temperature $T_r \sim 100$ MeV and increases the entropy by a factor of order 100. Finally, as the Universe cools again and reaches a temperature of about 10^{-13} eV the light moduli decay. They reheat the Universe to a temperature of about 30 MeV and a dilution factor of about 100 again. After this, all the moduli have decayed and the energy density is dominated by the decay of the light moduli. Since the final reheat temperature is well above that of nucleosynthesis, BBN can occur in the standard way.

Furthermore, since the entropy increases by a total factor of about 10^{14}, the gravtino density produced by moduli and meson decays is sufficiently diluted to an extent that it avoids existing bounds from BBN from gravitino decays.

Since the energy density is dominated by the decaying light moduli, the relic density of Wino LSP's is dominated by this final stage of decay. The initial density of LSP's at the time of production is such that the expansion rate is not large enough

to prevent self-interactions of LSP's. This is because

$$n_{LSP}^{initial} > \left.\frac{3H}{\langle\sigma v\rangle}\right|_{T_r} \tag{5.9}$$

where the right side is to be evaluated at the final reheating temperature and σv is the typical Wino annihilation cross-section $\sim 10^{-7}\text{GeV}^{-2}$. Therefore, the Wino's will annihilate until they reach the density given on the R.H.S., which is roughly 10^{12} eV^3 - an energy density of 10^{23} eV^4. Here we have assumed, as is reasonable, that since there is a lot of radiation produced at the time of decay, the LSPs quickly become non-relativistic by scattering with this 'background'. Since the entropy at the time of the last reheating $s \sim 10\,T^3 \sim 10^{23}$ eV^3, the ratio of the energy density to entropy, is around 1 eV. This should be compared to the observed value of this ratio today, which is 3.6 h^2 eV, where the Hubble parameter today is about 0.71.

Therefore, we see that the Wino LSP relic density is very reasonable in these models. The rest of this paper is devoted to a much more precise, detailed version of this calculation.

5.3.1 Scalar Decay and Reheating Temperatures

Here we collect some more precise formulae for the decay and reheat temperatures as a function of the moduli/meson masses.

The temperature at the time of decay can be found using

$$3H_d^2 = \frac{m_\psi Y_\psi}{M_P^2} s_d = \frac{m_\psi Y_\psi}{M_P^2}\left(\frac{2\pi^2}{45}\right) g_{*s}(T_d)\, T_d^3, \tag{5.10}$$

$$\longrightarrow T_d = \left(\frac{30}{\pi^2}\right)^{1/3}\left(\frac{\Gamma_\psi^2 M_P^2}{m_\psi Y_\psi g_{*s}(T_d)}\right)^{1/3}, \tag{5.11}$$

where $Y_\psi = n_\psi/s$ is the comoving number density and

$$s = \frac{\rho + p}{T} = \frac{2\pi^2}{45} g_{*s} T^3, \tag{5.12}$$

is the entropy density with g_{*s} the number of relativistic degrees for freedom[4]. Parameterizing the decay rate as above, i.e. $\Gamma_\psi = D_\psi m_\psi^3/M_P^2$ we find

$$T_d = \left(\frac{30}{\pi^2}\right)^{1/3} g_{*s}^{-1/3}(T_d) \left(\frac{D_\psi^2 m_\psi^5}{Y_\psi M_P^2}\right)^{1/3} \tag{5.13}$$

For later use we also note that if more than one modulus dominates at the time of decay then the temperature at the time of decay becomes

$$T_d = \left(\frac{30}{\pi^2}\right)^{1/3} g_{*s}^{-1/3}(T_d) \left(\frac{D_\psi^2 m_\psi^6}{M_P^2 \sum_i m_i Y_i}\right)^{1/3} \tag{5.14}$$

where the sum is over all moduli (including the one that decays). When the modulus decays, the relativistic decay products will reheat the universe to a temperature,

$$3H^2 = \frac{4\Gamma_\psi^2}{3} = M_P^{-2} \left(\frac{\pi^2}{30}\right) g_*(T_r)\, T_r^4, \tag{5.15}$$

$$\longrightarrow T_r = \left(\frac{40}{\pi^2}\right)^{1/4} g_*^{-1/4}(T_r) \sqrt{\Gamma_\psi M_P}, \tag{5.16}$$

or

$$T_r = \left(\frac{40}{\pi^2}\right)^{1/4} g_*^{-1/4}(T_r) \left(\frac{D_\psi m_\psi^3}{M_P}\right)^{1/2}. \tag{5.17}$$

Instead, if more than one modulus contributes to the energy density before decay the reheat temperature becomes

$$T_r = \left(\frac{40}{\pi^2}\right)^{1/4} g_*^{-1/4}(T_r) \left(\frac{m_\psi Y_\psi}{\sum_i m_i Y_i}\right)^{1/4} \left(\frac{D_\psi m_\psi^3}{M_P}\right)^{1/2}, \tag{5.18}$$

[4]We will take $g_{*s} = g_*$, which is true if all particles track the photon temperature. This is a good approximation for most of the history of the universe (prior to decoupling) [147].

where the sum is over all moduli (including the one that decays) and we note that this could lead to a subdominant radiation density compared to that of the remaining moduli. The entropy production is characterized by (assuming that $\Delta \gg 1$)

$$\Delta = \left(\frac{S_r}{S_d}\right) = \frac{g_{*s}(T_r)a^3(t_r)T_r^3}{g_{*s}(T_d)a^3(t_d)T_d^3}, \tag{5.19}$$

where T_d and T_r are the decay and reheat temperatures, respectively. Making use of Eq. (5.17), (5.19), and (5.13) we find

$$\begin{aligned} \Delta &= \frac{2}{15}\left(250\pi^2\right)^{1/4}\left(\frac{g_{*s}(T_r)}{g_{*s}(T_d)}\right)\left(\frac{g_{*s}(T_d)}{g_*^{3/4}(T_r)}\right)\frac{m_\psi Y_\psi}{\left(\Gamma_\phi M_P\right)^{1/2}}, \\ &= \frac{2}{15}\left(250\pi^2\right)^{1/4} g_*^{1/4}(T_r)\left(\frac{M_P}{D_\psi m_\psi}\right)^{1/2} Y_\psi, . \end{aligned} \tag{5.20}$$

For the case that more than one modulus dominates the energy density before ψ decays, we have instead

$$\Delta = \frac{2}{15}\left(250\pi^2\right)^{1/4} g_*^{1/4}(T_r)\left(\frac{M_P}{D_\psi m_\psi}\right)^{1/2}\left[\frac{\sum_i m_i Y_i}{m_\psi Y_\psi}\right]^{1/4} Y_\psi, \tag{5.21}$$

where the sum runs over all moduli that contribute to the energy density (including the decaying modulus ψ).

Moduli decay and BBN

From Eq. (5.21), we see that the decay of moduli can produce a substantial amount of entropy. Therefore, if any moduli present do not decay before the onset of BBN the resulting entropy production when decay occurs could result in devastating phenomenological consequences. However, another possibility is provided if the late-time decay of the moduli reheat the universe to temperatures greater than a few

MeV. Such reheating will then allow BBN to proceed as usual. Requiring that the modulus decay exceeds this temperature one finds from Eq. (5.17) that $m_\psi \gtrsim 10$ TeV.

5.4 Moduli Masses and Decay Widths

5.4.1 Moduli Masses

Since in this paper we are interested in the evolution of the moduli (and meson) fields, it is important to study their masses in the vacuum described above. The set of gauge-singlet scalar fields includes N geometric moduli s_i associated with G_2 manifold and a hidden sector meson field ϕ. Since these moduli and meson will mix in general, the physical moduli correspond to mass eigenstates. The mass matrix can be written as:

$$\left(m_X^2\right)_{i\,j} = \left((a_i a_j)^{1/2} K_1 + \delta_{ij} K_2\right)\, m_{3/2}^2 \tag{5.22}$$

$$\left(m^2\right)_{i\,\phi} = (a_i)^{1/2} K_3\, m_{3/2}^2 \tag{5.23}$$

$$\left(m^2\right)_{\phi\phi} = K_4\, m_{3/2}^2 \tag{5.24}$$

where K_1 to K_4 are obtained in [29]:

$$K_1 = \frac{16}{9261}\left(\frac{Q}{Q-3}\right)^2 P_{\rm eff}^4 \tag{5.25}$$

$$K_2 = \frac{22}{3} - \frac{8}{9\phi_0^2} - 2\phi_0^2 - (1+\frac{2}{3\phi_0^2})\frac{36}{P_{\rm eff}} \tag{5.26}$$

$$K_3 = \sqrt{\frac{2}{3}}\left(\frac{16}{1323}\right)\left(\frac{Q}{Q-3}\right)^2 \frac{P_{\rm eff}^3}{\phi_0} \tag{5.27}$$

$$K_4 = \frac{32}{567}\left(\frac{Q}{Q-3}\right)^4 \frac{P_{\rm eff}^4}{\phi_0^2} \tag{5.28}$$

where $\phi_0^2 \approx 0.734$. The special structure of the mass matrix allows us to find the eigenstates analytically. There is one heavy eigenstate with mass $m_{X_N} = (7K_1/3 +$

$K_2)^{1/2} m_{3/2}$, $(N-1)$ degenerate light eigenstates with mass $m_{X_j} = (K_2)^{1/2} m_{3/2}$ and an eigenstate with mass $m_\phi = (K_4 - \frac{K_3^2}{K_1})^{1/2} m_{3/2}$. These mass eigenstates of the moduli fields are given by:

$$\begin{aligned} X_j &= \sqrt{\frac{a_{j+1}}{(\sum_{k=1}^{j} a_k)(\sum_{k=1}^{j+1} a_k)}} \left(\sum_{k=1}^{j} \sqrt{a_k}\, \delta s'_k - \frac{\sum_{k=1}^{j} a_k}{\sqrt{a_{j+1}}}\, \delta s'_{j+1} \right);\ j = 1, 2 \cdots N-1 \\ X_N &= \sqrt{\frac{3}{7}} \sum_{k=1}^{N} \sqrt{a_k}\, \delta s'_k \end{aligned} \tag{5.29}$$

where $\delta s'_j = \sqrt{\frac{3a_j}{2s_j^2}}\, \delta s_j$ are the canonically normalized moduli fields. The normalized moduli fields can be related to the eigenstates by $\delta s'_i = U_{ij} X_j$, in which U_{ij} can be constructed using the eigenstates listed above. It is easy to show that $(\vec{X}_j)_i = U_{ij}$ for the eigenvector $\vec{X}_j$. In addition, there is another eigenstate X_ϕ corresponding to the meson field. Actually, the heavy eigenstate X_N and X_ϕ mix with each other. This mixing hardly changes the components of the eigenstate X_N and X_ϕ since $m_{X_N} \gg m_\phi$. However, the mass of the eigenstate X_ϕ is affected by the mixing. The masses m_{X_N} and m_ϕ only have a mild dependence on Q (for $P_{\text{eff}} = 84, Q - P = 3$), and do not depend on the number of moduli N at all. The mass of the light moduli m_{X_j} does not even depend on Q. Taking the expression for K_2, one immediately finds that $m_{X_j} \approx 1.96\, m_{3/2},\ j = 1, \cdots, N-1$. This result is very important since light moduli are then not allowed to decay into gravitinos, essentially eliminating the moduli induced gravitino problem. Choosing a reasonable value of Q to be of $\mathcal{O}(10)$, one finds that m_ϕ is roughly around $2\, m_{3/2}$ while m_{X_N} is roughly around $600\, m_{3/2}$. Changing values of Q by $\mathcal{O}(1)$ hardly changes the moduli masses m_{X_N} and m_ϕ. Therefore, the above typical values will be used henceforth in our analysis.

To summarize, the meson and moduli masses in the G_2 -MSSM can be robustly determined in terms of $m_{3/2}$.

5.4.2 Couplings and Decay Widths

Understanding the evolution of the moduli also requires a knowledge of the couplings of the moduli (meson) fields to the visible sector gauge and matter fields. Since all the moduli are stabilized explicitly in terms of the microscopic constants of the framework, all couplings of the moduli and meson fields to the MSSM matter and gauge fields can in principle be explicitly computed. Here we focus on the moduli couplings to MSSM matter and gauge fields. A different visible sector, as might arise from an explicit construction, will give rise to different couplings of the moduli fields in general, although with roughly the same moduli masses.

Here we will give a brief account of the important couplings of the moduli meson to visible gauge and matter fields and set the notation. Details are provided in Appendix C.2. The most important couplings of the moduli and meson fields involve two-body decays of the moduli and meson to gauge bosons, gauginos, squarks and slepton, quarks and leptons, higgses and higgsinos. The three-body decays are significantly more suppressed and will not be considered.

Let us start with the decay to gauge bosons and gauginos. The relevant part of the Lagrangian is given by:

$$\begin{aligned} \mathcal{L} \supset\ & g_{X_k gg}\, X_k\, \hat{F}^a_{\mu\nu} \hat{F}^{a,\mu\nu} + g_{X_k \tilde{g}\tilde{g}}\, X_k\, \hat{\lambda}^a \hat{\lambda}^a + \\ & g_{\delta\hat{\phi}_0 \tilde{g}\tilde{g}}\, \delta\hat{\phi}_0\, \hat{\lambda}^a \hat{\lambda}^a \end{aligned} \tag{5.30}$$

where $k = 1 \cdots N$ and $a = 1, 2, 3$. In addition, X_k, $\delta\hat{\phi}_0$, $\hat{F}^a_{\mu\nu}$ and $\hat{\lambda}^a$ are the normalized moduli, meson, gauge field strength and gaugino fields respectively. The expression for the couplings will be provided in Appendix C.2. It is important to note that the meson field does not couple to gauge bosons since the gauge kinetic function f_{sm} does not depend on ϕ_0. The normalized moduli eigenstates X_k have already been discussed. The others can be written as:

$$\delta\hat{\phi}_0 = \frac{\delta\phi_0}{\sqrt{2}};\ \hat{F}^a_{\mu\nu} = \frac{F^a_{\mu\nu}}{\sqrt{\langle \mathrm{Im}(f_{sm})\rangle}};\ \hat{\lambda}^a = \frac{\lambda^a}{\sqrt{\langle \mathrm{Im}(f_{sm})\rangle}} \tag{5.31}$$

where f_{sm} is the gauge kinetic function for the visible SM gauge group. In the rest of the paper, we will neglect the hats for these normalized fields and M_P in the couplings for convenience.

The coupling of the moduli and meson fields to the MSSM non-higgs scalars (ie sfermions) turn out to be important, as will be seen later. Since the Standard model fermion masses (including that of the top) are much smaller than that of the moduli, the decay of the moduli and meson to these fermions will not be considered. The coupling to the MSSM sfermions can be written as:

$$\begin{aligned} \mathcal{L} \ \supset\ & (g'_{X\tilde{f}\tilde{f}})_{i,\alpha\beta}\left[\partial_\mu(X_i\ \tilde{f}^{\alpha *})\partial^\mu \tilde{f}_\alpha\right] - g^\alpha_{X\tilde{f}\tilde{f}}\, X_i \tilde{f}^{*\bar{\alpha}} \tilde{f}^\alpha \\ +\ & (g'_{\delta\hat{\phi}_0\tilde{f}\tilde{f}})_{i,\alpha\beta}\left[\partial_\mu(\delta\phi_0\ \tilde{f}^{\alpha *})\partial^\mu \tilde{f}_\alpha\right] - g^\alpha_{\delta\hat{\phi}_0\tilde{f}\tilde{f}}\, \delta\hat{\phi}_0 \tilde{f}^{*\bar{\alpha}} \tilde{f}^\alpha \end{aligned} \tag{5.32}$$

where $\tilde{f}_\alpha$ are the canonically normalized scalar components of the visible chiral fields C_α, i.e. $\tilde{f}_\alpha = \frac{C_\alpha}{\sqrt{\tilde{K}_\alpha}}$. The couplings to the higgs and higgsinos are different due to the presence of the higgs bilinear $Z\, H_u H_d + h.c$ in the Kähler potential [30], which gives rise to contributions to the μ and $B\mu$ parameters. In addition to the couplings

similar as those in Eq. (5.32), there are additional couplings for scalar higgses, which can be schematically written as:

$$\begin{aligned}\mathcal{L} \supset\ & g_{XH_dH_u}\, X_j H_d H_u + g'_{XH_dH_u}\, \partial_\mu X_j \partial^\mu (H_d H_u) + c.c \\ +\ & g_{\delta\phi_0 H_d H_u}\, \delta\phi_0 H_d H_u + g'_{\delta\phi_0 H_d H_u}\, \partial_\mu \delta\phi_0 \partial^\mu (H_d H_u) + c.c \end{aligned} \tag{5.33}$$

As explained in [30], all higgs scalars except the SM-like higgs and all higgsinos are heavier than the gravitino, implying that the moduli and meson fields can only decay in this sector to the light SM-like higgs (h). The coupling to the SM-like higgs can be determined from the above coupling 5.33 as explained in appendix C.2.

Finally, the moduli and meson fields can also decay directly to the gravitino. In fact, it turns out that the (non-thermal) production of gravitinos from direct decays dominates the thermal production of gravitinos in the early plasma. Therefore, it is important to consider the moduli and meson couplings to the gravitinos. Since the meson and light moduli are lighter than twice the gravitino mass (as seen from the previous subsection), only the heavy modulus can decay to the gravitino.

The explicit form of these couplings in terms of the microscopic constants is provided in appendix C.2. An important point to note is that these couplings are computed from the theory at a high scale, presumably the unification scale. However, since the temperature at which the moduli decay is much smaller than the unification scale, one has to RG evolve these couplings to scales at which these moduli decay (around their masses). The RG evolution has also been discussed in appendix C.2 for the important couplings. Once the effective couplings of these moduli and meson

are determined, one can compute the decay widths, as shown below.

For the G_2-MSSM model, we have found that light moduli and meson dominantly decay to light higgses and squarks, while the heavy modulus dominantly decay to light higgses only. In appendix C.2, we have explicitly calculated the decay widths of the moduli X_k and meson. The widths of moduli can be schematically written as:

$$\begin{aligned}\Gamma^{total}_{X_k} \equiv \frac{D_{X_k} m^3_{X_k}}{M_P^2} &\approx \Gamma_{X_k\to gg} + \Gamma_{X_k\to \tilde{g}\tilde{g}} + \Gamma_{X_k\to \tilde{q}\tilde{q}} + \Gamma_{X_k\to hh} \\ &= \frac{7}{72\pi}\left(N_G(\mathcal{A}_1^{X_k} + \mathcal{A}_2^{X_k}) + \mathcal{A}_3^{X_k} + \mathcal{A}_4^{X_k}\right)\left(\frac{m^3_{X_k}}{M_P^2}\right),\end{aligned} \tag{5.34}$$

where $k = 1 \cdots N$ and $N_G = 12$ is the number of gauge bosons or gauginos. Note that $\mathcal{A}_3^{X_k}$ is significant only for $k = 1, 2..., N-1$ (see appendix C.2). For the meson, the width can be written as:

$$\begin{aligned}\Gamma^{total}_{\delta\phi_0} \equiv \frac{D_\phi m^3_\phi}{M_P^2} &\approx \Gamma_{\delta\phi_0\to \tilde{g}\tilde{g}} + \Gamma_{\delta\phi_0\to \tilde{q}\tilde{q}} + \Gamma_{\delta\phi_0\to hh} \\ &= \frac{7}{72\pi}(N_G\mathcal{A}_1^{\phi_0} + \mathcal{A}_2^{\phi_0} + \mathcal{A}_3^{\phi_0})\left(\frac{m^3_\phi}{M_P^2}\right).\end{aligned} \tag{5.35}$$

5.5 Evolution of Moduli in the G_2-MSSM

In this section, we apply the general discussion in Section 5.2 to the model of the G_2-MSSM reviewed in the previous section. For clarity we will summarize our main results focusing on the more salient aspects of the physics, leaving the more technical details of the calculations to Appendix C.1. We will illustrate our computations with benchmark values, in order to get concrete numerical results, and comment on the choice of the benchmark values in section 5.7.

As discussed in Section 5.2, we assume that cosmological inflation and (p)reheating

have provided adequate initial conditions for the post-inflationary universe.

5.5.1 Moduli Oscillations

As reviewed in the last section, we have a heavy modulus X_N, $N-1$ light moduli X_i, and the scalar meson ϕ. These will begin to oscillate in the radiation dominated universe once the temperature cools and the expansion rate becomes comparable to their masses.

For a benchmark gravitino mass value[5] of 50 TeV, the heavy modulus will begin oscillations first, at around $t_{X_N}^{osc} \approx 10^{-32}$ seconds, corresponding to a temperature of roughly $T = 10^{12}$ GeV. Following the heavy modulus, the other moduli will begin coherent oscillations around 10^{-30} s corresponding to a temperature of roughly 10^{11} GeV. These results are summarized in Table 5.1 below.

Modulus	Mass ($m_{3/2} = 50$ TeV)	Oscillation Time (seconds)
X_N	$m_{X_N} = 600\, m_{3/2}$	$t_{osc}^{X_N} = 2 \times 10^{-32}$
X_ϕ	$m_\phi \lesssim 2\, m_{3/2}$	$t_{osc}^{\phi} = 7 \times 10^{-30}$
X_i	$m_{X_i} \lesssim 2\, m_{3/2}$	$t_{osc}^{X_i} = 7 \times 10^{-30}$

Table 5.1: Oscillation times for the G_2-MSSM moduli

Since coherently oscillating moduli (ρ_m) scale relative to radiation as $\rho_m/\rho_r \sim a(t) \sim 1/T$, the moduli will quickly come to dominate the energy density of the universe, which is then matter dominated. Following the beginning of coherent oscillations of the heavy modulus, until the decay of all the moduli the universe

[5]We give detailed numerical values for $m_{3/2} = 50$ TeV. It will be clear that values a factor of two or so smaller or larger than this will not change any conclusions in this and related analyses.

will remain matter dominated. We will see that this, along with the entropy produced during moduli decays, results in negligible primordial thermal abundances of (s)particles compared with the non-thermal abundances coming from direct decays of the moduli. This will be crucial in addressing the gravitino problem and establishing a Wino-like LSP as a viable dark matter candidate through its non-thermal production.

5.5.2 Moduli Decays and Gravitino Production

As the universe continues to cool the expansion rate will eventually decrease enough so that the moduli are able to decay. This occurs when $H \sim \Gamma_X$, at which time the moduli will decay reheating the universe and producing substantial entropy. We will parameterize the decay rates of the G_2-MSSM moduli as:

$$\Gamma_X = D_X \frac{m_X^3}{M_P^2}, \tag{5.36}$$

where Γ_X is the decay width for particle X. The decay times will be computed for a set of benchmark values of D_X for the various moduli (meson) which can be obtained by choosing particular (reasonable) sets of values of the microscopic constants (see appendix C.2 for details).

Modulus	Decay Coefficient	Decay Time (seconds)
X_N	$D_{X_N} = 2$	$\tau_{X_N} = 9 \times 10^{-11}$
X_ϕ	$D_\phi = 710$	$\tau_\phi = 6 \times 10^{-6}$
X_i	$D_{X_i} = 4.00$	$\tau_{X_i} = 10 \times 10^{-4}$

Table 5.2: Decay coefficients and lifetimes for the G_2-MSSM moduli for a set of benchmark microscopic values

Heavy Modulus Decay and Initial Thermal Abundances

Given the G_2-MSSM values in Table 5.2 above, the heavy modulus will be the first to decay at around $10^{-11}s$. This decay will produce a large amount of entropy $\Delta_{X_N} = S_{after}/S_{before} \approx 10^{10}$ (even though the energy density of the heavy modulus is less than that of the meson and moduli), reheating the universe to a temperature $T_r^{X_N} = 41$ GeV. The entropy production will not only dilute the thermal abundances of all (s)particles, but also all the other moduli. One particularly important non-relativistic decay product of the heavy modulus is the gravitino. Gravitinos will be non-thermally produced by the modulus decay with a branching ratio $B_{3/2}^{X_N} = 0.07\%$, which yields a comoving abundance $Y_{3/2}^{(X_N)} = n_{3/2}/s \approx 10^{-9}$. This can be compared to the thermal abundance of gravitinos, which before modulus decay is $Y_{3/2}^{thermal} = 2.67 \times 10^{-8}$. This is further diluted by entropy production resulting from the decay, i.e. $Y_{3/2}^{thermal} \rightarrow Y_{3/2}^{thermal}/\Delta_{X_N} \approx 10^{-18}$. We see that the thermal contribution to the gravitino abundance is negligible compared to that from non-thermal production. A similar result follows for all other (s)particles that are thermally populated following inflation. Therefore, the primary source of (s)particles, and in particular gravitinos and Lightest SUSY Particles (LSPs), will result from non-thermal production resulting from decays of the moduli.

Meson/Light Moduli Decays and the Gravitino Problem

The decay of the heavy modulus is followed by the decay of the meson, at around $10^{-6}s$ (for benchmark values). The meson will decay before the light moduli because

of a larger decay width compared to that for the light moduli (see appendix C.2 for details). Similar to the heavy modulus, the meson contribution to the energy density is small compared to that of the $N-1$ light moduli. Nevertheless, it produces some entropy ($\Delta_\phi \approx 121$) and reheats the universe to a temperature of around 134 MeV. The entropy production will again dilute the abundance of light moduli, and any (s)particles present, including the gravitinos from the heavy modulus decay.

The decay of the meson to gravitinos is particularly important, as this can result in the well-known gravitino problem. If the scalar decay yields a large number of gravitinos, these gravitinos can later decay producing a substantial amount of entropy that could spoil the successes of BBN.

The entropy produced from the decay of the meson and the other light moduli further dilutes the gravitino abundance from the heavy modulus. The primary contribution to the gravitino relic abundance comes from the decay of the heavy modulus since the other fields have masses of order 2 $m_{3/2}$. After the decay of the meson, the energy density of the $N-1$ light moduli is the dominant contribution to the total energy density of the Universe.

Given that the $N-1$ light moduli are approximately degenerate in mass, their decays will occur at nearly the same time, after the decay of the meson. The resulting reheat temperature is found to be approximately 32 MeV, which is an acceptable temperature for consistency with the bound of 1 MeV set by BBN [148–151].

We note that the moduli decay rates have a strong dependence on the gravitino mass (as it sets the moduli mass scale). So, the decay of the light moduli being able

to avoid BBN constraints is a result of the fact that the gravitino mass is relatively large ($m_{3/2} \gtrsim 50$ TeV). However, as explained in detail in [30], the gauginos are significantly suppressed relative to the gravitinos allowing us to still obtain a light ($<$ TeV) spectrum which can be seen at the LHC. The decay of each modulus will contribute to the total entropy production, and one finds that the total entropy production for the set of benchmark values of the microscopic constants is given by $\Delta_{X_i} = 418$. We also note that the light moduli lifetime depends inversely on the decay coefficient D_{X_i}, so if instead of taking relatively large values $D_{X_i} = 4$ we take relatively small values $D_{X_i} = 0.4$, we find a reheat temperature of 10 MeV which is still compatible with BBN[6]. The decay of light moduli to gravitinos is kinematically suppressed for the same reason as for the meson. The final gravitino abundance is then just the contribution from the heavy modulus decay diluted by the decay of the meson and light moduli and is $Y_{3/2}^{final} = Y_{3/2}^{\phi}/\Delta_{X_i} \approx 10^{-14}$. The above gravitino abundance is well within the upper bound on the gravitino abundance set by BBN constraints, as it will not lead to any significant entropy production at the time the gravitinos decay. Thus, we find that there is *no gravitino problem* in the G_2-MSSM. In addition to the relativistic decay products, the light moduli will also decay appreciably into neutralinos (LSPs), which we consider in detail in the next section.

[6]See appendix A for a discussion of the range of the coefficients D_{X_i}.

5.6 Dark Matter from the G_2-MSSM

Natural models of electroweak symmetry breaking (EWSB) require additional symmetries and particles beyond those of the Standard Model. The additional particles typically come charged under additional discrete symmetries suppressing their decay to Standard Model particles (e.g. R-parity, KK-parity, etc.), so such models predict an additional, stable, weakly interacting particle with an electroweak scale mass, i.e. they naturally predict a candidate for Weakly Interacting Massive Particle (WIMP) cold dark matter. In the case of the G_2-MSSM, this gives rise to a Wino-like neutralino which is the lightest supersymmetric particle (LSP) of the theory.

For completeness in section 5.6.1 we will review the standard calculation for computing the (thermal) dark matter relic density today. In section 5.6.2, we will then revisit this calculation for non-thermal production of LSPs resulting from scalar decay. In Section 5.6.3, we examine how non-thermal production is naturally realized in the G_2-MSSM and predicts the Wino LSP as a viable WIMP candidate.

5.6.1 Standard Thermal Dark Matter

In the standard calculation of the relic abundance of LSPs it is assumed that prior to BBN the universe is radiation dominated. In particular, it is assumed that the dark matter particles are created from a thermal bath of radiation created from (p)reheating after inflation. In this radiation dominated universe, the Friedmann equation reads $3H^2 = M_P^{-2}\rho_r$, with $\rho_r = (\pi^2/30)g_*T^4$ the radiation density and g_* the number of relativistic degrees of freedom at temperature T.

The evolution of LSPs are given by the Boltmann equation

$$\dot{n}_X = -3Hn_X - \langle\sigma v\rangle \left[n_X^2 - n_{eq}^2\right], \tag{5.37}$$

where $\langle\sigma v\rangle$ is the thermally averaged cross-section, n_X is the number density, and n_{eq} is the number density of the species in chemical equilibrium, i.e. $XX \leftrightarrow \gamma\gamma$, where γ is a relativistic particle such as the photon.

Assuming that initially the dark matter particles are relativistic ($m_X < T$) and in chemical equilibrium, then they will pass through three phases as the universe expands and cools. Initially their density will be determined by all the factors on the right side of (5.37). As long as the interactions of the particles take place on smaller time scales than the cosmic expansion then the particles will remain close to their equilibrium distributions. While the species is relativistic ($m_X < T$) this means that their comoving abundance is given by $Y_X = n_X/s \approx Y_X^{eq} = const.$. Once the universe cools enough from the cosmological expansion so that X becomes non-relativistic ($T < m_X$) then particle creation becomes more difficult (Boltzmann suppressed) and the comoving abundance tracks that of a non-relativistic species $Y_X \approx Y_X^{eq} = 0.145\, x^{3/2} \exp(-x)$ where $x \equiv m_X/T$. The particle density will continue to decrease until the number of particles becomes so scarce that the expansion rate exceeds the annhiliation rate and the particle species undergoes 'freeze-out'. From (5.37) we see that at this time the number density is given by:

$$n_X = \left.\frac{3H}{\langle\sigma v\rangle}\right|_{T_f}, \tag{5.38}$$

where T_f indicates that this relation only holds at the time of freeze-out. Using (5.38)

and $Y_X \approx Y_X^{eq}$ at the time of freeze-out, we find that freeze-out is only logarithmically sensitive to the parameters of the model, $x_f \equiv \frac{m_X}{T_f} \approx \ln\left[m_X M_P \langle\sigma v\rangle\right]$ and corrections are $\mathcal{O}(\ln\ln x_f)$. Taking both the cross-section and mass m_X to be weak scale at around 100 GeV we find that $x_f = 4$ and thus the freeze-out temperature is $T_f = m_X/25 \approx 4$ GeV. From (5.38) and (5.12), we find the comoving density at freeze-out:

$$\begin{aligned} Y_f &= \frac{3H}{s\langle\sigma v\rangle}, && (5.39)\\ &= \frac{45}{2\pi\sqrt{10}}\frac{1}{\sigma_0 g_*^{1/2}}\left(\frac{1}{M_P\langle\sigma v\rangle T_f}\right), && (5.40)\\ &= \frac{45}{2\pi\sqrt{10}}\frac{1}{\sigma_0 g_*^{1/2}}\left(\frac{m_X}{M_P}\right)x_f, && (5.41) \end{aligned}$$

where we have taken $\langle\sigma v\rangle = \sigma_0\, m_X^{-2}$. We note that this answer is rather insensitive to the details of freeze-out, and the abundance is determined solely in terms of the properties of the produced dark matter (mass and cross-section). In particular, there is no dependence on the underlying microscopic physics of the theory.

5.6.2 Non-thermal Production from Scalar Decay

We know from the successes of BBN that at the time the primordial light elements were formed the universe was radiation dominated at a temperature greater than around an MeV. However, perhaps surprisingly, there is no evidence for a radiation dominated universe prior to BBN. In particular, we have seen that in the presence of additional symmetries and flat directions, scalar moduli can easily dominate the energy density of the universe and then later decay. The presence of these decaying scalars can alter the standard cold dark matter picture of the last section in significant ways.

To understand this, consider the decay of an oscillating scalar condensate ϕ, which decays at a rate $\Gamma_\phi \sim m_\phi^3/M_P^2$. When the expansion rate becomes of order the scalar decay rate ($H \sim \Gamma$) the scalars will decay into LSPs along with relativistic (s)particles which reheat the universe to a temperature T_r. If this reheat temperature is below that of the thermal freeze-out temperature of the particles $T_f \sim m_X/25$ then the LSPs will never reach chemical equilibrium. As an example, if we consider a scalar mass $m_\phi \sim 10-100$ TeV this gives rise to a reheat temperature $T_r \sim \sqrt{\Gamma_\phi M_P} \gtrsim$ MeV where $\Gamma_\phi \sim m_\phi^3/M_P^2$. The decay of ϕ in a supersymmetric setup could lead to LSPs with weak-scale masses $m_X \sim 100$ GeV, which have a thermal freeze-out temperature $T_f \sim m_X/25 \sim$ few GeV. We see that in this case $T_r < T_f$ is quite natural and the particles are non-thermally produced at a temperature below standard thermal freeze-out. Thus, the particles will be unable to reach chemical equilibrium.

Depending on the yield of dark matter particles from scalar decay, there are two possible outcomes of the non-thermally produced particles.

Case one: LSP Yield Above the Fixed Point

If the production of LSPs coming from scalar decay is large enough, then some rapid annihilation is possible at the time of their production. Since the particles are produced at the time of reheating, we know from the Boltzmann equation (5.37) that the critical density for annihilations to take place is:

$$n_X^c = \left.\frac{3H}{\langle\sigma v\rangle}\right|_{T_r}, \tag{5.42}$$

which is different from the result (5.38) in that here the reheat temperature and not the thermal freeze-out is the important quantity. This is very important because $T_r \sim \sqrt{\Gamma_\phi M_P}$ depends on the microscopic parameters of the theory as the reheat temperature is set by the decay rate of the scalar. In the standard case, we saw that the freeze-out temperature, or more precisely, the parameter $x_f \equiv m_X/T_f$ was only logarithmically sensitive to the parameters of the dark matter and gave no information at all about the underlying theory from which the dark matter was produced (e.g. scalars from the underlying microscopic physics).

Given that the initial number density of particles exceeds the above bound ($n_X(0) > n_X^c$), the LSPs will quickly annihilate until they reach the density (5.42). Thus, the critical value n_X^c serves as a fixed point for the number density, since any production above this limit will always result in the same yield of particles given by n_X^c. From this one finds the comoving density [131]

$$Y_X = \frac{c_1}{g_*^{1/2}} \frac{1}{M_P \langle \sigma v \rangle T_r} = Y_X^{std} \left(\frac{T_f}{T_r} \right), \tag{5.43}$$

where $c_1 = 45/(2\pi\sqrt{10})$. We see that non-thermal production can yield a greater comoving density than standard thermal production by a factor (T_f/T_r). For the example considered above, namely $m_\phi \sim 10 - 100$ TeV, $m_X \sim 100$ GeV, and $T_r \sim$ few MeV we find the comoving density is enhanced by a factor $\sim 10^2 - 10^3$. One interesting consequence of this is it allows room for larger annihilation cross-sections for the LSPs. For example, in standard thermal production a Wino-like LSP leads to too small a relic density since its annihilation cross section is only s-wave suppressed

. In the case of the G_2-MSSM, non-thermal production is a natural consequence of the microscopic physics and a Wino LSP will provide a perfectly suitable WIMP candidate.

Case two: LSP Yield Below the Fixed Point

The other possibility is that the decay of the scalar yields few enough LSPs ($n_X(0) < n_X^c$) so that annihilation does not occur. Then the comoving abundance is simply given by

$$Y_X = B_\phi \Delta_\phi^{-1} Y_\phi^{(0)} \sim \frac{B_\phi n_\phi^{(0)}}{T_r^3}, \tag{5.44}$$

where B_ϕ is the branching ration of scalars to LSPs and $Y_\phi^{(0)}$ is the initial abundance of scalars in the decaying condensate. We note that again this result depends on the underlying physics of the UV theory, since both the branching ratio and the reheat temperature are coming from the physics of the scalar.

5.6.3 Dark Matter in the G_2-MSSM

As shown in [30], the LSP in the G_2-MSSM is predominantly Wino-like. There are two significant sources of these LSPs in the G_2-MSSM – direct production from decays of both the gravitino and the light moduli. As explained earlier, the thermal abundance of LSPs in the early plasma after inflation is vastly diluted by the entropy productions from the heavy modulus, meson and the light moduli. Therefore, the thermal abundance of LSPs is negligible. In addition, the LSPs produced from decays of the heavy modulus and the meson field are also diluted by the entropy production from the light moduli and are negligible as well.

The light moduli may decay to LSPs directly, or via decay to superpartners. From Section 5.4 the branching ratio for this process to occur for a set of benchmark values of the microscopic paramaters is $B_{LSP}^{X_i} \sim 25\%$ and the comoving abundance is then found to be:

$$Y_{LSP}^{(X^i)} = \Delta_{X_i}^{-1} B_{LSP}^{X_i} (N-1) Y_{X_i}^{(\phi)} = 1.19 \times 10^{-7}, \tag{5.45}$$

where $\Delta_{X_i} = 417.7\ [(N)/100]^{3/4}$ is the entropy production from the decay of all the light moduli X_i. Here we have taken benchmark value for the number of light moduli to be 100. The corresponding number density at the time of reheating is

$$\begin{aligned} n_{LSP} &= s(T_r^{X_i}) Y_{LSP}, & (5.46) \\ &= 1.79 \times 10^{-11}\ \text{GeV}^3 & (5.47) \end{aligned}$$

As discussed in the last section, we must compare this number density of LSPs to that of the critical density for annihilations (5.42). At the time of reheating from the light moduli the Hubble parameter is given by

$$H(t_r) = \left(\frac{\pi^2 g_*}{90}\right)^{1/2} \frac{(T_r^{X_i})^2}{M_P} = 4.48 \times 10^{-22}\ \text{GeV}. \tag{5.48}$$

The dominant (s-wave) annihilation cross section for the LSPs ($\tilde{W}^0 \tilde{W}^0 \to W^+ W^-$) is given by

$$\langle \sigma v \rangle = \sigma_0\, m_{LSP}^{-2} = \frac{1}{m_{LSP}^2} \frac{g_2^4}{2\pi} \frac{(1-x_w)^{3/2}}{(2-x_w)^2} = 3.26 \times 10^{-7}\ \text{GeV}^{-2}, \tag{5.49}$$

where $x_w = m_w^2/m_{LSP}^2$, $m_w = 80.4$ GeV is the W-boson mass, and $g_2 \approx 0.65$ is the gauge coupling constant of $SU(2)_L$ at temperatures $T_r \sim$ MeV, and this defines σ_0. It

is crucial that the cross-section is s-wave so that there is no temperature dependence in $\langle \sigma v \rangle$. We will comment more on this in section 5.7. Using (5.42) we find the fixed point density for annihilations

$$n^c_{LSP} = 4.12 \times 10^{-15} \text{ GeV}^3. \tag{5.50}$$

We see that the produced density is greater than the fixed point value $n^{X_i}_{LSP} > n^c_{LSP}$ and annihilations will occur. This corresponds to the "LSP yield above the fixed point" case discussed above. Thus, the LSPs produced will quickly annihilate down toward the fixed point value in less than a Hubble time. The relic density of dark matter is then given by the fixed point value (5.50) and the critical density of LSPs today coming from decay of the light moduli is

$$\Omega^{X_i}_{LSP} = \frac{m_{LSP} Y^c_{LSP}}{\rho_c/s_0} = \frac{1}{\rho_c/s_0} \left(\frac{45}{2\pi\sqrt{10 g_*}\sigma_0} \right) \left(\frac{m^3_{LSP}}{M_P \, T^{X_i}_r} \right) = 0.76 \; h^{-2} \tag{5.51}$$

where s_0 and ρ_c are the entropy density and critical density today, respectively, and we have used the experimental value $\rho_c/s_0 = 3.6 \times 10^{-9} h^2 \; GeV$ with h parameterizing the Hubble parameter today with median value $h = 0.71$.

In addition to this contribution, there is also the contribution from the decay of non-thermal gravitinos produced from the heavy modulus which have a final abundance $Y^{final}_{3/2} \approx 10^{-14}$. The contribution from gravitinos to the critical density of dark matter is then

$$\Omega^{(3/2)}_{LSP} = \frac{m_{LSP} Y^{final}_{3/2} s_0}{\rho_c} = 0.0008 h^{-2}, \tag{5.52}$$

which is negligible compared with that coming from the light moduli.

Thus, the total critical density in dark matter coming from the LSPs of the G_2-MSSM is :

$$\begin{aligned}\Omega_{LSP}\, h^2 \;&\approx\; 0.27 \left(\frac{m_{LSP}}{100\,\mathrm{GeV}}\right)^3 \left(\frac{10.75}{g_*(T_r)}\right)^{1/4} \left(\frac{3.26\times 10^{-7}\mathrm{GeV}^{-2}}{\langle\sigma v\rangle}\right) \\ &\quad\times \left(\frac{4}{D_{X_i}}\right)^{1/2} \left(\frac{2\, m_{3/2}}{m_{X_i}}\right)^{3/2} \left(\frac{100\ \mathrm{TeV}}{m_{3/2}}\right)^{3/2}, \end{aligned} \tag{5.53}$$

where we have included all the parametric dependence of the answer derived in Appendix C.2. This value should be compared to the experimental value $\Omega_{CDM}h^2 = 0.111 \pm 0.006$ [152]. For those used to $\langle\sigma v\rangle$ in other units, note that $1\,\mathrm{GeV}^{-2} = 0.4\times 10^{-27} cm^2$.

This result is not presented in terms of central values – rather it is the best value we can obtain. The LSP mass can be larger than 100 GeV, but not smaller. The constant D_{X_i} can be order 4, but a scan of the microscopic parameter space suggests a somewhat smaller value for the only calculable example so far known (see appendix C.2.4). A better understanding of the string theory could give 4 or a larger value. Whereas $m_{3/2}$ is somewhat constrained to be at most about 100 TeV by the parameters of the framework, as explained in [30]. Therefore, this framework is rather constrained and predictive. We view the closeness of this result as a success, and as an indication that improving the underlying theory may improve the agreement with data.

5.7 Discussion of Results

We have seen in the previous sections that for natural values of microscopic parameters, there is no moduli and gravitino probem in realistic G_2 compactifications.

In addition, within the G_2-MSSM, the non-thermal production of Wino LSPs from the light moduli give rise to a relic density with the right order of magnitude (up to factors of a few). It is possible that with a more sophisticated understanding of the theory, one could obtain a result more consistent with the observational results. It is also worthwhile to understand these results from a physical point of view. The results obtained above depend surprisingly little on many of the details of the microscopic parameters. In particular, there is essentially no dependence of the final relic density on the total number of moduli (N), the masses (m_{X_N}, m_ϕ) and couplings (D_{X_N}, D_ϕ) of the heavy modulus and meson fields as well as the initial amplitudes of the moduli (f_{X_k}) and meson (f_ϕ) fields. This is good in a sense since our understanding of the underlying theory and many of the above microscopic parameters is incomplete. However, the result does depend crucially on certain qualitative (and also some quantitative) features of the underlying physics, as we discuss below. In general it is better if results depend on the microscopic theory, since then data can tell us about the underlying theory.

One very important feature which helps avoid the gravitino problem is that the meson and light moduli have masses which are of order (actually slightly below) two gravitino masses, as we saw explicitly in Section 4.1, This kinematically suppresses their decays to the gravitino. The gravitino abundace is thus dominated by decay of the heavy modulus which is further diluted by entropy production from the decays of the meson and light moduli. Therefore, a natural mechanism for solving the gravitino problem in a generic setup is that the modulus which decays last does not decay to

the gravitino, The moduli problem can also be easily solved in frameworks where the gravitino mass is $\gtrsim 10$ TeV, which is naturally satisfied in the G_2 framework.

Another qualitative feature of the G_2 framework is that there is a hierarchy in the time scales of decay of the various moduli (meson) fields. Since the mass of the heavy modulus is much larger (~ 300 times) than that of the other moduli (meson), it decays much earlier. Also, from our current understanding of the Kähler potential of the meson and moduli fields, one finds (see appendix C.2) that the meson decays before the light moduli due to a larger decay width. The precise computation of the decay width depends on the nature of the Kähler potential for the meson and moduli and the Kähler metric for matter fields, and one might argue that there are inherent uncertainties in our understanding of these quantities. However, the only qualitative feature relevant for cosmological evolution is that the meson decays before the light moduli. As long as the light moduli decay last (which we have argued in the appendix to be the natural case from our current understanding of the Kähler potential), the result does not depend on any of the masses and couplings of the heavy modulus or the meson field. The final result depends only on the masses and couplings of the light moduli which decay last. The same qualitative feature could be present in other frameworks arising from other limits of string/M-theory.

Now that it is clear that it is the light moduli decaying at the end which affect the final relic density, it is important to understand their effect more closely. In any theory of (soft) supersymmetry breaking, the mass of the light moduli will be set by the gravitino mass scale. In the context of low energy supersymmetry, the gravitino

mass will typically be in the range $1 - 100$ TeV. Therefore, the light moduli will also be typically in the above range[7]. Since the reheat temperature of the moduli basically depends on the moduli masses (assuming the coefficient D_{X_i} is $\mathcal{O}(1)$), the light moduli will typically give rise to a reheat temperature $T_r^{X_i}$ of $\mathcal{O}(1-100)$ MeV, which is far smaller than the freezeout temperature of the LSPs ($T_f^{LSP} \sim$ GeV) which could be produced from the light moduli. This is true for the G_2 framework and could be true for many other frameworks as well. Therefore, with $T_r^{X_i} < T_f^{LSP}$, the final outcome for the relic density will depend on the whether the number density of the LSPs produced from the light moduli ($n_{LSP}^{(X_i)}$) is greater or smaller than the critical number density at $T_r^{X_i}$ ($n_{LSP}^{(c)}|_{T_r^{X_i}}$).

For the G_2 framework, for natural values of the microscopic parameters one finds that $n_{LSP}^{(X_i)} > n_{LSP}^{(c)}|_{T_r^{X_i}}$ as shown in section 5.6.3. This is equivalent to the inequality:

$$\begin{aligned} B_{LSP}^{(X_i)} D_{X_i} &> \frac{1.5}{\sigma_0} \left(\frac{m_{LSP}^2}{m_{X_i}^2}\right) \approx 120\,\gamma^2 \\ \text{with } \gamma &\equiv \frac{m_{LSP}}{m_{3/2}} \end{aligned} \tag{5.54}$$

where σ_0 is defined by (5.49) and we have used $m_{X_i} \approx 1.96\, m_{3/2}$. As explained in [30], the quantity γ depends predominantly on δ, which characterizes the threshold correction to the gauge couplings at the unification scale. The dependence on other microscopic parameters such as V_7 and C_2 (see section 5.4) is largely absorbed into the gravitino mass. The suppression factor γ depends almost linearly on $|\delta|$, and typically takes value in the range $\sim (1-6)\times 10^{-3}$. Now, the constraint (5.54) is easy

[7]This is however not true for Large Volume compactifications as the lightest modulus in that case is much lighter than $m_{3/2}$ [20].

to understand. For natural values of microscopic parameters in the G_2 framework, one has $B_{LSP}^{(X_i)} = \mathcal{O}(25\%)$, $D_{X_i} = \mathcal{O}(1)$ (see appendix C.2) which easily satisfy (5.54) above. In order for other frameworks to realize this situation, a criterion similar to (5.54) needs to be satisfied.

When (5.54) is satisfied, the final relic density can be written as (see (5.50) and (5.53)):

$$\begin{aligned}
\Omega_{LSP}\, h^2 &\approx \frac{m_{LSP} Y_{LSP}^c}{\rho_c/s_0} = \frac{1}{\rho_c/s_0}\left(\frac{45}{2\pi\sqrt{10 g_*}\sigma_0}\right)\left(\frac{m_{LSP}^3}{M_P\, T_r^{X_i}}\right) \\
&\approx \frac{1}{\rho_c/s_0}\left(\frac{45}{2\sqrt{10\pi}(40 g_*)^{1/4}\sigma_0}\right)\left(\frac{m_{LSP}^3}{D_{X_i}^{1/2} M_P^{1/2} m_{X_i}^{3/2}}\right) \\
&\approx 18\ \mathrm{GeV}^{-3/2}\left(\frac{m_{LSP}^{3/2}\gamma^{3/2}}{D_{X_i}^{1/2}}\right) = 18\ \mathrm{GeV}^{-3/2}\left(\frac{m_{3/2}^{3/2}\gamma^3}{D_{X_i}^{1/2}}\right) \qquad (5.55)
\end{aligned}$$

An upper bound on the observed value of the relic density implies that smaller values of γ and m_{LSP} and larger values of D_{X_i} are preferred. A small γ implies that for a given LSP mass a heavier gravitino is preferred implying that the moduli be correspondingly heavier. Also, since γ is roughly linear in $|\delta|$, smaller values of $|\delta|$ are preferred. These features can be seen easily from the plots in figures 5.1 and 5.2. Figure 5.1 shows a contour plot of the relic density in the $D_{X_i} - m_{3/2}$ plane for two (large and small) values of $|\delta|$ which correspond to two (large and small) values of γ.

Figure 5.2 shows the dependence of the relic density on the reheat temperature of the light moduli ($T_r^{X_i}$). As seen from the first line in Eq. (5.55), the relic density is inversely proportional $T_r^{X_i}$ implying that a higher reheat temperature is preferred. A higher $T_r^{X_i}$ corresponds precisely to a larger D_{X_i} and m_{X_i} (larger $m_{3/2}$) as explained

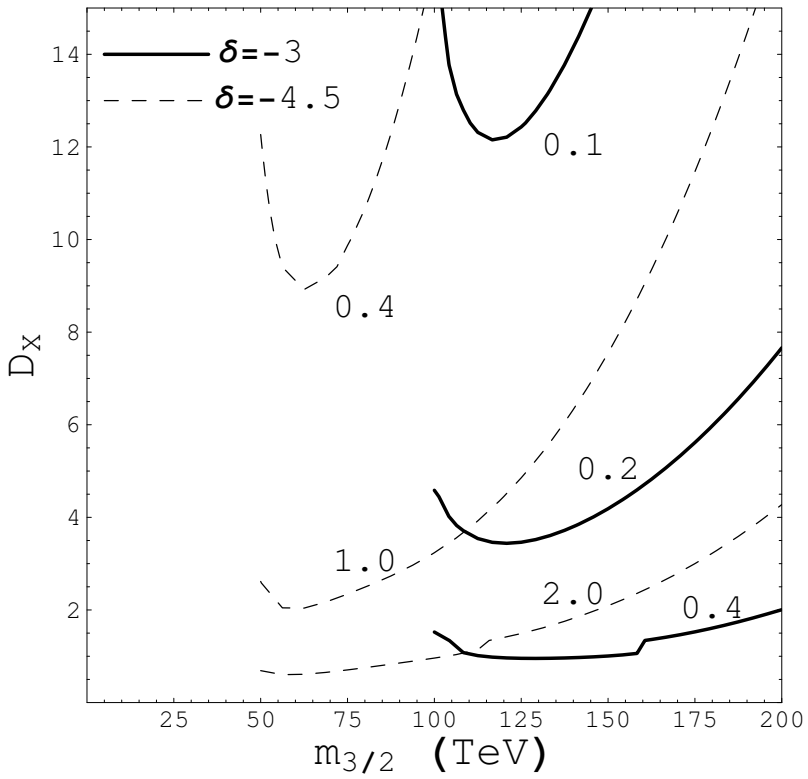

Figure 5.1: The contour plot of the relic density in the G_2-MSSM in the $D_{X_i} - m_{3/2}$ plane for two (large and small) values of $|\delta|$ which correspond to two (large and small) values of γ. The solid lines are for $\delta = -3$ (a correction to α_{unif}^{-1} of order 3/26), and the dashed lines for $\delta = -4.5$.

above.

As explained in section 5.6.3, the nature of the LSP is also crucial to the final result for the relic density. For the G_2 framework, the annihilation cross-section is s-wave and does not depend on $T_r^{X_i}$. On the other hand, if the LSP were Bino, the cross-section would be p-wave suppressed and would depend linearly on $T_r^{X_i}/m_{LSP}$, thereby making it suppressed relative to the s-wave result. This would make the relic density much larger than the result obtained for the s-wave case above. Therefore, the upper bound on relic density prefers small mixing angles (or vanishing mixing

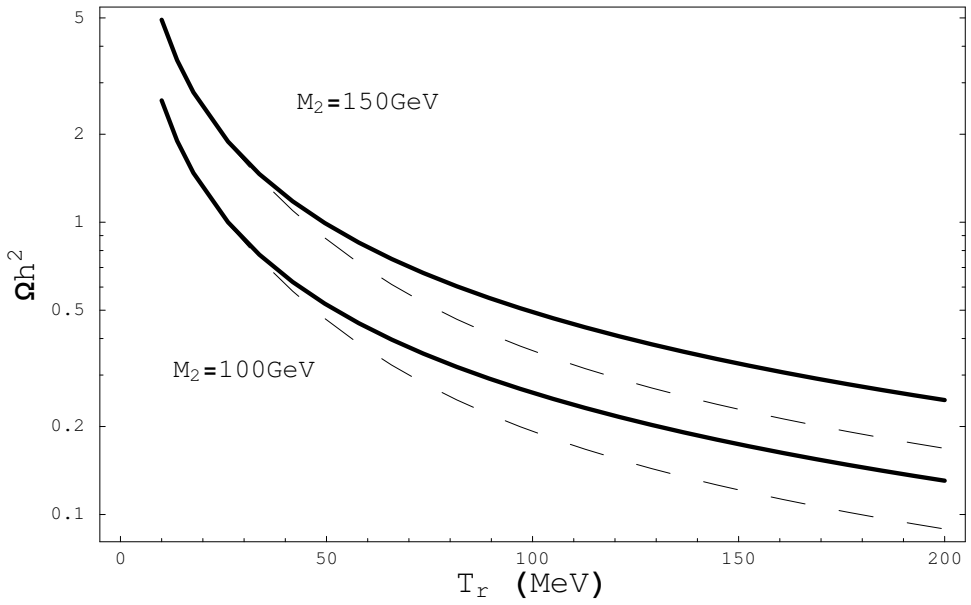

Figure 5.2: The LSP relic density for the G_2-MSSM plotted as a function of the reheat temperature of the light moduli. The solid line assumes no coannihilation with charged Winos; the dashed line includes coannihilation with charged Winos.

angles, as in the G_2-MSSM) with the Bino and Higgsino components. This can be seen from figure 5.3.

5.8 Summary and Future Directions

In this paper we have emphasized the importance of the cosmological moduli and gravitino problems and the relation to adequate generation of dark matter in thermal equilibrium, or generation of too much dark matter non-thermally in string/M theory frameworks. Focussing on G_2 compactifications, in particular on the G_2-MSSM, we have found that the decay of moduli in this framework is rather naturally consistent

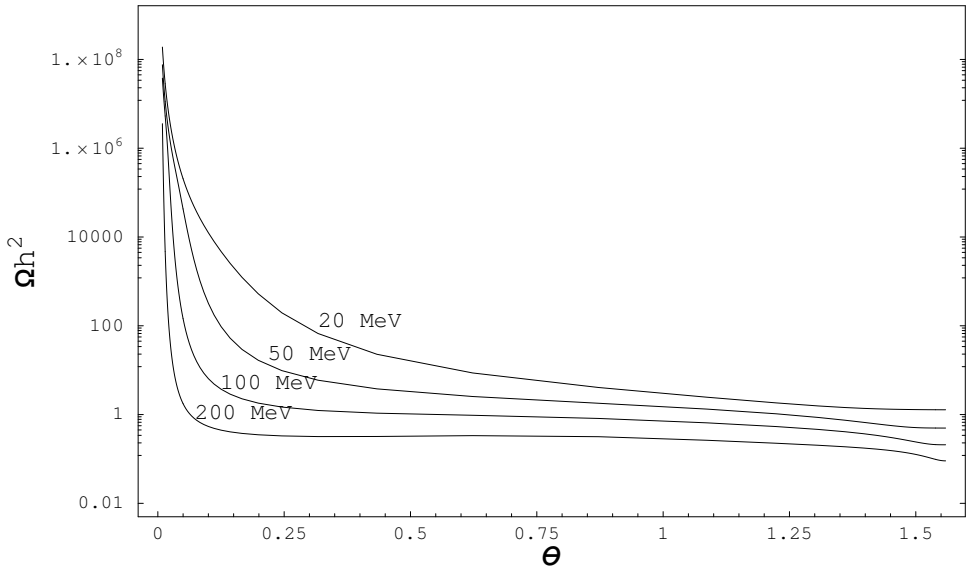

Figure 5.3: The LSP relic density in the G_2-framework plotted as a function of the mixing angle of Bino and Wino for $M_2 = 100$GeV.

with BBN constraints, and the associated large entropy production at late times (but before BBN) results in an avoidance of the gravitino problem(s). Moreover, we have seen that the late decay of the light moduli into Wino-like neutralinos leads to a nearly acceptable relic density of cold dark matter. This result arises from a combination of entropy production and LSPs from moduli decay giving an adequate relic density from non-thermal production of dark matter. This process offers an explicit example of how *thermal dark matter production is not the dominant source of cosmological dark matter, especially in the presence of moduli.* The LSP is Wino-like here as well as in anomaly mediated theories, but for interestingly different

reasons – here the tree level gaugino masses are universal but about the same size as the anomaly mediated ones, and the finite one loop Higgsino is comparable with both.

The result for the final relic density depends parametrically on the couplings and mass of the light moduli (which decay last) and the mass of the LSP. The masses of the light moduli and the LSP are set by the gravitino mass scale and depend on a set of underlying microscopic parameters of the theory. The couplings of the moduli depend on the Kähler potential of the theory. Since our understanding of the Kähler potential is incomplete, it is only possible to make reasonable assumptions to proceed, which is what we have done, but one can see that most of the results are insensitive to these uncertainties. That is because the moduli decays produce a large number density of LSPs, which then annihilate down to the final relic density that only depends on the reheating temperature. From Eq. (5.55) and figure 5.1, we see that an upper bound on the relic density prefers a light LSP, heavy gravitino and large couplings to the visible sector parameterized by D_{X_i} (defined in Eq. (5.34)). These results obtained have been explained in terms of the underlying qualitative features of the framework. These qualitative features could be present in other string/M theory frameworks as well, leading to similar results.

There is not yet a satisfactory inflation mechanism for the G_2-MSSM. This is under study. Fortunately, our results are not sensitive to that. We assume only that at an early time inflation ends and the energy density of the universe is dominated by moduli settling into the minimum of the potential.

In future, one would like to understand the origin of the baryon asymmetry in the Universe (BAU) within string/M-theory frameworks. In the G_2 framework, the large entropy production resulting from the decay of the moduli was crucial for addressing the gravitino problem. However, this entropy will also act to reduce any initial baryon asymmetry. Therefore, one requires a large initial asymmetry or a late-time mechanism for regeneration of the asymmetry. For example, a large initial baryon asymmetry could arise from the Affleck-Dine mechanism [153], or it could happen that the superpartner parameter space allows for late-time electroweak baryogenesis. This is work in progress.

Understanding the above issues would be crucial to solving the "cosmological inverse problem" (see [154, 155] for some preliminary work in this direction), usually considered separate from the "LHC Inverse Problem" [156]. Within the context of realistic string/M-theory frameworks, however, the two inverse problems merge into one "inverse problem" as the microscopic parameters characterizing the underlying physics of any framework have predictions (at least in principle) for both particle physics as well as cosmological observables, thereby providing unique connected insights into these basic issues.

CHAPTER VI

Conclusion

With the start of the LHC and many other experiments soon, interpreting new data and testing theories will be the main subject in the following many years. For theorists, it is crucial to bring their favorite theory into contact with experiments. In this thesis, I focus on a quite generic setup of G_2 compactification of M-theory with moduli stabilized. This scenario has several notable appealing features: first, moduli are stabilized by gaugino condensation and supersymmetry is broken dynamically at the same time. Second, the TeV scale can be qualitatively obtained in the allowed region of parameter space. Third, there is a unique de Sitter minimum in the potential. This makes it interesting to perform a detailed phenomenology analysis. Along this line, I have studied in detail the soft supersymmetry breaking terms, and calculate the low energy superpartner mass spectra. Then I have systematically studied several important phenomenological topics, for example, the prospects for the LHC, CP violation and EDMs predications, dark matter and cosmological issues.

The M-Theory scenario in our study is very distinctive in that it will lead to four-top signatures in the LHC. Thus it can be discovered at the early stage after the LHC

starts. In addition, the CP violating phases in this scenario is naturally suppressed. The main CP violation comes from the non-universal A-terms, which gives non-trivial predictions for EDMs of electron, neutron and Mercury. The aspects of dark matter is also promising. The dark matter relic density could be generated non-thermally and qualitatively in consistent with the current observation. Moreover, the notorious moduli and gravitino problems are naturally solved due to mass relation between different moduli fields and gravitino. Of course, there are still much to be done to get a complete scenario for phenomenology. Particularly, inflation, axion and strong CP problem which could be discussed in the near future.

There are many directions for future research. From a theoretical perspective, one of the most outstanding problems is to explicitly construct a visible sector with MSSM or its extension. Although this is a difficult task in general, substantial progress has been made based on constructions of local singularities using the techniques of geometric engineering [157–160]. Of course, the more ambitious goal is to construct global examples of G_2 manifolds with the right structure of conical and orbifold singularities. This would require a major breakthrough from a mathematical point of view. However, a better understanding of the dualities from Heterotic and Type IIA string theory could also lead to important insights.

From the phenomenological perspective, it would be extremely useful to study variations of the minimal proposal which could solve important phenomenological problems while still retaining the desirable features. A good feature of this framework is that important phenomenological issues such as inflation, generation of small

neutrino masses, explanation of quark mass hierarchy and strong CP problem etc. can in principle be addressed within this framework.

Although restricted to the M-Theory scenario, most of the techniques and ideas can be generalized to other corners of String/M-Theory. Similar analysis for other types of string frameworks will certainly be interesting and must be done in parallel with the bottom-up study. With the LHC data, one hopes certain string framework can be favored and others disfavored if the corresponding LHC signatures are studied in detail. This will eventually allows us to learn about the correct string vacuum in which we are living.

APPENDICES

APPENDIX A

Calculation of P_{eff}

A.1 General Discussion

As we have seen in section 2.3, a large P_{eff} is crucial for the validity of our solutions and the supergravity approximation. It also leads to the the suppression of tree-level gaugino masses compared to the gravitino mass. Finally, in order to tune the cosmological constant, one requires $P_{\text{eff}} = 84$ (83 if one includes higher order corrections) for $Q - P = 3$. In this paper, until now we have just used P_{eff} as one of the parameters which could vary within a certain range. However, in an explicit microscopic construction of the hidden sector, it is computable from first principles. From the definition:

$$P_{\text{eff}} \equiv P \ln \left(\frac{C_1}{C_2} \right) \tag{A.1}$$

it is easy to see that for a large P_{eff} such as 83, a large splitting in the coefficients C_1 and C_2 is required. Here for the convenience of the discussion, we have introduced C_1 and C_2 through $C_1 = A_1/P$ and $C_2 = A_2/Q$. At tree level, these coefficients are

simply determined by the cutoff scale of the effective gauge theory and are given by $(\Lambda_{\rm cutoff}/M_P)^3$. This would not give a large $P_{\rm eff}$. However, one has to take into account threshold corrections to the gauge couplings of the hidden sectors. To compute the threshold corrections, one has to specify the concrete setup of the hidden sector $\mathcal{Q}$, as well as the geometry of the three-cycle where the hidden sector lives. Generally the one-loop gauge couplings can be written as:

$$\frac{16\pi^2}{g^2(\mu)} = \frac{16\pi^2}{g_M^2} + b\log(\Lambda^2/\mu^2) + S, \tag{A.2}$$

where b is the one-loop beta function coefficient, and S is the one-loop threshold correction. For instance, the contribution from KK modes has the form [50]:

$$S = S' + 2N_c\log(\mathrm{Vol}(\mathcal{Q})\Lambda_{\rm cutoff}^3), \tag{A.3}$$

where $\mathrm{Vol}(\mathcal{Q})$ is the volume of the hidden-sector three-cycle $\mathcal{Q}$ and S' can be expressed in terms of certain topological invariants of $\mathcal{Q}$, known as the "Ray-Singer analytic torsion". Before we go to explicit examples, we would like to show the general requirement on the threshold corrections. Let us first denote the gauge kinetic function as $f = f_0 + \Delta f_1$ and $f_2 = f_0 + \Delta f_2$, where $\Delta f_{1,2}$ are the corresponding threshold correction. The superpotential from strong gauge dynamics can be written as:

$$W \sim \Lambda_{\rm cutoff}^{3+\alpha}\,|\phi|^{-\alpha}\,P\,e^{-\frac{2\pi}{P}(f+\Delta f_1)} + \Lambda_{\rm cutoff}^3\,Q\,e^{-\frac{2\pi}{Q}(f+\Delta f_2)} \tag{A.4}$$

We can easily identify the coefficient $C_{1,2}$ as follows:

$$C_1 = \left(\frac{\Lambda_{\rm cutoff}}{M_P}\right)^{3+\alpha} e^{-\frac{2\pi}{P}\Delta f_1} \tag{A.5}$$

$$C_2 = \left(\frac{\Lambda_{\rm cutoff}}{M_P}\right)^{3} e^{-\frac{2\pi}{P}\Delta f_2} \tag{A.6}$$

Since $\alpha = 2/P$ is small, we have

$$\frac{C_1}{C_2} \approx e^{-\frac{2\pi}{P}\Delta f_1 + \frac{2\pi}{Q}\Delta f_2}. \tag{A.7}$$

For the case $Q - P = 3$ and $P_{\rm eff} = 84$, using Eq.(A.1) and (A.7) we have the estimate

$$\Delta f_1 - \Delta f_2 \sim 14. \tag{A.8}$$

In view of the fact that $f_0 \approx \frac{14}{3}Q = \mathcal{O}(50)$, the requirement Eq.(A.8) is not completely unreasonable.

A.2 A Particular Example - $\mathcal{Q} = S^3/Z_k$

As a particular example, we consider the three-cycle $\mathcal{Q}$ to be the lens space S^3/Z_k as in this case the threshold corrections can be computed. In addition, for concreteness, we consider a situation where the first hidden sector gauge group is obtained from a larger group $SU(P+M+1)$ by Wilson line breaking $SU(P+M+1) \to SU(P+1) \times SU(M) \times U(1)$, while the second hidden sector group is still $SU(Q)$ without breaking. Again we assume one flavor of charged matter Q and $\bar{Q}$. As long as M is sufficiently smaller than P (such as $< P/2$), we can neglect its contribution to the superpotential and also in moduli stabilization. The calculation of the threshold correction is similar to that in [50]. For the first hidden sector, it is

given by $S_1' = 2(P+1)\,T_{\mathcal{O}} + 2M\,T_\lambda$, while for the second one it is $S_2' = 2Q\,T_{\mathcal{O}}$. T_λ and $T_{\mathcal{O}}$ are the relevant torsions:

$$T_{\mathcal{O}} = -\log(k), \quad T_\lambda = \log(4\sin^2(G\pi\lambda/k)), \tag{A.9}$$

where $G = P + M + 1$, and λ is an integer specifying the Wilson line. As discussed above, $C_{1,2}$ can be calculated straightforwardly, which are

$$C_1 = M_P^{-3}\,\langle \mathrm{Vol}(\mathcal{Q})^{-(1+1/P)}\rangle\,\Lambda_{\mathrm{cutoff}}^{-1/P}\,e^{-\frac{S_1'}{2P}} \tag{A.10}$$

$$C_2 = M_P^{-3}\,\langle \mathrm{Vol}(\mathcal{Q})^{-1}\rangle\,e^{-\frac{S_2'}{2Q}}. \tag{A.11}$$

Here, $\mathrm{Vol}(\mathcal{Q})$ is the dimensionful volume of the hidden-sector three-cycle $\mathcal{Q}$. It is important to remember that C_1, C_2 should be thought of as depending on the vacuum expectation value of $\mathrm{Vol}(\mathcal{Q})$ as shown in the above equation. Therefore, this dependence does not invalidate the holomorphicity of the superpotential. One can now compute the P_{eff} from the above equations:

$$\begin{aligned} P_{\mathrm{eff}} &\approx P(-\frac{S_1'}{2P} + \frac{S_2'}{2Q}) \\ &= -T_{\mathcal{O}} - M\,T_\lambda \\ &= \log(k) - M\log(4\sin^2(G\pi\lambda/k)) \end{aligned} \tag{A.12}$$

It is obvious that k has to be very large to get a large P_{eff}. For example, $P = 15$, $Q = 18$, $M = 10$, $V_7 = 50$, $\lambda = 80$ and $k = 99$ gives $P_{\mathrm{eff}} = 58$ and $C_2 = 1.5 \times 10^{-4}$. Notice C_2 is much smaller than one. The gravitino for this case is about 0.8TeV. One can also consider other patterns of symmetry breaking, e.g. $SO(2(P+1)) \to SU(P+1)\times U(1)$. In this case smaller values of k compared to the previous example

can give rise to a large P_{eff}, although in general a large k is still needed. Large values of k may seem unrealistic, but that is not clear since the allowed possibilities for compact G_2 manifolds fibred over Lens spaces with large k are not known. In addition, although at present it is not known how to compute the torsion for other three-cycles, it is possible that a large P_{eff} can be obtained more "naturally" in other examples.

A.3 More Possibilities

Other three manifolds might give rise to a large P_{eff} more naturally. Rather than study further explicit examples we give a toy model which illustrates this possibility. The model has parameters which extend the previous example and is given by

$$T_{\mathcal{O}} = -\gamma_0 \log(k), \quad T_{\lambda_1} = \gamma_1 \log(\alpha \sin^2(G\pi\lambda_1/k)),\ T_{\lambda_2},\ T_{\lambda_3}, ... \tag{A.13}$$

where G is an integer and $\gamma_{0,1}$ are determined by the topology of the manifold and are kept as free parameters. α is determined by group theory. In general, there could be other non-trivial torsions $T_{\lambda_2}, T_{\lambda_3}$, etc. depending on how the higher gauge group is broken by the Wilson lines. In order to illustrate the idea, we will restrict to $T_{\mathcal{O}}$ and T_{λ_1}. Let's again consider the case where the first hidden sector group $SU(P+1)$ arises from the breaking $SU(P+M+1) \to SU(P+1) \times SU(M) \times U(1)$. Now, it is possible to get both $P_{\text{eff}} \approx 84$ and $C_2 \sim \mathcal{O}(1)$. For example, the set of parameters $\gamma_0 = \gamma_1 = 6.3$, $P = 15$, $Q = 18$, $M = 10$, $V_7 = 50$ and $k = 11$ gives $P_{\text{eff}} = 84.2$ and $C_2 = 5.4$.

The above example was shown just to illustrate the fact that with more general

three-cycles $\mathcal{Q}$, it may be possible to obtain a large $P_{\rm eff}$ quite naturally. As another possibility, if $\mathcal{Q}$ is such that the relevant torsions $T_{\mathcal{O}}, T_{\lambda_1}, T_{\lambda_2}$, etc. in (A.13) have a linear dependence on k instead of logarithmic one, it is quite easy to obtain a large $P_{\rm eff}$ naturally. In addition, if there are massive quarks[1] which are charged under the hidden sector gauge group, the strong coupling scale will be lowered and both the values of $P_{\rm eff}$ and C_2 will be affected.

To summarize, the values of $P_{\rm eff}$ and C_2 depend crucially on the microscopic details of the hidden sector and can take a wide range of values. Therefore, in our phenomenological analysis, we have simply assumed that $P_{\rm eff}$ and C_2 can take values in the range of phenomenological interest.

[1]Of course, their masses should be larger than the strong coupling scale.

APPENDIX B

Calculation of Electric Dipole Moments

B.1 Dynamical Alignment of Phases in the Superpotential

The dynamical alignment of phases is crucial for solving the SUSY CP problem. It means that all terms in the superpotential dynamically align to acquire the same phase in the vacuum. To show that, we start with the generic moduli superpotential

$$W = \sum_{n=1}^{N_W} |W_n| e^{i\gamma_n} \tag{B.1}$$

The superpotential depends on geometric moduli z_i as well as other chiral superfields ϕ_i in general. It is generically a polynomial and/or exponential function of these fields (for example, see Eq. (4.6)), and so γ_n are functions of $\mathrm{Im}(z_i)$ and the phase of ϕ_i, which are collectively denoted by ψ_i. The scalar potential in $\mathcal{N} = 1$ supergravity is written as:

$$V = e^K \left(K^{i\bar{j}} D_i W D_{\bar{j}} \overline{W} - 3|W|^2 \right) \tag{B.2}$$

In the following, we consider the Kähler metric to be diagonal for simplicity, but the results are independent of this assumption. Then we have:

$$V \sim \sum_i K^{i\bar{i}} |D_i W|^2 - 3|W|^2, \tag{B.3}$$

where

$$\begin{aligned} |W|^2 &= \sum_n |W_n|^2 + 2 \sum_{n \neq m} |W_n||W_m| \cos(\gamma_n - \gamma_m), \\ |D_i W|^2 &= \sum_n |D_i W_n|^2 + 2 \sum_{n \neq m} |D_i W_n||D_i W_m| \times \cos(\gamma_n - \gamma_m). \end{aligned} \tag{B.4}$$

The second line in Eq. (B.4) can be obtained by utilizing the fact that the superpotential is generically a polynomial and/or exponential function of fields. For fields ϕ_i occurring polynomially, one has $\partial_i W_n \sim W_n/\phi_i = \text{real} \times e^{i\gamma_n - i\gamma_{\phi_i}}$ as well as $\partial_i K\, W_n = \text{real} \times e^{i\gamma_n - i\gamma_{\phi_i}}$. Similarly, for fields z_i occurring exponentially in the superpotential, one has $\partial_i W_n = \text{real} \times e^{i\gamma_n}$ as well as $\partial_i K\, W_n = \text{real} \times e^{i\gamma_n}$, giving rise to the expressions in Eq. (B.4) above. This then implies that the first and second terms in Eq. (B.3) contain the same functional dependence on γ_n.

Therefore, the minimization of the scalar potential with respect to ψ_i gives

$$\sum_{n \neq m} A_{nm} \sin(\gamma_n - \gamma_m) \partial_{\psi_i} \left[\gamma_n(\psi_i) - \gamma_m(\psi_i)\right] = 0 \tag{B.5}$$

where A_{nm} is a real matrix and the explicit form is not important here. Since γ_n is a combination of several phases, $\partial_{\psi_i}(\gamma_n - \gamma_m)$ is non-zero for some i in general. Therefore, the solution to the system of equations in Eq. (B.5) is:

$$\sin(\gamma_n - \gamma_m) = 0 \tag{B.6}$$

Generically, the number of degree of freedom ψ_k is more than the number of γ_n, and the above equations can be solved by $\gamma_n = \gamma_m$ for any n and m. As an example, for the superpotential in (4.6), there is only one independent equation corresponding to the combination $((b_1 - b_2)\vec{N} \cdot \vec{t} + a\gamma_\phi)$ but $N + 1$ degree of freedom corresponding to N axion t_i and the phase of the meson γ_ϕ. This means all W_n share the same phase, which proves that the phases are dynamically aligned in the vacuum. Of course, if the number of dynamical phases is less than the number of independent equations, then there could be relative phases between different terms in the superpotential. However, that is not generic.

B.2 One-loop Diagrams

The fermion EDMs can be generated at one-loop in supersymmetric models with CP-violating phases in the soft supersymmetry breaking sector. Within the framework considered in this paper, the CP-violating phases only reside in the trilinear terms and therefore appear in the mass mixing terms of the left- and right-handed sfermions. Therefore, the main contribution to the quark EDM and CEDM comes from diagrams involving gluinos because of the large gauge coupling. For the electron EDM, the dominant contribution comes from the diagram involving neutralinos. This is because the diagrams with charginos in the loop require CP-violating phases in the chargino sector which do not arise within the M-theory framework considered.

Let us first consider the diagrams contributing to quark EDM and CEDM with

gluino running in the loop

$$d_q^{\tilde{g}(E)} = \frac{-2e\alpha_s}{3\pi}\sum_{k=1}^{2}\mathrm{Im}(\Gamma_q^{1k})\frac{m_{\tilde{g}}}{m^2_{\tilde{q}_k}}Q_{\tilde{q}}B\left(\frac{m^2_{\tilde{g}}}{m^2_{\tilde{q}_k}}\right) \quad \text{(B.7)}$$

$$d_q^{\tilde{g}(C)} = \frac{g_s\alpha_s}{4\pi}\sum_{k=1}^{2}\mathrm{Im}(\Gamma_q^{1k})\frac{m_{\tilde{g}}}{m^2_{\tilde{q}_k}}C\left(\frac{m^2_{\tilde{g}}}{m^2_{\tilde{q}_k}}\right) \quad \text{(B.8)}$$

where $\Gamma_q^{1k} = D_{q2k}D^*_{q1k}$ and D_q is the 2×2 matrix which diagonalizes the squark mass matrix $m^2_{\tilde{q}}$

$$D_q^\dagger m_q^2 D_q = \mathrm{Diag}(m^2_{\tilde{q}1}, m^2_{\tilde{q}2}). \quad \text{(B.9)}$$

More explicitly

$$\begin{aligned}\tilde{q}_L &= D_{q11}\tilde{q}_1 + D_{q12}\tilde{q}_2\\ \tilde{q}_R &= D_{q21}\tilde{q}_1 + D_{q22}\tilde{q}_2.\end{aligned} \quad \text{(B.10)}$$

Here $B(r)$ and $C(r)$ are loop functions defined as:

$$\begin{aligned}B(r) &= \frac{1}{2(r-1)^2}\left(1 + r + \frac{2r\ln(r)}{1-r}\right)\\ C(r) &= \frac{1}{6(r-1)^2}\left(10r - 26 + \frac{2r\ln(r)}{1-r} - \frac{18\ln(r)}{1-r}\right)\end{aligned}$$

In the above equations, we assume no flavor mixing in the squark mass matrices as argued in the main body of the paper. Using the fact that $\mathrm{Im}(\Gamma_q^{11}) = -\mathrm{Im}(\Gamma_q^{12})$, we have:

$$d_q^{\tilde{g}(E)} \approx \frac{-2e\alpha_s Q_{\tilde{q}}}{3\pi}\frac{\mathrm{Im}(m^2_{\tilde{q}})_{LR}}{m^3_{\tilde{g}}}r^2\left(B(r) + r\,B'(r)\right) \quad \text{(B.11)}$$

Similarly

$$d_q^{\tilde{g}(C)} \approx \frac{g_s\alpha_s}{4\pi}\frac{\mathrm{Im}(m^2_{\tilde{q}})_{LR}}{m^3_{\tilde{g}}}r^2\left(C(r) + r\,C'(r)\right) \quad \text{(B.12)}$$

In the calculation above, we assume the mass splitting of squarks is small compared to the squark mass. This is usually true since we are only interested in the up and down squarks. When $r = m_{\tilde{g}}^2/M_{\tilde{q}}^2 \ll 1$, one finds that $C(r) \gg A(r), B(r)$. It is easy to see that $d_q^{\tilde{g}(C)} \gg d_q^{\tilde{g}(E)}$. For other diagrams which involve neutralino and charginos, the structure is very similar. However, they are much smaller than $d_q^{\tilde{g}}$ and can be neglected.

Now let us turn to the one-loop diagrams contributing to the electron EDM

$$d_e^{\tilde{\chi}^+} = \frac{e\alpha_{em}}{4\pi \sin^2\theta_W} \sum_{k=1}^{2} \mathrm{Im}(\Gamma_{ei}) \frac{m_{\tilde{\chi}^+}}{m_{\tilde{\nu}}^2} A\left(\frac{m_{\tilde{\chi}^+}^2}{m_{\tilde{\nu}}^2}\right) \tag{B.13}$$

$$d_e^{\tilde{\chi}^0} = \frac{e\alpha_{em}}{4\pi \sin^2\theta_W} \sum_{k,i=1,1}^{2,4} \mathrm{Im}(\eta_{eik}) \frac{m_{\tilde{\chi}^0}}{m_{\tilde{e}_k}^2} B\left(\frac{m_{\tilde{\chi}^0}^2}{m_{\tilde{e}_k}^2}\right) \tag{B.14}$$

where $\Gamma_{ei} = U_{i2}^* V_{i1}^*$, and

$$\eta_{eik} = \Big[-\sqrt{2}\left\{\tan\theta_W (Q_f - T_{3e}) X_{1i} + T_{3e} X_{2i}\right\} D_{e1k}^* + \kappa_e X_{bi} D_{e2k}^* \Big] \left(\sqrt{2}\tan\theta_W Q_e X_{1i} D_{e2k} - \kappa_e X_{bi} D_{e1k}\right)$$

Here we have

$$\kappa_e = \frac{m_e}{\sqrt{2} m_W \cos\beta} \tag{B.15}$$

The loop function $A(r)$ is given by

$$A(r) = \frac{1}{2(1-r)^2}\left(3 - r + \frac{2\ln(r)}{1-r}\right) \tag{B.16}$$

In the above equations, $U(V)$, X and D_e are the conventional chargino, neutralino and selectron mixing matrices. It is easy to see that the chargino diagram do not contribute to the electron EDM in the framework considered, since there is no CP-violating phases in the chargino sector. In the absence of the neutralino mixing, the

expression of $d_e^{\tilde{\chi}^0}$ can be significantly simplified

$$d_e^E \approx \frac{e\alpha_{em}}{4\pi\cos^2\theta_w}\frac{\mathrm{Im}(m_{\tilde{e}}^2)_{LR}}{m_{\tilde{B}}^3}\, r_1^2\,[B(r_1)+r_1B'(r_1)] \tag{B.17}$$

where $r_1 = m_{\tilde{B}}^2/m_{\tilde{e}}^2$ with $m_{\tilde{e}}$ denoting the average mass of the selectrons. In the above result, the higgsino contribution is neglected since it is suppressed by the small Y_e^2.

B.3 Barr-Zee Type Diagrams

As we have discussed in subsection 4.2.4, we are concerned with the Barr-Zee diagram with the third generation squarks, i.e. $\tilde{t}$ and $\tilde{b}$, running in the inner loop. Here we give the detailed derivation of Eq. (4.33) and (4.34). We start with the general results of EDM and CEDM for the Barr-Zee diagram [93]

$$\begin{aligned} d_f^E &= Q_f\frac{3e\alpha_{em}}{32\pi^3}\frac{R_f m_f}{M_A^2}\sum_{q=t,b}\xi_q Q_q^2\,[F(r_1)-F(r_2)] \\ d_f^C &= \frac{g_s\alpha_s}{64\pi^3}\frac{R_f m_f}{M_A^2}\sum_{q=t,b}\xi_q\,[F(r_1)-F(r_2)] \end{aligned} \tag{B.18}$$

where M_A is the mass of pseudoscalar higgs A_0, $r_{1,2} = m_{\tilde{q}_{1,2}}^2/M_A^2$, $R_f = \cot\beta(\tan\beta)$ for $I_3 = 1/2(-1/2)$ and $F(z)$ is the two-loop function

$$F(z) = \int_0^1 dx \frac{x(1-x)}{z-x(1-x)}\ln\left[\frac{x(1-x)}{z}\right]. \tag{B.19}$$

The CP-violating couplings are given by

$$\begin{aligned} \xi_t &= -\frac{\sin 2\theta_{\tilde{t}} m_t \mathrm{Im}(\mu e^{i\delta_t})}{2v^2\sin^2\beta} \\ \xi_b &= -\frac{\sin 2\theta_{\tilde{b}} m_b \mathrm{Im}(A_b e^{-i\delta_b})}{2v^2\sin\beta\cos\beta} \end{aligned} \tag{B.20}$$

where $\theta_{\tilde{t},\tilde{b}}$ are the stop and sbottom mixing angles, and $\delta_q = \mathrm{Arg}(A_q + R_q\mu^*)$. The mixing angle of the squark sector is given by

$$\begin{aligned}\tan(2\theta_q) &= -\frac{2m_q|\mu R_q + A_q^*|}{M_{\tilde{Q}}^2 - M_{\tilde{q}}^2 + \cos 2\beta M_Z^2(T_z^q - 2e_q s_w^2)} \\ &\approx -\frac{2m_q|\mu R_q + A_q^*|}{M_{\tilde{Q}}^2 - M_{\tilde{q}}^2}\end{aligned} \tag{B.21}$$

Therefore, Eq. (B.20) becomes

$$\begin{aligned}\xi_t &\approx \frac{y_t^2|A_t^* + \mu\cot\beta|\mathrm{Im}(\mu e^{i\delta_t})}{M_{\tilde{Q}}^2 - M_{\tilde{t}}^2} \\ \xi_b &\approx \cot\beta\frac{y_b^2|A_b^* + \mu\tan\beta|\mathrm{Im}(A_b e^{-i\delta_b})}{M_{\tilde{Q}}^2 - M_{\tilde{b}}^2}\end{aligned} \tag{B.22}$$

Using Eq. (B.20) and (B.21), we can rewrite Eq. (B.18) as

$$\begin{aligned}d_f^E &\approx Q_f\frac{3e\alpha_{em}}{32\pi^3}\frac{R_f m_f}{M_A^4}\mathrm{Im}\Bigg[\frac{4}{9}y_t^2\mu(A_t + \mu^*\cot\beta)F'(r_1) \\ &\qquad + \frac{1}{9}y_b^2 A_b(A_b^* + \mu\tan\beta)\cot\beta F'(r_2)\Bigg] \\ d_f^C &\approx \frac{g_s\alpha_s}{64\pi^3}\frac{R_f m_f}{M_A^4}\mathrm{Im}\Bigg[y_t^2\mu(A_t + \mu^*\cot\beta)F'(r_1) \\ &\qquad + y_b^2 A_b(A_b^* + \mu\tan\beta)\cot\beta F'(r_2)\Bigg]\end{aligned} \tag{B.23}$$

where $r_1 \equiv m_{\tilde{t}}^2/M_A^2$ and $r_2 \equiv m_{\tilde{b}}^2/M_A^2$ with $m_{\tilde{t},\tilde{b}}$ being the average masses of the stops and sbottoms respectively.

APPENDIX C

Cosmological Evolution of the Moduli

C.1 Cosmology of the G_2-MSSM Moduli – A Detailed Treatment

In this appendix, we include detailed calculations leading to the abundances, entropy production, and reheat temperatures quoted in the paper for sets of benchmark values of the microscopic parameters. The computation of couplings and decay widths of the moduli and meson fields in terms of the microscopic parameters which motivate the benchmark values will be given in appendix C.2. We have retained the parametric sensitivity to the gravitino mass, number of moduli (topology), and the overall couplings of the moduli (meson) in order to address the robustness and plausibility of the framework.

C.1.1 Heavy modulus oscillations

At the time the heavy moduli (X_N) starts coherent oscillations the universe is radiation dominated and the Hubble equation is given by

$$3H^2 = 3\left(\frac{1}{2}m_{X_N}\right)^2 = M_P^{-2}\left(\frac{\pi^2}{30}\right)g_* T^4. \tag{C.1}$$

The temperature at which the modulus starts oscillating is then given by

$$\begin{aligned} T_{osc}^{X_N} &= \left(\frac{90}{4\pi^2}\right)^{1/4} g_*^{-1/4}(T_{osc}^{X_N}), \\ &= 2.70 \times 10^{12} \left(\frac{228.75}{g_*(T_{osc}^{X_N})}\right)^{1/4} \left(\frac{m_{X_N}}{600\, m_{3/2}}\right)^{1/2} \text{GeV}. \end{aligned} \tag{C.2}$$

From this we find the entropy density

$$s(T_{osc}^{X_N}) = \frac{2\pi^2}{45} g_{osc} T_{osc}^3, \tag{C.3}$$

$$= 1.98 \times 10^{39} \left(\frac{g_{osc}}{228.75}\right)^{1/4} \left(\frac{m_{X_N}}{600\, m_{3/2}}\right)^{3/2} \text{GeV}^3, \tag{C.4}$$

and the comoving abundance is then

$$\begin{aligned} Y_{X_N}^{(0)} &= = \frac{1}{2} m_{X_N} f_{X_N}^2 s^{-1}(T_{osc}^{X_N}), \\ &= 4.51 \times 10^4 \left(\frac{228.75}{g_*(T_{osc})}\right)^{1/4} \left(\frac{f_{X_N}}{M_P}\right)^2 \left(\frac{600\, m_{3/2}}{m_{X_N}}\right)^{1/2}, \end{aligned} \tag{C.5}$$

The oscillating modulus will quickly come to dominate the radiation density and the temperature at this time is given by

$$T_{eq}^{X_N} = 1.80 \times 10^{12} \left(\frac{228.75}{g_*(T_{osc}^{X_N})}\right)^{1/4} \left(\frac{m_{X_N}}{600\, m_{3/2}}\right)^{1/2} \left(\frac{f_{X_N}}{M_P}\right)^2 \text{GeV}, \tag{C.6}$$

so that we see once the modulus starts coherent oscillations it quickly overtakes the energy density (i.e., $T_{eq}^{X_N} \approx T_{osc}^{X_N}$).

C.1.2 Meson and Light Moduli Oscillations

Because the meson and light moduli are approximately degenerate in mass (i.e. $m_\phi = m_{X_i}$) they will begin to oscillate at the same time,

$$3H^2 = 3\left(\frac{2}{3} m_\phi\right)^2 = M_P^{-2} \left(\frac{\pi^2}{30} g_*(T_{osc}^\phi) \left(T_{osc}^\phi\right)^4 + m_{X_N} Y_{X_N} s(T_{osc}^\phi)\right). \tag{C.7}$$

Noting that the radiation term has already become negligible compared to the heavy modulus density we find the temperature at this time is given by

$$\begin{aligned} T_{osc}^{\phi} &= \left(\frac{30}{\pi^2}\right)^{1/3} \left[\frac{m_\phi^2 M_P^2}{g_{*s}(T_{osc}^{\phi}) m_{X_N} Y_{X_N}}\right]^{1/3} \\ &= 8.24 \times 10^{10} \left(\frac{228.75}{g_*(T_{osc}^{X_N})}\right)^{\frac{1}{4}} \left(\frac{m_\phi}{2m_{3/2}}\right)^{\frac{2}{3}} \left(\frac{600 m_{3/2}}{m_{X_N}}\right)^{\frac{1}{6}} \left(\frac{M_P}{f_{X_N}}\right)^{\frac{2}{3}} \text{ GeV} \end{aligned} \quad \text{(C.8)}$$

which is in excellent agreement with the exact answer obtained numerically (including radiation) $T_{osc}^{\phi} = 9.97 \times 10^{10}$ GeV. The entropy density at this time is

$$s(T_{osc}^{\phi}) = 5.62 \times 10^{34} \left(\frac{g_*(T_{osc}^{X_N})}{228.75}\right)^{\frac{1}{4}} \left(\frac{m_\phi}{2m_{\frac{3}{2}}}\right)^{2} \left(\frac{600 m_{3/2}}{m_{X_N}}\right)^{\frac{1}{2}} \left(\frac{M_P}{f_{X_N}}\right)^{2} \text{ GeV}^3. \quad \text{(C.9)}$$

The meson ϕ initial abundance is then

$$Y_\phi^{(0)} = 5.30 \times 10^6 \left(\frac{228.75}{g_*(T_{osc})}\right)^{1/4} \left(\frac{f_\phi}{M_P}\right)^2 \left(\frac{f_{X_N}}{M_P}\right)^2 \left(\frac{m_{X_N}}{600 m_{3/2}}\right)^{1/2} \left(\frac{2m_{3/2}}{m_\phi}\right). \quad \text{(C.10)}$$

The light moduli will begin coherent oscillations at roughly the same time as the meson. Their abundance is then given by

$$\begin{aligned} Y_{X_i}^{(0)} &= (N-1)\, Y_\phi^{(0)} \\ &= 5.25 \times 10^8 \left(\frac{N-1}{99}\right) \left(\frac{228.75}{g_*(T_{osc})}\right)^{1/4} \left(\frac{f_{X_i}}{M_P}\right)^2 \left(\frac{f_{X_N}}{M_P}\right)^2 \\ &\quad \times \left(\frac{m_{X_N}}{600 m_{3/2}}\right)^{1/2} \left(\frac{2m_{3/2}}{m_{X_i}}\right), \end{aligned} \quad \text{(C.11)}$$

where we have implicitly assumed that because the masses of the meson and light moduli are approximately degenerate they will have equal oscillation amplitudes[1].

[1]We note that initially this may not be the case, but at the onset of coherent oscillations (much less than a Hubble time) the system will settle into this symmetric configuration.

C.1.3 Heavy Modulus Decay

Once the Hubble parameter decreases to the point when $H \approx \Gamma_{X_N}$, the heavy modulus decays and from (5.18) the corresponding reheat temperature is,

$$\begin{aligned} T_r^{X_N} &= 41.40 \left(\frac{10.75}{g_*(T_r^{X_N})}\right)^{1/4} \left(\frac{D_{X_N}}{1.6}\right)^{1/2} \left(\frac{m_{X_N}}{600\, m_{3/2}}\right)^{3/2} \\ &\quad \times \left(\frac{M_P}{f_\phi}\right)^{1/2} \left(\frac{100}{N}\right)^{1/4} \text{GeV}. \end{aligned} \tag{C.12}$$

To understand the N and ϕ dependence in this expression, we note that from (5.18) the reheat temperature includes the factor,

$$\left(\frac{m_{X_N} Y_{X_N} + m_\phi Y_\phi + m_{X_i} Y_{X_i}}{m_{X_N} Y_{X_N}}\right)^{1/4} \tag{C.13}$$

Using that the meson and light moduli have degenerate mass and therefore equal oscillation amplitudes (i.e. $m_{X_i} Y_{X_i} = (N-1) m_\phi Y_\phi$) we find

$$\left(1 + N \frac{m_\phi Y_\phi}{m_{X_N} Y_{X_N}}\right)^{-1/4} \approx \left(N \frac{m_\phi Y_\phi}{m_{X_N} Y_{X_N}}\right)^{-1/4} \tag{C.14}$$

which leads to the parametric dependence in the reheat temperature.

Using (5.21) the entropy increase resulting from the heavy modulus decay is

$$\begin{aligned} \Delta_{X_N} &= 4.35 \times 10^{10} \left(\frac{g_*(T_r^{X_N})}{10.75}\right)^{1/4} \left(\frac{228.75}{g_*(T_{osc}^{X_N})}\right)^{1/4} \left(\frac{f_{X_N}}{M_P}\right)^2 \\ &\quad \times \left(\frac{1.6}{D_{X_N}}\right)^{1/2} \left(\frac{600\, m_{3/2}}{m_{X_N}}\right) \left(\frac{f_\phi}{M_P}\right)^{1/2} \left(\frac{N}{100}\right)^{1/4}, \end{aligned} \tag{C.15}$$

where we have again used (C.14). Therefore, after the decay the other moduli abun-

dances are given by

$$\begin{aligned} Y_{\phi}^{(X_N)} &= \Delta_{X_N}^{-1} Y_{\phi}^{(0)}, \\ &= 1.22 \times 10^{-4} \left(\frac{10.75}{g_*(T_r^{X_N})}\right)^{1/4} \left(\frac{D_{X_N}}{1.6}\right)^{1/2} \left(\frac{f_\phi}{M_P}\right)^{3/2} \\ &\quad \times \left(\frac{m_{X_N}}{600\, m_{3/2}}\right)^{3/2} \left(\frac{2\, m_{3/2}}{m_\phi}\right) \left(\frac{100}{N}\right)^{1/4} \end{aligned} \tag{C.16}$$

$$\begin{aligned} Y_{X_i}^{(X_N)} &= \Delta_{X_N}^{-1} Y_{X_i}^{(0)}, \\ &= 1.21 \times 10^{-2} \left(\frac{10.75}{g_*(T_r^{X_N})}\right)^{1/4} \left(\frac{D_{X_N}}{1.6}\right)^{1/2} \left(\frac{f_{X_i}}{M_P}\right)^{3/2} \\ &\quad \times \left(\frac{m_{X_N}}{600\, m_{3/2}}\right)^{3/2} \left(\frac{2\, m_{3/2}}{m_{X_i}}\right) \left(\frac{N}{100}\right)^{3/4}, \end{aligned} \tag{C.17}$$

where we have again used $N - 1 \approx N$. There is also a decay to gravitinos with branching ratio $B_{3/2}^{(X_N)} = 0.2\% = 0.002$. The corresponding comoving abundance is thus,

$$\begin{aligned} Y_{3/2}^{(X_N)} &= 2 \times B_{3/2} \times \frac{Y_{X_N}^{(0)}}{\Delta_{X_N}}, \\ &= 1.45 \times 10^{-9} \left(\frac{B_{3/2}}{0.07\%}\right) \left(\frac{10.75}{g_*(T_r^{X_N})}\right)^{1/4} \left(\frac{D_{X_N}}{1.6}\right)^{1/2} \\ &\quad \times \left(\frac{m_{X_N}}{600 m_{3/2}}\right)^{1/2} \left(\frac{M_P}{f_\phi}\right)^{1/4} \left(\frac{100}{N}\right)^{1/4}, \end{aligned} \tag{C.18}$$

C.1.4 Meson Decay

When the meson decays, its contribution to the total energy density will be less than that of the other $N - 1$ light moduli. The universe will be matter dominated before and after the decay, but because the two energy sources are comparable there is a somewhat significant entropy production. The meson decay reheats the universe

to a temperature

$$T_r^{\phi} = 134 \times \left(\frac{100}{N}\right)^{1/4} \left(\frac{10.75}{g_*(T_r)}\right)^{1/4} \left(\frac{D_\phi}{711.6}\right)^{1/2} \left(\frac{m_\phi}{2\,m_{3/2}}\right)^{3/2} \text{MeV}. \quad \text{(C.19)}$$

The entropy increase is given by

$$\Delta_\phi = 121 \times \left(\frac{D_{X_N}}{1.6}\right)^{1/2} \left(\frac{711.6}{D_\phi}\right)^{1/2} \left(\frac{m_{X_N}}{600\,m_{3/2}}\right)^{3/2} \left(\frac{2\,m_{3/2}}{m_\phi}\right)^{3/4} \left(\frac{f_\phi}{M_P}\right)^{3/2}. \quad \text{(C.20)}$$

The decay of the meson will further dilute the other moduli, we find

$$\begin{aligned} Y_{X_i}^{(\phi)} &= \Delta_{X_N}^{-1} \Delta_\phi^{-1} Y_{X_i}^{(0)}, \\ &= 9.94 \times 10^{-5} \left(\frac{N}{100}\right)^{3/4} \left(\frac{10.75}{g_*(T_r)}\right)^{1/4} \left(\frac{D_\phi}{711.6}\right)^{1/2} \left(\frac{2\,m_{3/2}}{m_{X_i}}\right)^{1/4}. \end{aligned} \quad \text{(C.21)}$$

The decay of both the meson and the light moduli to gravitinos is kinematically suppressed, so that the only source of gravitinos comes from the decay of the heavy modulus. This abundance after the decay of the meson is then

$$\begin{aligned} Y_{m_{3/2}}^{(\phi)} &= \Delta_\phi^{-1} Y_{m_{3/2}}^{(X_N)}, \\ &= 1.19 \times 10^{-11} \left(\frac{B_{3/2}^{(X_N)}}{0.07\%}\right) \left(\frac{100}{N}\right)^{1/4} \left(\frac{10.75}{g_*(T_r)}\right)^{1/4} \\ &\quad \times \left(\frac{D_\phi}{711.6}\right)^{1/2} \left(\frac{m_\phi}{2\,m_{3/2}}\right)^{3/4} \left(\frac{600\,m_{3/2}}{m_{X_N}}\right) \left(\frac{M_P}{f_\phi}\right)^{7/4}. \end{aligned} \quad \text{(C.22)}$$

C.1.5 Light Moduli Decays

The decay of the light moduli results in a reheating temperature

$$T_r^{X_i} = 31.7 \times \left(\frac{10.75}{g_*(T_r)}\right)^{1/4} \left(\frac{m_{X_i}}{2\,m_{3/2}}\right)^{3/2} \left(\frac{D_{X_i}}{4}\right)^{1/2} \text{MeV}, \quad \text{(C.23)}$$

which agrees with the bounds set by BBN (i.e. $T_r^{X_i} > 1\,\text{MeV}$). The resulting entropy production is

$$\Delta_{X_i} = 417.7 \times \left(\frac{D_\phi}{711.6}\right)^{1/2} \left(\frac{4}{D_{X_i}}\right)^{1/2} \left(\frac{2\,m_{3/2}}{m_{X_i}}\right)^{3/4} \left(\frac{N}{100}\right)^{3/4}. \quad \text{(C.24)}$$

The new gravitino abundance is given by

$$\begin{aligned} Y_{m_{3/2}}^{(X_i)} &= \Delta_{X_i}^{-1} Y_{m_{3/2}}^{(\phi)}, \\ &= 2.86\times10^{-14}\left(\frac{B_{3/2}^{(X_N)}}{0.07\%}\right)\left(\frac{100}{N}\right)\left(\frac{10.75}{g_*(T_r)}\right)^{1/4}\left(\frac{m_\phi}{2\,m_{3/2}}\right)^{3/2} \\ &\quad\times\left(\frac{600\,m_{3/2}}{m_{X_N}}\right)\left(\frac{D_{X_i}}{4}\right)^{1/2}\left(\frac{M_P}{f_\phi}\right)^{7/4} \end{aligned} \tag{C.25}$$

which is small enough to avoid the gravitino problem. The light moduli will decay into LSPs yielding an abundance

$$\begin{aligned} Y_{LSP}^{(X^i)} &= \Delta_{X_i}^{-1} B_{LSP}^{X_i} Y_{X_i}^{(\phi)}, \\ &= 1.19\times10^{-7}\left(\frac{B_{LSP}^{X_i}}{25\%}\right)\left(\frac{10.75}{g_*(T_r)}\right)^{1/4}\left(\frac{m_{X_i}}{2\,m_{3/2}}\right)^{1/2}\left(\frac{D_{X_i}}{4}\right)^{1/2}, \end{aligned} \tag{C.26}$$

where $B_{LSP}^{X_i}$ is the branching ratio for the decay of the light moduli to LSPs. This corresponds to a number density at the time of decay of $n_{LSP} = 1.79\times10^{-11}\,\mathrm{GeV}^3$.

As we noted in the text, this abundance is produced below the freeze-out temperature of the LSPs (non-thermal production) and is greater than the critical density (5.42) for annihilations to take place, which is $n_{X_i}^c = 4.12\times10^{-15}\,\mathrm{GeV}^3$. Thus, the LSPs will quickly annihilate (in less than a Hubble time) and the final abundance will be given by the critical value.

Thus, the relic density coming from the decay of the light moduli is given by

$$\begin{aligned} \Omega_{LSP} &= \frac{m_{LSP} Y_{LSP}^c s_0}{\rho_c}, \\ &= 0.26\,h^{-2}\left(\frac{m_{LSP}}{100\,\mathrm{GeV}}\right)^3\left(\frac{10.75}{g_*(T_r)}\right)^{1/4}\left(\frac{3.26\times10^{-3}\mathrm{GeV}^{-2}}{\sigma_0}\right) \\ &\quad\times\left(\frac{4}{D_{X_i}}\right)^{1/2}\left(\frac{2\,m_{3/2}}{m_{X_i}}\right)^{3/2}\left(\frac{100\,\mathrm{TeV}}{m_{3/2}}\right)^{3/2}, \end{aligned} \tag{C.27}$$

where s_0 and ρ_c are the entropy density and critical density today respectively, and we have used the experimental value $\rho_c/s_0 = 3.6 \times 10^{-9} h^2$ GeV where h parametrizes the Hubble parameter today with median value $h = 0.71$.

C.2 Couplings and Decay Widths of the Moduli and Meson Fields

In this section, we discuss the moduli couplings to MSSM particles and then calculate their decay widths in terms of the microscopic parameters of the G_2-MSSM framework. This will motivate the benchmark values used for numerical results throughout the paper. We will find that the moduli decay into scalars is very important.

C.2.1 Moduli Couplings

Let us first consider the couplings associated with N eigenstates X_j of the geometric moduli s_i. For simplicity, we neglect the small mixing with the meson modulus ϕ (we will return to that later). First consider the moduli coupling to gauge bosons through the gauge kinetic function f^{sm}. The relevant term is:

$$\mathcal{L} \supset -\frac{1}{4}\mathrm{Im}(f_{sm}) F^a_{\mu\nu} F^{a\mu\nu} \tag{C.28}$$

$$= -\frac{1}{4}\langle \mathrm{Im}(f_{sm}) \rangle F^a_{\mu\nu} F^{a\mu\nu} - \frac{1}{4}\sum_i N_i^{sm} \delta s_i F^a_{\mu\nu} F^{a\mu\nu} \tag{C.29}$$

where we have expanded the moduli as $s_i = \langle s_i \rangle + \delta s_i$. After normalizing the gauge fields and the moduli fields, the interaction term can be written as:

$$\mathcal{L}_{X_j gg} = \frac{1}{4\, f_{sm}} \sum_{i=1}^{N} N_i^{sm} \sqrt{\frac{2\langle s_i \rangle}{3a_i}} U_{ij}\ X_j F^a_{\mu\nu} F^{a\mu\nu} \tag{C.30}$$

$$= \frac{\sqrt{7}}{6\sqrt{2}} \mathcal{B}\, \mathcal{C}_j\ X_j F^a_{\mu\nu} F^{a\mu\nu}, \tag{C.31}$$

where $\mathcal{B}$ and $\mathcal{C}_j$ are defined as:

$$\mathcal{B} \equiv \left(\sum_{i=1}^{N} \frac{N_i^{sm}}{N_i}\ a_i \right)^{-1} \tag{C.32}$$

$$\mathcal{C}_j \equiv \sum_{i=1}^{N} \frac{N_i^{sm}}{N_i}\ (\vec{X}_N)_i (\vec{X}_j)_i. \tag{C.33}$$

For the heavy modulus, since $(X_N)_i^2 = \frac{3}{7} a_i$, we have $\mathcal{C}_N = \frac{3}{7}\mathcal{B}^{-1}$ while for the light moduli $X_i, i = 1, \cdots, (N-1)$, it is easy to show:

$$\sum_{i=1}^{N-1} \mathcal{C}_i^2 = l^2 \sin^2\theta, \tag{C.34}$$

where l is the length of the vector $\vec{X}_N^{\,\prime}$ defined as $(\vec{X}_N^{\,\prime})_i \equiv (\vec{X}_N)_i\, N_i^{sm}/N_i$ and θ is the angle between $\vec{X}_N^{\,\prime}$ and $\vec{X}_N$. So, generically $\mathcal{C}_i$ are less than one. There are two extreme cases: one when $N_i^{sm} = kN_i$ in which the moduli couplings to gauge bosons vanish since the vector $\vec{X}_N$ is orthogonal to $\vec{X}_j$, and the other when $\vec{X}_N^{\,\prime}$ equal to one of the X_i's in which all $\mathcal{C}_i$'s are zero except one.

For the couplings to gauginos, the dominant contribution comes from the following terms in the lagrangian:

$$\mathcal{L} \supset -\frac{i}{4} \partial_i f_{sm} F^i \lambda^a \lambda^a + h.c. \tag{C.35}$$

where $\partial_i f_{sm} = N_i^{sm}$ and $-i$ arises because of the convention of the moduli chiral fields $z_i = t_i + is_i$ we used. Expanding the F-terms of the moduli fields around their *vevs*, we have:

$$F^i \;=\; \langle F^i\rangle + \langle \partial_{s_k} F^i\rangle \delta s_k \tag{C.36}$$

The derivative of the F-term can be calculated as follows:

$$\begin{aligned}
\partial_{s_k} F^i &= \partial_{s_k}\Big(e^{K/2} K^{i\bar{j}} (K_{\bar{j}} W^* + W^*_{\bar{j}})\Big) \\
&= -ie^{-i\gamma} m_{3/2} \left(\frac{4}{3}\frac{a_i}{N_i} N_k \nu^2 \frac{\tilde{z}}{\tilde{x}} + \frac{4}{3}\frac{N_k}{N_i}(3a_i - 2\delta_{ik})\nu\frac{\tilde{y}}{\tilde{x}} + \frac{N_k}{N_i}(3a_i - 2\delta_{ik})\right) \\
&= -ie^{-i\gamma} m_{3/2} \left(-\frac{4}{3} s_i N_k b_1 b_2 \nu - 3\frac{N_k}{N_i} a_i + 2\delta_{ik} + \cdots\right)
\end{aligned} \tag{C.37}$$

where in the last line, the subleading terms are not explicitly shown. γ is the phase in the superpotential which will be set to zero for simplicity without affecting any result here. We have used the following equations:

$$\partial_{s_i} K = -\frac{3a_i}{s_i}, \quad K^{i\bar{j}} = \frac{4s_i^2}{3a_i}\delta_{i\bar{j}}, \quad \partial_{s_k} K^{i\bar{j}} = \frac{2}{s_k} K^{i\bar{j}}\delta_{ik} \tag{C.38}$$

After normalizing the moduli fields and the gauge fields, the couplings are given by:

$$\begin{aligned}
\mathcal{L}_{X_i\lambda\lambda} &\approx \frac{1}{4}\sqrt{\frac{2}{3}} m_{3/2} \left[\left(\frac{4}{3}\nu^2 b_1 b_2\right)\sum_{k=1}^{N} a_k^{1/2} U_{ki} - \frac{1}{f_{\rm sm}} 2\nu \sum_{k=1}^{N} \frac{N_k^{sm}}{N_k} a_k^{1/2} U_{ki}\right] X_i \lambda^a\lambda^a + h.c. \\
&= \frac{\sqrt{14}}{12} m_{3/2}\left[\frac{4}{3}\nu^2 b_1 b_2 (\vec{X}_N \cdot \vec{X}_i) - 2\mathcal{B}\,(\vec{X}'_N \cdot \vec{X}_i)\right] X_i\lambda^a\lambda^a + h.c.
\end{aligned} \tag{C.39}$$

For the light moduli fields, the first term vanishes and the couplings turn out to be:

$$\mathcal{L}_{X_l\lambda\lambda} \approx -\frac{\sqrt{14}}{6}\mathcal{B}\,\mathcal{C}_i m_{3/2}\, X_i\lambda^a\lambda^a + h.c. \tag{C.40}$$

For the heavy modulus field, the first dot product is unity and the coupling is:

$$\mathcal{L}_{X_l\lambda\lambda} \approx \frac{\sqrt{14}}{12} m_{3/2}\left(\frac{4}{3}\nu^2 b_1 b_2\right)\; X_i\lambda^a\lambda^a + h.c. \tag{C.41}$$

The moduli couplings to other MSSM particles can be derived generically by expanding all the moduli around their *vevs* in the supergravity lagrangian:

$$\mathcal{L} \supset \tilde{K}_{\bar{\alpha}\beta}\mathcal{D}_\mu \tilde{f}^{*\bar{\alpha}}\mathcal{D}^\mu \tilde{f}^\beta + i\tilde{K}_{\bar{\alpha}\beta} f^{\dagger\bar{\alpha}}\bar{\sigma}^\mu \mathcal{D}_\mu f^\beta - V(\tilde{f}^*, \tilde{f}) + \cdots \tag{C.42}$$

where f^α and $\tilde{f}^\alpha$ are fermions and their superpartners. The other derivative terms involving moduli and matter fields are not explicitly shown for simplicity. The relevent coupling here are the moduli-sfermion-sfermion coupling and the moduli-fermion-fermion coupling. They are found to be

$$\mathcal{L} \supset \partial_{s_i}\tilde{K}_{\bar{\alpha}\beta}\left[\delta s_i\, \partial_\mu \tilde{f}^{*\bar{\alpha}}\partial^\mu \tilde{f}^\beta + i\delta s_i\, f^{\dagger\bar{\alpha}}\bar{\sigma}^\mu\partial_\mu f^\beta\right] - \partial_{s_i} m'^2_{\bar{\alpha}\beta}\,\delta s_i \tilde{f}^{*\bar{\alpha}}\tilde{f}^\beta + \cdots \tag{C.43}$$

$$= g'^{\alpha}_{X_i\tilde{f}\tilde{f}}\left[\partial_\mu(X_i\, \tilde{f}_c^{*\bar{\alpha}})\partial^\mu \tilde{f}_c^\alpha + c.c. + iX_i\, \bar{f}_c^{\bar{\alpha}}\bar{\sigma}^\mu\partial_\mu f_c^\alpha\right] - g^\alpha_{X_i\tilde{f}\tilde{f}} X_i \tilde{f}_c^{*\bar{\alpha}}\tilde{f}_c^\alpha + \cdots \tag{C.44}$$

where $\tilde{f}_c^\alpha$ and f_c^α are the canonical normalized fields. For simplicity, we consider the Kahler metric to be diagonal $\tilde{K}_{\bar{\alpha}\beta} = \tilde{K}_\alpha \delta_{\bar{\alpha}\beta}$, then

$$g^\alpha_{X_j\tilde{f}\tilde{f}} \approx m^2_{3/2}\partial_{s_i}\log(\tilde{K}_\alpha)\sqrt{\frac{2s_i^2}{3a_i}}U_{ij}$$

$$= \frac{\sqrt{14}}{3}m^2_{3/2}\,(\vec{X}''_N)^\alpha \cdot \vec{X}_j \tag{C.45}$$

$$g'^{\alpha}_{X_j\tilde{f}\tilde{f}} = \frac{\sqrt{14}}{6}\,(\vec{X}''_N)^\alpha \cdot \vec{X}_j \tag{C.46}$$

where $(\vec{X}''_N)^\alpha_i \equiv \xi_{i,\alpha}(X_N)_i/a_i$ and $\xi_{i,\alpha} \equiv s_i\partial_{s_i}\log(K_\alpha)$. In this calculation, we have used the fact that $\partial_{\phi_0}\tilde{K}_\alpha = 0$ and have neglected terms involving F-terms of geometric moduli F^i which are suppressed relative to $m_{3/2}$.

For the couplings to the higgs doublets, there are differences from other scalars. The kinetic terms and the mass terms for the higgs fields in the MSSM can be written

as:

$$\begin{aligned}\mathcal{L} &\supset \tilde{K}_{H_u}\left[\partial_\mu H_u^* \partial^\mu H_u + i\bar{\tilde{H}}_u \bar{\sigma}^\mu \partial_\mu \tilde{H}_u\right] + \cdots \\ &- (\tilde{K}_{H_d}^{-1}|\mu'|^2 + m'^2_{H_u}) H_u^* H_u + (H_u \leftrightarrow H_d) \\ &- (B\mu' H_d H_u + c.c.) \end{aligned} \tag{C.47}$$

where

$$\mu' = m_{3/2} Z - \bar{F}^{\bar{m}} \partial_{\bar{m}} Z \tag{C.48}$$

is only generated by the higgs bilinear term in the Kahler potential [30]. To derive the modular couplings to higgs doublets, one needs $\partial_{s_i}\mu'$, which is:

$$\partial_{s_i}\mu' = (\partial_{s_i} m_{3/2}) Z + m_{3/2}\partial_{s_i} Z - (\partial_{s_i}\bar{F}^{\bar{m}})\partial_{\bar{m}} Z - \bar{F}^{\bar{m}}\partial_{s_i}\partial_{\bar{m}} Z \tag{C.49}$$

One can see that the second and the third terms are of order $m_{3/2}$ while the rest are suppressed. Therefore, the dominant contribution is:

$$\partial_{s_i}\mu' \approx \frac{1}{2} m_{3/2}(\partial_{s_m} Z)\left(-\frac{4}{3} s_m N_i b_1 b_2 \nu + 4\delta_{im}\right) \tag{C.50}$$

For simplicity, taking all the phases of the superpotential and that of Z to be vanishing, we find:

$$-\mathcal{L} \supset g_{X_j H_u H_u} X_j H_u^* H_u \tag{C.51}$$

$$\begin{aligned} g_{X_j H_u H_u} &\approx m_{3/2}^2 \Bigg[Z_{\text{eff}}^2 \partial_{s_m} \log Z \left(-\frac{4}{3} s_m N_i b_1 b_2 \nu + 4\delta_{im}\right) - Z_{\text{eff}}^2 \partial_{s_i} \log \tilde{K}_{H_d} \\ &+ \partial_{s_i} \log \tilde{K}_{H_u} \Bigg] \sqrt{\frac{2s_i^2}{3a_i}} U_{ij} \\ &= \frac{\sqrt{14}}{3} m_{3/2}^2 Z_{\text{eff}}^2 \Bigg(-\frac{4}{3}\nu^2 b_1 b_2 \left(\sum_{m=1}^{N} \zeta_m\right) \vec{X}_N \cdot \vec{X}_j + 4\vec{X}_N''' \cdot \vec{X}_j \\ &- (\vec{X}_N'')^{H_d} \cdot \vec{X}_j \Bigg) + \frac{\sqrt{14}}{3} m_{3/2}^2 (\vec{X}_N'')^{H_u} \cdot \vec{X}_j \end{aligned} \tag{C.52}$$

where $(\vec{X}'''_N)_i \equiv \frac{\zeta_i}{a_i}(X_N)_i$ and $\zeta_i \equiv s_i\partial_{s_i}\log(Z)$. We also use the fact that $\partial_{\phi_0}Z = 0$ and the F-terms $F_i/M_P \ll m_{3/2}$ for geometric moduli. To get the corresponding couplings for H_d, we can simply replace H_u by H_d in the above equations. The coupling of moduli to higgs through the kinetic term is similar to the non-higgs scalar

$$g'^{\alpha}_{X_iH_uH_u} = \frac{\sqrt{14}}{6}(\vec{X}''_N)^{H_u}\cdot\vec{X}_i \tag{C.53}$$

Let us now consider the $B\mu$ term, which is given by:

$$\begin{aligned} B\mu' &= (2m_{3/2}^2 + V_0)Z - m_{3/2}\bar{F}^{\bar{m}}\partial_{\bar{m}}Z + m_{3/2}F^m[\partial_m Z - \partial_m\log(\tilde{K}_{H_u}\tilde{K}_{H_d})\,Z] \\ &- \bar{F}^{\bar{m}}F^n[\partial_{\bar{m}}\partial_n Z - \partial_n\log(\tilde{K}_{H_u}\tilde{K}_{H_d})\partial_{\bar{m}}Z]. \end{aligned} \tag{C.54}$$

The corresponding derivative is given by:

$$\partial_{s_i}B\mu' \approx \frac{1}{2}m_{3/2}^2\,Z\,\partial_{s_i}\log(\tilde{K}_{H_u}\tilde{K}_{H_d})\left(-\frac{4}{3}s_iN_kb_1b_2\nu + 2\delta_{ik}\right) + 2m_{3/2}^2\partial_{s_i}Z, \tag{C.55}$$

which gives rise to the coupling:

$$-\mathcal{L} \supset g_{X_jH_dH_u}X_jH_dH_u + c.c. \tag{C.56}$$

$$\begin{aligned} g_{X_jH_dH_u} &\approx \frac{\sqrt{14}}{6}m_{3/2}^2\,Z_{\rm eff}\Bigg(-\frac{4}{3}\nu^2b_1b_2\left(\sum_{m=1}^{N}\xi_m^{H_u}\right)\vec{X}_N\cdot\vec{X}_j \\ &+ 2(\vec{X}''_N)^{H_u}\cdot\vec{X}_j + (H_u\to H_d) + 4\vec{X}'''_N\cdot\vec{X}_j\Bigg) \end{aligned} \tag{C.57}$$

Besides the term mentioned above there is another coupling from the bilinear term in the kähler potential $K \sim Z(s_i)H_dH_u + h.c.$ [131]. This term leads to a coupling:

$$\mathcal{L} \supset g'_{X_jH_dH_u}\partial_\mu X_j\partial^\mu(H_dH_u) + c.c. \tag{C.58}$$

$$g'_{X_jH_dH_u} = \frac{\sqrt{14}}{6}Z_{\rm eff}\,\vec{X}'''_N\cdot\vec{X}_j \tag{C.59}$$

This coupling could be very important since it is proportional to the moduli mass squared if equations of motion of X_i are used. Again for the coupling to be unsuppressed, the bilinear coefficient Z should have a sizable dependence on the geometric moduli s_i, which is natural. This coupling is essential for electroweak symmetry breaking in the G_2-MSSM.

C.2.2 Meson Couplings

In the G_2-MSSM framework, the hidden sector is not sequestered from the visible sector and there are couplings between the hidden sector meson field ϕ and various MSSM particles, which we want to compute. First since the tree level gauge kinetic function does not depend on ϕ, there is no coupling to gauge bosons. However there are couplings to the gauginos which depend on ∂_{ϕ_0}, which are computed to be

$$\partial_{\phi_0} F^i = -ie^{-i\gamma}\frac{4s_i}{3\phi_0}\mathcal{F}m_{3/2}, \tag{C.60}$$

$$\mathcal{F} = \frac{2QP_{\text{eff}}}{21P} + 2 + \frac{3}{P} + \mathcal{O}(P_{\text{eff}}^{-1}). \tag{C.61}$$

After normalization of fields, the coupling of meson to the gauginos is given by:

$$\mathcal{L}_{\delta\phi_0\lambda\lambda} = e^{-i\gamma}\frac{1}{3\sqrt{2}\phi_0}\mathcal{F}m_{3/2}\delta\phi_0\lambda\lambda \tag{C.62}$$

We now move on to the couplings of the meson field to scalars. We will assume that the Kähler metric and the higgs bilinear Z do not depend on ϕ_0. We then have for

the non-higgs scalars:

$$\begin{aligned}\mathcal{L}_{\delta\phi_0\tilde{f}\tilde{f}} &= \frac{1}{\sqrt{2}\tilde{K}_\alpha}\frac{\partial m_\alpha'^2}{\partial\phi_0}\delta\phi_0\tilde{f}^*\tilde{f} \\ &= \sqrt{2}m_{3/2}\left(\partial_{\phi_0} m_{3/2}\right)\delta\phi_0\tilde{f}^*\tilde{f} \\ &\approx \sqrt{2}m_{3/2}^2\phi_0(1+\frac{2}{3\phi_0^2})\delta\phi_0\tilde{f}^*\tilde{f} \end{aligned} \tag{C.63}$$

In the above, we have neglected terms proportional to F_i/M_P which are $\ll m_{3/2}$. There are various kinds of couplings of the meson to the Higgs fields H_u and H_d. The coupling originating from the term $\int d^4\theta\,(ZH_uH_d + c.c)$ does *not* give rise to any contribution since Z is assumed to be independent of ϕ_0. The couplings $\mathcal{L}_{\delta\phi_0 H_u^* H_u}$ and $\mathcal{L}_{\delta\phi_0 H_d^* H_d}$ are computed as follows:

$$\begin{aligned}\mathcal{L}_{\delta\phi_0 H_u H_u} &= g_{\delta\phi_0 H_u H_u}\delta\phi_0\tilde{H}_u^*\tilde{H}_u \\ g_{\delta\phi_0 H_u H_u} &= \frac{1}{\sqrt{2}\tilde{K}_{H_u}}\frac{\partial(\tilde{K}_{H_d}^{-1}|\mu'|^2 + m_{H_u}'^2)}{\partial\phi_0} \\ &\approx \sqrt{2}(Z_{\text{eff}}^2+1)\,m_{3/2}^2\phi_0\left[(1+\frac{2}{3\phi_0^2}) + (\frac{Z_{\text{eff}}^2}{Z_{\text{eff}}^2+1})\frac{2\mathcal{F}}{3\phi_0^2}\sum_{i=1}^{N}\zeta_i\right] \end{aligned} \tag{C.64}$$

$\mathcal{L}_{\delta\phi_0\hat{H}_d^*\hat{H}_d}$ can be obtained from the above by replacing H_u with H_d. Again, we have neglected terms proportional to F_i/M_P. Finally, we look at the coupling $\mathcal{L}_{\delta\phi_0 H_d H_u}$. It is given by:

$$\begin{aligned}\mathcal{L}_{\delta\phi_0 H_d H_u} &= g_{\delta\phi_0 H_d H_u}\delta\phi_0\tilde{H}_d\tilde{H}_u \\ g_{\delta\phi_0 H_d H_u} &= \frac{1}{\sqrt{2}(\tilde{K}_{H_u}\tilde{K}_{H_d})^{1/2}}\frac{\partial(B\mu')}{\partial\phi_0} \\ &\approx \sqrt{2}m_{3/2}^2\,\phi_0 Z_{\text{eff}}\left[2(1+\frac{2}{3\phi_0^2}) + \frac{\mathcal{F}}{3\phi_0^2}\sum_{i=1}^{N}(\xi_i^{H_u}+\xi_i^{H_d})\right] \end{aligned} \tag{C.65}$$

The coupling $\mathcal{L}_{\delta\phi_0 H_u^* H_d^*}$ can be computed by taking the complex conjugate of the above expression.

C.2.3 RG Evolution of the Couplings

In the last subsection, we computed all the relevant couplings of the moduli and meson at a high scale, presumably around the unification scale. However, since the scale at which moduli decay is much smaller than the unification scale, one should in principle use the effective couplings at that scale to compute the decay widths. The RG running of the moduli-scalar-scalar couplings are especailly important for the third generation squarks and the higgs doublets and are the main focus of this subsection. The leading contribution to the β functions are terms proportional to $|y_t|^2$ and g_3^{22}, which are given below:

$$\begin{aligned}
\beta(g_{X_j H_d H_u}) &\approx \frac{1}{16\pi^2} 3|y_t|^2 g_{X_j H_d H_u}, \\
\beta(g'_{X_j H_d H_u}) &\approx \frac{1}{16\pi^2} 3|y_t|^2 g'_{X_j H_d H_u}, \\
\beta(g_{X_j H_u H_u}) &\approx \frac{1}{16\pi^2} 6|y_t|^2 \left(g_{X_j H_u H_u} + X_t\right), \\
\beta(g'_{X_j H_u H_u}) &\approx \frac{1}{16\pi^2} 6|y_t|^2 g'_{X_j H_u H_u}, \\
\beta(g_{X_j \tilde{Q}_3 \tilde{Q}_3}) &\approx \frac{1}{16\pi^2}\left[g_{X_j \tilde{Q}_3 \tilde{Q}_3}\left(2|y_t|^2 - \frac{16}{3} g_3^2\right) + 2|y_t|^2 X_t\right], \\
\beta(g'_{X_j \tilde{Q}_3 \tilde{Q}_3}) &\approx \frac{1}{16\pi^2} g'_{X_j \tilde{Q}_3 \tilde{Q}_3}\left(2|y_t|^2 - \frac{16}{3} g_3^2\right), \\
\beta(g_{X_j \tilde{u}_3 \tilde{u}_3}) &\approx \frac{1}{16\pi^2}\left[g_{X_j u_3 u_3}\left(8|y_t|^2 - \frac{16}{3} g_3^2\right) + 4|y_t|^2 X_t\right], \\
\beta(g'_{X_j \tilde{u}_3 \tilde{u}_3}) &\approx \frac{1}{16\pi^2} g'_{X_j u_3 u_3}\left(8|y_t|^2 - \frac{16}{3} g_3^2\right),
\end{aligned} \tag{C.66}$$

where $X_t \equiv g_{X_j H_u H_u} + g_{X_j \tilde{Q}_3 \tilde{Q}_3} + g_{X_j \tilde{u}_3 \tilde{u}_3}$. For other beta functions not listed above, the RGE effects can be neglected.

[2]Here we have not included the digrams proportional to $g_{X_j gg}$ and $g_{X_j \tilde{g}\tilde{g}}$, since their contributions are relatively smaller

To examine the RG effects on the moduli-scalar-scalar couplings, we take all the weighted dot products involved in the moduli-scalar-scalar couplings to be equal for simplicity[3],

$$\vec{X}_N''' \cdot \vec{X}_i = (\vec{X}_N'')^\alpha \cdot \vec{X}_i = \Pi. \tag{C.67}$$

This is reasonable as their structure is very similar. So the high scale couplings can be written as:

$$\begin{aligned}
g_{X_j H_u H_u} &= g_{X_j H_d H_d} = \frac{\sqrt{14}}{3} m_{3/2}^2 (3Z_{\rm eff}^2 + 1)\Pi && \text{(C.68)}\\
g'_{X_j H_u H_u} &= g'_{X_j H_d H_d} = \frac{\sqrt{14}}{6}\Pi && \text{(C.69)}\\
g_{X_j H_d H_u} &= \frac{4\sqrt{14}}{3} m_{3/2}^2 Z_{\rm eff}\Pi && \text{(C.70)}\\
g'_{X_j H_d H_u} &= \frac{\sqrt{14}}{6} Z_{\rm eff}\Pi && \text{(C.71)}
\end{aligned}$$

Using the beta functions given in Eq.(C.66), we can see that at low scale $g_{X_j H_u H_u}$ is squashed because of the large yukawa couplings. Similarly $g_{X_j \tilde{Q}_3 \tilde{Q}_3}$ and $g_{X_j \tilde{u}_3 \tilde{u}_3}$ decrease significantly and become negative at low scales.

One important thing to compute for moduli decay to light higgs is the effective coupling $g^{eff}_{X_j hh}$, which can be written in terms of the couplings to higgs doublets

$$\begin{aligned}
g^{eff}_{X_i hh} &= (g_{X_i H_u H_u} - 2m_h^2 g'_{X_i H_u H_u})\cos^2\alpha + (g_{X_i H_d H_d} - 2m_h^2 g'_{X_i H_d H_d})\sin^2\alpha \\
&- (g_{X_i H_d H_u} - m_{X_i}^2 g'_{X_i H_d H_u})\sin 2\alpha && \text{(C.72)}
\end{aligned}$$

where all the couplings involved should be evaluated at low scales and α is the higgs mixing angle. For the G_2-MSSM, the higgs sector is almost in the "decoupling

[3]The more general case will be studied later.

region", which implies $\alpha \approx \beta - \frac{\pi}{2}$. Now with universal boundary condition for the weighted dot products for concreteness and simplicity, the effective coupling of moduli to hh final state is given by:

$$g^{eff}_{X_i hh} \approx \frac{\sqrt{14}}{3} m^2_{3/2} \left[(3Z^2_{\rm eff} + 1)(\sin^2\alpha + K_1 \cos^2\alpha) - 2K_2 Z_{\rm eff} \sin(2\alpha) \right] \Pi \quad \text{(C.73)}$$

where K_1 and K_2 are the RG factors. To estimate these factors, we take $y_t = 1$, $\alpha^{-1}_{unif} = 26.7$ and $Z_{\rm eff} = 1.58$, which is the same as the first Benchmark G_2-MSSM. Then, typically we find $K_1 \sim 0.2$ and $K_2 \sim 0.5$. For readers not familiar with the details of the G_2-MSSM, it is helpful to know that generically $\tan\beta \sim 1$ and $Z_{\rm eff} \sim 1.5$. For the effective coupling to third generation squarks, including the RG effects, we have:

$$g^{eff}_{X_j \tilde{u}_3 \tilde{u}_3} \approx g^{eff}_{X_j \tilde{Q}_3 \tilde{Q}_3} \sim \frac{\sqrt{14}}{3} m^2_{3/2} \Pi \quad \text{(C.74)}$$

where $g^{eff}_{X_j \tilde{f}\tilde{f}} \equiv g_{X_j \tilde{f}\tilde{f}} - m^2_{\tilde{f}} g'_{X_j \tilde{f}\tilde{f}}$. From the above RGE results, we find that the couplings to the non-higgs scalars and higgs should be roughly of the same order because of the large radiative correction even when some of them are suppressed relative to the other at the high scale boundary. Therefore, if the couplings to scalars are large, then we should expect a significant branching ratio of the moduli to LSPs.

For the coupling of the meson field to scalars, the β functions are exactly the same. Similar to the analysis of light moduli, we introduce factors K_1 and K_2 to account for the RG effects on $g_{\phi H_u H_u}$ and $g_{\phi H_d H_u}$. Typically one has $K_1 \sim 0.25$ and $K_2 \sim 0.5$. From Eq.(C.64) and (C.63), we find the coupling $g_{\phi H_u H_u}$ is at least $Z^2_{\rm eff}\mathcal{F} \sim 30$ times

larger than $g_{\phi\tilde{f}\tilde{f}}$ at the high scale. Because of this large coupling $g_{\phi H_u H_u}$, even if the couplings $g_{\phi\tilde{Q}_3\tilde{Q}_3}$ and $g_{\phi\tilde{u}_3\tilde{u}_3}$ are zero at the high scale, they can still be generated at the low scale, which is proportional to $g_{\phi H_u H_u}$ by a factor $K_3 \sim 0.1$.

C.2.4 Decay Rates of the Moduli

Now that we have computed all the the relevant couplings for moduli decay, we can proceed to compute the corresponding decay widths. In the following, we give the result of decay widths for all the moduli, calculated from the two-body width formulae. There could be contribution from three-body decays, which is generally small because of the phase space. Although certain three-body decays, e.g. moduli to top quarks and higgs [116, 131] is relatively large, it is still comparatively small in the current framework compared to the two-body decay modes.

For light moduli $X_i, i = 1, \cdots, (N-1)$, the total decay width is

$$\Gamma(X_i) \equiv \frac{D_{X_i} m_{X_i}^3}{M_P^2} = \frac{7}{72\pi}\left(N_G \mathcal{A}_1^{X_i} + N_G \mathcal{A}_2^{X_i} + \mathcal{A}_3^{X_i} + \mathcal{A}_4^{X_i}\right)\frac{m_{X_i}^3}{M_P^2}, \tag{C.75}$$

where $\mathcal{A}_1^{X_i}$, $\mathcal{A}_2^{X_i}$, $\mathcal{A}_3^{X_i}$ and $\mathcal{A}_4^{X_i}$ are the corresponding coefficients for the decays to gauge bosons gg, gauginos $\tilde{g}\tilde{g}$, non-higgs scalars $\tilde{f}\tilde{f}$ and light higgs bosons hh

respectively. They are given by:

$$\mathcal{A}_1^{X_i} = \frac{1}{2}\left(\sum_{i=1}^{N}\frac{N_i^{sm}}{N_i}\,a_i\right)^{-2}(\vec{X}'_N\cdot X_i)^2, \tag{C.76}$$

$$\mathcal{A}_2^{X_i} = \left(\frac{m_{3/2}^2}{2m_{X_i}^2}\right)\left(\sum_{k=1}^{N}\frac{N_k^{sm}}{N_k}\,a_k\right)^{-2}(\vec{X}'_N\cdot X_i)^2, \tag{C.77}$$

$$\mathcal{A}_3^{X_i} \approx \sum_{\alpha=\tilde{t}_L,\tilde{t}_R,\tilde{b}_L} 3\left(\frac{m_{3/2}^4}{m_{X_i}^4}\right)\left(1-4\frac{m_{\tilde{f}_\alpha}^2}{m_{X_i}^2}\right)^{1/2}\Pi^2, \tag{C.78}$$

$$\mathcal{A}_4^{X_i} \approx \left(\frac{m_{3/2}^4}{2m_{X_i}^4}\right)\left[(3Z_{\rm eff}^2+1)(\sin^2\alpha+K_1\cos^2\alpha)-2K_2Z_{\rm eff}\sin(2\alpha)\right]^2\Pi^2 \tag{C.79}$$

Here, weighted dot products in the scalar couplings are assumed to be equal and are denoted as Π as in the last subsection. In addition, the RGE effects on the couplings are included. In the above result, the gaugino and gauge bosons are treated as massless. The two-body decay to the standard model fermions is suppressed by $(\frac{m_f}{m_{X_i}})^2 \ll 10^{-4}$, so it is neglected in our result; even the top quark contribution is small. For the decay to non-higgs scalars, naively there is a large kinematic suppression since these scalars have mass close to $m_{3/2}$. However, the RGE running significantly decreases the third generation squark mass at the scale much lower than the unification scale. In G_2 MSSM framework, the lightest stop is $\tilde{t}_R$ which is about 4 times lighter than the gravitino. It, therefore, has a large contribution to the partial width. In addition, $\tilde{Q}_3$ ($\tilde{b}_L$ and $\tilde{t}_L$) are also light enough such that they contribute to the decay width.

The above result for $\mathcal{A}$'s depend on the specific choices of the fundamental parameters, such as a_i, N_i and N_i^{sm}, through several weighted dot products of vectors $\vec{X}_N$ and $\vec{X}_i$. These quantities are different for different moduli. However from Eq.(C.34)

they are constrained by:

$$\sum_{i=1}^{N}(\vec{X}'_N \cdot \vec{X}_i)^2 = |\vec{X}'_N|^2 \sin^2\theta. \tag{C.80}$$

Similar constraints apply for other products. From the above equation, one expects that on average

$$(\vec{X}'_N \cdot \vec{X}_i)^2 \sim \frac{1}{N-1}|\vec{X}'_N|^2 \sin^2\theta \tag{C.81}$$

which is suppressed by $1/(N-1)$. It is obvious that this symmetric configuration is favored in cosmology. If one wants the moduli to decay before BBN, then the most dangerous modulus is the one with the smallest total decay width, which is bounded by the average width. This gives rise to a strong constraint on the geometry of the G_2 manifold, since the width is suppressed by the number of moduli N. In the following discussion, we will focus on this symmetric configuration.

In order to evaluate the decay width and the branching ratio, one needs to know the typical values of these weighted dot products of $\vec{X}_N$ and $\vec{X}_i$. To do the estimation, we generate a set of fundamental parameters a_i, N_i, N_i^{sm}, ξ_i and ζ_i randomly with the following conditions:

$$\sum_{i=1}^{N} a_i = \frac{7}{3}, \quad 1 < N_i^{sm} < 2, \quad 2 < N_i < 6, \quad -1 < \xi_i < 0, \quad -1 < \zeta_i < 0. \tag{C.82}$$

The above ranges are chosen based on constraints arising from the G_2 framework and our current understanding of the Kähler metric of visible matter fields in realistic constructions. We also impose the supergravity condition $V_7 > 1$ and volume of three-cycle $V_Q^{sm} \approx 26$. The ranges of N_i and N_i^{sm} are chosen such that the efficiency

of the parameter generation is maximized when the above constraints are imposed. Due to our primitive understanding about the kähler metric, the modular weights (corresponding to ξ_i and ζ_i) are taken randomly in the allowed range. We plot the distribution for $\mathcal{B}^{-2}(\vec{X}'_N \cdot \vec{X}_i)^2$ and $(\vec{X}'''_N \cdot \vec{X}_i)^2$ in Fig.C.1, where we can see the typical values are 2×10^{-4} and 20. This result can be understood from the very rough estimate $(\vec{X}'_N \cdot \vec{X}_i) \sim \sqrt{a_i} \sim 1/\sqrt{N}$ and $(\vec{X}'''_N \cdot \vec{X}_i) \sim 1/\sqrt{a_i} \sim \sqrt{N}$. The distribution of $((\vec{X}''_N)^\alpha \cdot \vec{X}_i)^2$ is expected to be about the same as $(\vec{X}'''_N \cdot \vec{X}_i)^2$, since they all have the same structure. However, one should be aware that all the weighted dot products are independent and so are not necessarily equal.

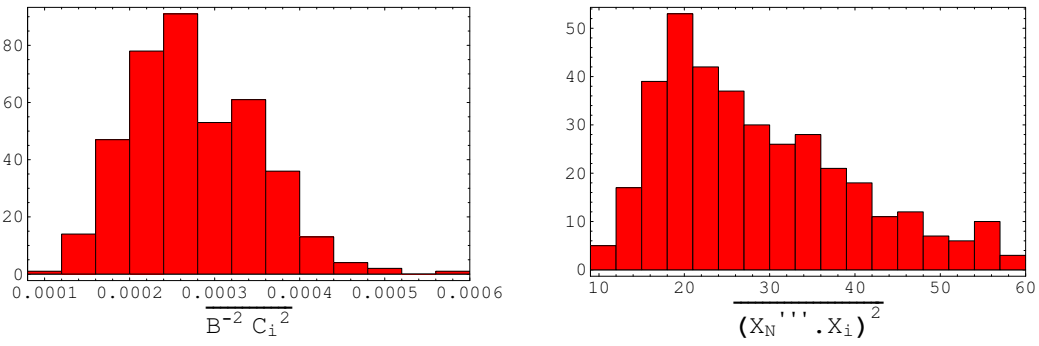

Figure C.1: Left: distribution of the average of $\mathcal{B}^{-2}(\vec{X}'_N \cdot \vec{X}_i)^2$. Right: distribution of the average of the weighted dot product $(\vec{X}'''_N \cdot \vec{X}_i)^2$.

Now let us estimate the decay width for the light moduli. Consider the first benchmark model of G_2-MSSM [30] for example, assuming the weighed dot products take their average value, we find $\mathcal{A}_1^{X_i} \approx \mathcal{A}_2^{X_i} \sim 10^{-4}$, $\mathcal{A}_3^{X_i} \sim 7.3$ and $\mathcal{A}_4^{X_i} \sim 20.5$. To summarize, the main channels of interest for light moduli decays and their partial widths are $\Gamma(gg) = \Gamma(\tilde{g}\tilde{g}) \approx 0.024$ sec^{-1}, $\Gamma(\tilde{t}_R\tilde{t}_R) \approx 60$ sec^{-1}, $\Gamma(\tilde{t}_L\tilde{t}_L) = \Gamma(\tilde{b}_L\tilde{b}_L) \approx 43$ sec^{-1} and $\Gamma(hh) \approx 412$ sec^{-1}. The total width is the sum of these partial width.

LSPs arise mainly from gauginos (including LSPs), $\tilde{t}\tilde{t}$ and $\tilde{b}\tilde{b}$, so the LSP branching ratio is the sum of the gaugino and squark channels divided by the total width. One can see that the decay to higgs and scalar dominate the decay of the light moduli. The total decay width is about 558 sec^{-1} or the corresponding $\mathcal{D}_{X_i} = 0.86$. The branching ratio of the light moduli to LSP is about 26%. These results should still be roughly correct for other benchmarks, differing at most by $\mathcal{O}(1)$ since the dependence on the mass spectrum is mild as seen from the explicit result of $\mathcal{A}_i^{X_i}$. The main uncertainty arises from the deviation of those weighted dot products from their typical values. To explore the more general case, one can relax the condition that all the weighted dot products are equal. Instead we choose:

$$\vec{X}_N''' \cdot \vec{X}_i = (\vec{X}_N'')^{H_u} \cdot \vec{X}_i = (\vec{X}_N'')^{H_d} \cdot \vec{X}_i = \Pi_1 \tag{C.83}$$

$$(\vec{X}_N'')^{\tilde{Q}_3} \cdot \vec{X}_i = (\vec{X}_N'')^{\tilde{u}_3} \cdot \vec{X}_i = \Pi_2 \tag{C.84}$$

Then we vary Π_1 and Π_2 according to the distributions of the weighted dot products in Fig.C.1. The distribution for D_{X_i} and the branching ratio to LSPs is shown in Fig.C.2. One can see that the branching ratio has a very small variation, but the distribution of D_{X_i} has a long tail. In the paper, we will use $0.4 < D_{X_i} < 4$ for concreteness, although other values may be possible.

For the heavy modulus X_N, the total decay width is

$$\Gamma(X_N) = \frac{7}{72\pi} \left(N_G \mathcal{A}_1^{X_N} + N_G \mathcal{A}_2^{X_N} + \mathcal{A}_4^{X_N} \right) \frac{m_{X_N}^3}{M_P^2}, \tag{C.85}$$

where $\mathcal{A}_i^{X_N}$ corresponds to the decay to gauge bosons gg, gauginos $\tilde{g}\tilde{g}$ and higgs

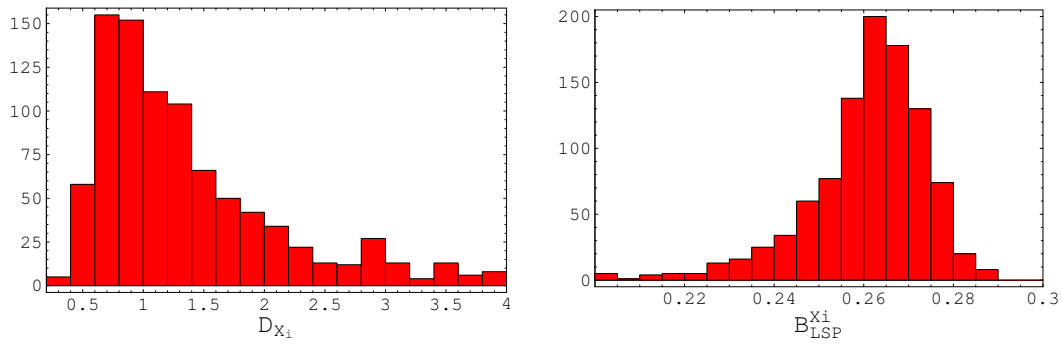

Figure C.2: Left: distribution of D_{X_i}. Right: distribution of moduli branching ratio to LSP.

bosons, and are given by

$$\mathcal{A}_1^{X_N} = \frac{9}{98} \tag{C.86}$$

$$\mathcal{A}_2^{X_N} = \frac{2}{9}\left(\frac{m_{3/2}}{m_{X_N}}\right)^2 \left(\nu^2 b_1 b_2\right)^2 \tag{C.87}$$

$$\mathcal{A}_4^{X_N} = Z_{\text{eff}}^2 \left(\vec{X}_N''' \cdot \vec{X}_i\right)^2 . \tag{C.88}$$

In the above result, we have not included the contributions from the decay to non-higgs scalars and fermions since they are suppressed by $(m_{3/2}/m_{X_N})^4$ and $(m_f/m_{X_N})^2$ given the large mass of the heavy modulus $m_{X_N} \sim 600 \times m_{3/2}$. Taking benchmark 1 of G_2-MSSM in [30] and typical values for weighted dot products, we get $\mathcal{A}_1^{X_N} \approx 0.1$, $\mathcal{A}_2^{X_N} \approx 0.01$ and $\mathcal{A}_4^{X_N} \approx 50$. The total width is about 3×10^{10} sec^{-1} or the corresponding $D_{X_N} \approx 1.6$. The branching ratio to LSPs is about 3×10^{-3}.

The decays of moduli to gravitinos is also very important. The decay of a modulus to gravitinos can be calculated using the following formula: [117]

$$\Gamma(X \to 2\psi_{3/2}) \simeq \frac{|\mathcal{G}_X^{(eff)}|^2}{288\pi} \frac{m_X^5}{m_{3/2}^2 M_P^2} \tag{C.89}$$

where $\mathcal{G}_X^{(eff)}$ is the effective coupling of the modulus field to gravitinos which includes

effects of moduli mixing. For the heavy modulus, the coupling arises from the mixing with meson field, since the goldstino is mainly the fermionic partner of the meson. Since the heavy modulus is much heavier than the meson a rough estimate[4] gives $\mathcal{G}_X^{(eff)} \sim m_{3/2}/m_{X_N}$. Therefore, for the heavy modulus, the decay rate to gravitino is

$$\Gamma(X_N \to 2\psi_{3/2}) \sim \frac{1}{288\pi}\frac{m_{X_N}^3}{M_P^2} \tag{C.90}$$

This corresponds to $B_{3/2}^{X_N} \sim 7 \times 10^{-4}$. In addition, since the heavy modulus decays much earlier than other moduli, the gravitino produced will be diluted by the subsequent moduli decays. So this estimate is enough for our discussion of gravitino problem. For both the light moduli and the meson fields, the decay to gravitino is kinematically suppressed since $m_{X_i}, m_{\phi_0} \approx 2m_{3/2}$.

C.2.5 Decay Width of the Meson

The total decay width of meson modulus is:

$$\Gamma(\delta\phi_0) \equiv \frac{D_\phi m_\phi^3}{M_P^2} = \frac{1}{72\pi}\left(N_G\mathcal{A}_1^{\phi_0} + \mathcal{A}_2^{\phi_0} + \mathcal{A}_3^{\phi_0}\right)\frac{m_\phi^3}{M_P^2}, \tag{C.91}$$

[4]There could be an additional suppression in special cases as discussed in [115,122]. We thank Fuminobu Takahashi for discussions regarding this point.

where $\mathcal{A}_i^{\phi}$ corresponds to the decay to gauginos $\tilde{g}\tilde{g}$, non-higgs scalar $\tilde{f}\tilde{f}$ and light higgs bosons hh, and are given by:

$$\mathcal{A}_1^{\phi_0} = \frac{1}{2\phi_0^2}\mathcal{F}^2\left(\frac{m_{3/2}}{m_\phi}\right)^2, \tag{C.92}$$

$$\begin{aligned}\mathcal{A}_2^{\phi_0} &= \sum_\alpha 27\phi_0^2 K_3^2 Z_{\rm eff}^4\left((1+Z_{\rm eff}^{-2})(1+\frac{2}{3\phi_0^2})+\frac{2\mathcal{F}}{3\phi_0^2}\sum_{i=1}^N\zeta_i\right)^2 \\ &\times \left(\frac{m_{3/2}^4}{m_\phi^4}\right)\left(1-4\frac{m_{\tilde{f}_\alpha}^2}{m_\phi^2}\right)^{1/2},\end{aligned} \tag{C.93}$$

$$\begin{aligned}\mathcal{A}_3^{\phi_0} &= \frac{9}{2}\phi_0^2\left(\frac{m_{3/2}^4}{m_{\phi_0}^4}\right)\left[Z_{\rm eff}^2\left((1+Z_{\rm eff}^{-2})(1+\frac{2}{3\phi_0^2})+\frac{2\mathcal{F}}{3\phi_0^2}\sum_{i=1}^N\zeta_i\right)(\sin^2\alpha+K_1\cos^2\alpha)\right. \\ &- \left. K_2 Z_{\rm eff}\left(2(1+\frac{2}{3\phi_0^2})+\frac{\mathcal{F}}{3\phi_0^2}\sum_{i=1}^N(\xi_i^{H_u}+\xi_i^{H_d})\right)\sin 2\alpha\right]^2.\end{aligned} \tag{C.94}$$

Here, as discussed in the last subsection, the low scale couplings to third-generation squarks are dominantly generated from RG running and are related to the coupling $g_{\phi H_u H_u}$ by a factor $K_3 \sim 0.1$. For the first benchmark of G_2-MSSM in [30] and taking the simplest assumption $\xi_i = \zeta_i = -1/2$, we get $\mathcal{A}_1^{\phi_0} \approx 13.7$, $\mathcal{A}_2^{\phi_0} \approx 2.9\times 10^4$ and $\mathcal{A}_3^{\phi_0} \approx 1.3\times 10^5$. One can see that this result is enhanced from the naive estimate by the total number of moduli $\sim N$ and large (hidden-sector) three-cycle volume ν. The total decay width is about 4.6×10^5 sec^{-1}, corresponding to $D_\phi = 711$. The branching ratio to LSPs is about 18%. Again, this can change by $\mathcal{O}(1)$ for other benchmarks.

BIBLIOGRAPHY

BIBLIOGRAPHY

[1] A. Djouadi, M. M. Muhlleitner, and M. Spira, "Decays of Supersymmetric Particles: the program SUSY-HIT (SUspect-SdecaY-Hdecay-InTerface)," *Acta Phys. Polon.* **B38** (2007) 635–644, hep-ph/0609292.

[2] L. Susskind, "The anthropic landscape of string theory," hep-th/0302219.

[3] R. Bousso and J. Polchinski, "Quantization of four-form fluxes and dynamical neutralization of the cosmological constant," *JHEP* **06** (2000) 006, hep-th/0004134.

[4] R. Bousso and J. Polchinski, "The string theory landscape," *Sci. Am.* **291** (2004) 60–69.

[5] G. L. Kane, P. Kumar, and J. Shao, "LHC String Phenomenology," *J. Phys.* **G34** (2007) 1993–2036, hep-ph/0610038.

[6] G. L. Kane, P. Kumar, and J. Shao, "Unravelling Strings at the LHC," *Phys. Rev.* **D77** (2008) 116005, 0709.4259.

[7] S. Kachru, R. Kallosh, A. Linde, and S. P. Trivedi, "De Sitter vacua in string theory," *Phys. Rev.* **D68** (2003) 046005, hep-th/0301240.

[8] V. Balasubramanian, P. Berglund, J. P. Conlon, and F. Quevedo, "Systematics of Moduli Stabilisation in Calabi-Yau Flux Compactifications," *JHEP* **03** (2005) 007, hep-th/0502058.

[9] F. Denef, M. R. Douglas, B. Florea, A. Grassi, and S. Kachru, "Fixing all moduli in a simple F-theory compactification," *Adv. Theor. Math. Phys.* **9** (2005) 861–929, hep-th/0503124.

[10] K. Becker, M. Becker, C. Vafa, and J. Walcher, "Moduli stabilization in non-geometric backgrounds," *Nucl. Phys.* **B770** (2007) 1–46, hep-th/0611001.

[11] M. R. Douglas and S. Kachru, "Flux compactification," *Rev. Mod. Phys.* **79** (2007) 733–796, hep-th/0610102.

[12] F. Denef, M. R. Douglas, and S. Kachru, "Physics of string flux compactifications," *Ann. Rev. Nucl. Part. Sci.* **57** (2007) 119–144, hep-th/0701050.

[13] K. Choi, A. Falkowski, H. P. Nilles, M. Olechowski, and S. Pokorski, "Stability of flux compactifications and the pattern of supersymmetry breaking," *JHEP* **11** (2004) 076, hep-th/0411066.

[14] K. Choi, A. Falkowski, H. P. Nilles, and M. Olechowski, "Soft supersymmetry breaking in KKLT flux compactification," *Nucl. Phys.* **B718** (2005) 113–133, hep-th/0503216.

[15] M. Endo, M. Yamaguchi, and K. Yoshioka, "A bottom-up approach to moduli dynamics in heavy gravitino scenario: Superpotential, soft terms and sparticle mass spectrum," *Phys. Rev.* **D72** (2005) 015004, hep-ph/0504036.

[16] K. Choi, K. S. Jeong, and K.-i. Okumura, "Phenomenology of mixed modulus-anomaly mediation in fluxed string compactifications and brane models," *JHEP* **09** (2005) 039, hep-ph/0504037.

[17] A. Falkowski, O. Lebedev, and Y. Mambrini, "SUSY Phenomenology of KKLT Flux Compactifications," *JHEP* **11** (2005) 034, hep-ph/0507110.

[18] K. Choi, K. S. Jeong, T. Kobayashi, and K.-i. Okumura, "Little SUSY hierarchy in mixed modulus-anomaly mediation," *Phys. Lett.* **B633** (2006) 355–361, hep-ph/0508029.

[19] H. Baer, E.-K. Park, X. Tata, and T. T. Wang, "Collider and dark matter searches in models with mixed modulus-anomaly mediated SUSY breaking," *JHEP* **08** (2006) 041, hep-ph/0604253.

[20] J. P. Conlon, F. Quevedo, and K. Suruliz, "Large-volume flux compactifications: Moduli spectrum and D3/D7 soft supersymmetry breaking," *JHEP* **08** (2005) 007, hep-th/0505076.

[21] B. C. Allanach, F. Quevedo, and K. Suruliz, "Low-energy supersymmetry breaking from string flux compactifications: Benchmark scenarios," *JHEP* **04** (2006) 040, hep-ph/0512081.

[22] J. P. Conlon, S. S. Abdussalam, F. Quevedo, and K. Suruliz, "Soft SUSY breaking terms for chiral matter in IIB string compactifications," *JHEP* **01** (2007) 032, hep-th/0610129.

[23] J. P. Conlon and F. Quevedo, "Gaugino and scalar masses in the landscape," *JHEP* **06** (2006) 029, hep-th/0605141.

[24] J. P. Conlon, C. H. Kom, K. Suruliz, B. C. Allanach, and F. Quevedo, "Sparticle Spectra and LHC Signatures for Large Volume String Compactifications," *JHEP* **08** (2007) 061, 0704.3403.

[25] J. P. Conlon and F. Quevedo, "Astrophysical and Cosmological Implications of Large Volume String Compactifications," *JCAP* **0708** (2007) 019, 0705.3460.

[26] S. S. AbdusSalam, J. P. Conlon, F. Quevedo, and K. Suruliz, "Scanning the Landscape of Flux Compactifications: Vacuum Structure and Soft Supersymmetry Breaking," *JHEP* **12** (2007) 036, 0709.0221.

[27] M. Cicoli, J. P. Conlon, and F. Quevedo, "General Analysis of LARGE Volume Scenarios with String Loop Moduli Stabilisation," *JHEP* **10** (2008) 105, 0805.1029.

[28] B. S. Acharya, K. Bobkov, G. Kane, P. Kumar, and D. Vaman, "An M theory solution to the hierarchy problem," *Phys. Rev. Lett.* **97** (2006) 191601, hep-th/0606262.

[29] B. S. Acharya, K. Bobkov, G. L. Kane, P. Kumar, and J. Shao, "Explaining the electroweak scale and stabilizing moduli in M theory," *Phys. Rev.* **D76** (2007) 126010, hep-th/0701034.

[30] B. S. Acharya, K. Bobkov, G. L. Kane, J. Shao, and P. Kumar, "The G_2-MSSM - An M Theory motivated model of Particle Physics," *Phys. Rev.* **D78** (2008) 065038, 0801.0478.

[31] B. S. Acharya *et. al.*, "Non-thermal Dark Matter and the Moduli Problem in String Frameworks," *JHEP* **06** (2008) 064, 0804.0863.

[32] G. L. Kane, J. Shao, and P. Kumar, "CP violation in M-theory and the implication for EDMs," *To Appear* (2009).

[33] B. S. Acharya, "M theory, Joyce orbifolds and super Yang-Mills," *Adv. Theor. Math. Phys.* **3** (1999) 227–248, hep-th/9812205.

[34] M. Atiyah and E. Witten, "M-theory dynamics on a manifold of G(2) holonomy," *Adv. Theor. Math. Phys.* **6** (2003) 1–106, hep-th/0107177.

[35] B. S. Acharya and E. Witten, "Chiral fermions from manifolds of G(2) holonomy," hep-th/0109152.

[36] B. S. Acharya and S. Gukov, "M theory and Singularities of Exceptional Holonomy Manifolds," *Phys. Rept.* **392** (2004) 121–189, hep-th/0409191.

[37] P. Joseph, *String Theory: volume 2*. Cambridge University Press, 1998.

[38] M. B. Green, J. H. Schwarz, and W. Edward, *Superstring Theory: volume 2*. Cambridge University Press, 1988.

[39] R. Blumenhagen, B. Kors, D. Lust, and S. Stieberger, "Four-dimensional String Compactifications with D-Branes, Orientifolds and Fluxes," *Phys. Rept.* **445** (2007) 1–193, hep-th/0610327.

[40] F. Marchesano, "Progress in D-brane model building," *Fortsch. Phys.* **55** (2007) 491–518, hep-th/0702094.

[41] S. K. Soni and H. A. Weldon, "Analysis of the Supersymmetry Breaking Induced by N=1 Supergravity Theories," *Phys. Lett.* **B126** (1983) 215.

[42] V. S. Kaplunovsky and J. Louis, "Model independent analysis of soft terms in effective supergravity and in string theory," *Phys. Lett.* **B306** (1993) 269–275, hep-th/9303040.

[43] A. Brignole, L. E. Ibanez, and C. Munoz, "Towards a theory of soft terms for the supersymmetric Standard Model," *Nucl. Phys.* **B422** (1994) 125–171, hep-ph/9308271.

[44] A. Brignole, L. E. Ibanez, and C. Munoz, "Soft supersymmetry-breaking terms from supergravity and superstring models," hep-ph/9707209.

[45] J. A. Bagger, T. Moroi, and E. Poppitz, "Anomaly mediation in supergravity theories," *JHEP* **04** (2000) 009, hep-th/9911029.

[46] B. S. Acharya and K. Bobkov, "Kahler Independence of the G2-MSSM," 0810.3285.

[47] B. S. Acharya, F. Denef, and R. Valandro, "Statistics of M theory vacua," *JHEP* **06** (2005) 056, hep-th/0502060.

[48] E. Witten, "Deconstruction, G(2) holonomy, and doublet-triplet splitting," hep-ph/0201018.

[49] E. Witten, "Strong Coupling Expansion Of Calabi-Yau Compactification," *Nucl. Phys.* **B471** (1996) 135–158, hep-th/9602070.

[50] T. Friedmann and E. Witten, "Unification scale, proton decay, and manifolds of G(2) holonomy," *Adv. Theor. Math. Phys.* **7** (2003) 577–617, hep-th/0211269.

[51] D. J. H. Chung *et. al.*, "The soft supersymmetry-breaking Lagrangian: Theory and applications," *Phys. Rept.* **407** (2005) 1–203, hep-ph/0312378.

[52] S. Kachru, L. McAllister, and R. Sundrum, "Sequestering in string theory," *JHEP* **10** (2007) 013, hep-th/0703105.

[53] K. Choi and H. P. Nilles, "The gaugino code," *JHEP* **04** (2007) 006, hep-ph/0702146.

[54] S. P. Martin, "A Supersymmetry Primer," hep-ph/9709356.

[55] D. M. Pierce, J. A. Bagger, K. T. Matchev, and R.-j. Zhang, "Precision corrections in the minimal supersymmetric standard model," *Nucl. Phys.* **B491** (1997) 3–67, hep-ph/9606211.

[56] T. Gherghetta, G. F. Giudice, and J. D. Wells, "Phenomenological consequences of supersymmetry with anomaly-induced masses," *Nucl. Phys.* **B559** (1999) 27–47, hep-ph/9904378.

[57] N. Arkani-Hamed, A. Delgado, and G. F. Giudice, "The well-tempered neutralino," *Nucl. Phys.* **B741** (2006) 108–130, hep-ph/0601041.

[58] A. Delgado and G. F. Giudice, "On the tuning condition of split supersymmetry," *Phys. Lett.* **B627** (2005) 155–160, hep-ph/0506217.

[59] A. Arvanitaki, C. Davis, P. W. Graham, and J. G. Wacker, "One loop predictions of the finely tuned SSM," *Phys. Rev.* **D70** (2004) 117703, hep-ph/0406034.

[60] **ALEPH** Collaboration, A. Heister *et. al.*, "Search for charginos nearly mass degenerate with the lightest neutralino in e+ e- collisions at centre-of-mass energies up to 209-GeV," *Phys. Lett.* **B533** (2002) 223–236, hep-ex/0203020.

[61] T. Sjostrand, S. Mrenna, and P. Skands, "PYTHIA 6.4 Physics and Manual," *JHEP* **05** (2006) 026, hep-ph/0603175.

[62] N. Arkani-Hamed and S. Dimopoulos, "Supersymmetric unification without low energy supersymmetry and signatures for fine-tuning at the LHC," *JHEP* **06** (2005) 073, hep-th/0405159.

[63] G. F. Giudice and A. Romanino, "Split supersymmetry," *Nucl. Phys.* **B699** (2004) 65–89, hep-ph/0406088.

[64] N. Arkani-Hamed, S. Dimopoulos, G. F. Giudice, and A. Romanino, "Aspects of split supersymmetry," *Nucl. Phys.* **B709** (2005) 3–46, hep-ph/0409232.

[65] A. J. Barr, C. G. Lester, M. A. Parker, B. C. Allanach, and P. Richardson, "Discovering anomaly-mediated supersymmetry at the LHC," *JHEP* **03** (2003) 045, hep-ph/0208214.

[66] J. L. Feng, T. Moroi, L. Randall, M. Strassler, and S.-f. Su, "Discovering supersymmetry at the Tevatron in Wino LSP scenarios," *Phys. Rev. Lett.* **83** (1999) 1731–1734, hep-ph/9904250.

[67] C. A. Baker *et. al.*, "An improved experimental limit on the electric dipole moment of the neutron," *Phys. Rev. Lett.* **97** (2006) 131801, hep-ex/0602020.

[68] P. G. Harris *et. al.*, "New experimental limit on the electric dipole moment of the neutron," *Phys. Rev. Lett.* **82** (1999) 904–907.

[69] B. C. Regan, E. D. Commins, C. J. Schmidt, and D. DeMille, "New limit on the electron electric dipole moment," *Phys. Rev. Lett.* **88** (2002) 071805.

[70] M. V. Romalis, W. C. Griffith, and E. N. Fortson, "A new limit on the permanent electric dipole moment of Hg- 199," *Phys. Rev. Lett.* **86** (2001) 2505–2508, hep-ex/0012001.

[71] W. C. Griffith *et. al.*, "Improved Limit on the Permanent Electric Dipole Moment of Hg-199," *Phys. Rev. Lett.* **102** (2009) 101601.

[72] A. Masiero and L. Silvestrini, "CP violation in low-energy SUSY," hep-ph/9709242.

[73] S. Abel, S. Khalil, and O. Lebedev, "EDM constraints in supersymmetric theories," *Nucl. Phys.* **B606** (2001) 151–182, hep-ph/0103320.

[74] T. Ibrahim and P. Nath, "The chromoelectric and purely gluonic operator contributions to the neutron electric dipole moment in N = 1 supergravity," *Phys. Lett.* **B418** (1998) 98–106, hep-ph/9707409.

[75] T. Ibrahim and P. Nath, "The neutron and the electron electric dipole moment in N = 1 supergravity unification," *Phys. Rev.* **D57** (1998) 478–488, hep-ph/9708456.

[76] T. Ibrahim and P. Nath, "The neutron and the lepton EDMs in MSSM, large CP violating phases, and the cancellation mechanism," *Phys. Rev.* **D58** (1998) 111301, hep-ph/9807501.

[77] M. Brhlik, G. J. Good, and G. L. Kane, "Electric dipole moments do not require the CP-violating phases of supersymmetry to be small," *Phys. Rev.* **D59** (1999) 115004, hep-ph/9810457.

[78] K. Choi, "Small SUSY phases in string inspired supergravity," *Phys. Rev. Lett.* **72** (1994) 1592–1595, hep-ph/9311352.

[79] J. P. Conlon, "Mirror Mediation," *JHEP* **03** (2008) 025, 0710.0873.

[80] S. Abel, S. Khalil, and O. Lebedev, "Additional stringy sources for electric dipole moments," *Phys. Rev. Lett.* **89** (2002) 121601, hep-ph/0112260.

[81] I. Affleck, M. Dine, and N. Seiberg, "Dynamical Supersymmetry Breaking in Supersymmetric QCD," *Nucl. Phys.* **B241** (1984) 493–534.

[82] R. D. Peccei and H. R. Quinn, "CP Conservation in the Presence of Instantons," *Phys. Rev. Lett.* **38** (1977) 1440–1443.

[83] G. F. Giudice and A. Masiero, "A Natural Solution to the mu Problem in Supergravity Theories," *Phys. Lett.* **B206** (1988) 480–484.

[84] E. Witten, "Anomaly cancellation on G(2) manifolds," hep-th/0108165.

[85] P. Berglund and A. Brandhuber, "Matter from G(2) manifolds," *Nucl. Phys.* **B641** (2002) 351–375, hep-th/0205184.

[86] N. Arkani-Hamed and M. Schmaltz, "Hierarchies without symmetries from extra dimensions," *Phys. Rev.* **D61** (2000) 033005, hep-ph/9903417.

[87] E. A. Mirabelli and M. Schmaltz, "Yukawa hierarchies from split fermions in extra dimensions," *Phys. Rev.* **D61** (2000) 113011, hep-ph/9912265.

[88] D. E. Kaplan and T. M. P. Tait, "New tools for fermion masses from extra dimensions," *JHEP* **11** (2001) 051, hep-ph/0110126.

[89] H. Abe, K. Choi, K.-S. Jeong, and K.-i. Okumura, "Scherk-Schwarz supersymmetry breaking for quasi-localized matter fields and supersymmetry flavor violation," *JHEP* **09** (2004) 015, hep-ph/0407005.

[90] C. D. Froggatt and H. B. Nielsen, "Hierarchy of Quark Masses, Cabibbo Angles and CP Violation," *Nucl. Phys.* **B147** (1979) 277.

[91] S. M. Barr and A. Zee, "ELECTRIC DIPOLE MOMENT OF THE ELECTRON AND OF THE NEUTRON," *Phys. Rev. Lett.* **65** (1990) 21–24.

[92] D. Bowser-Chao, D. Chang, and W.-Y. Keung, "Electron electric dipole moment from CP violation in the charged Higgs sector," *Phys. Rev. Lett.* **79** (1997) 1988–1991, hep-ph/9703435.

[93] D. Chang, W.-Y. Keung, and A. Pilaftsis, "New two-loop contribution to electric dipole moment in supersymmetric theories," *Phys. Rev. Lett.* **82** (1999) 900–903, hep-ph/9811202.

[94] A. Pilaftsis, "Higgs-boson two-loop contributions to electric dipole moments in the MSSM," *Phys. Lett.* **B471** (1999) 174–181, hep-ph/9909485.

[95] D. Chang, W.-F. Chang, and W.-Y. Keung, "Additional two-loop contributions to electric dipole moments in supersymmetric theories," *Phys. Lett.* **B478** (2000) 239–246, hep-ph/9910465.

[96] D. Chang, W.-F. Chang, and W.-Y. Keung, "New constraint from electric dipole moments on chargino baryogenesis in MSSM," *Phys. Rev.* **D66** (2002) 116008, hep-ph/0205084.

[97] A. Pilaftsis, "Higgs-mediated electric dipole moments in the MSSM: An application to baryogenesis and Higgs searches," *Nucl. Phys.* **B644** (2002) 263–289, hep-ph/0207277.

[98] D. Chang, W.-F. Chang, and W.-Y. Keung, "Electric dipole moment in the split supersymmetry models," *Phys. Rev.* **D71** (2005) 076006, hep-ph/0503055.

[99] Y. Li, S. Profumo, and M. Ramsey-Musolf, "Higgs-Higgsino-Gaugino Induced Two Loop Electric Dipole Moments," *Phys. Rev.* **D78** (2008) 075009, 0806.2693.

[100] M. Pospelov and A. Ritz, "Electric dipole moments as probes of new physics," *Annals Phys.* **318** (2005) 119–169, hep-ph/0504231.

[101] A. Manohar and H. Georgi, "Chiral Quarks and the Nonrelativistic Quark Model," *Nucl. Phys.* **B234** (1984) 189.

[102] R. L. Arnowitt, J. L. Lopez, and D. V. Nanopoulos, "KEEPING THE DEMON OF SUSY AT BAY," *Phys. Rev.* **D42** (1990) 2423–2426.

[103] R. L. Arnowitt, M. J. Duff, and K. S. Stelle, "SUPERSYMMETRY AND THE NEUTRON ELECTRIC DIPOLE MOMENT," *Phys. Rev.* **D43** (1991) 3085–3088.

[104] D. A. Demir, O. Lebedev, K. A. Olive, M. Pospelov, and A. Ritz, "Electric dipole moments in the MSSM at large tan(beta)," *Nucl. Phys.* **B680** (2004) 339–374, `hep-ph/0311314`.

[105] T. Falk, K. A. Olive, M. Pospelov, and R. Roiban, "MSSM predictions for the electric dipole moment of the Hg- 199 atom," *Nucl. Phys.* **B560** (1999) 3–22, `hep-ph/9904393`.

[106] S. Abel and O. Lebedev, "Neutron electron EDM correlations in supersymmetry and prospects for EDM searches," *JHEP* **01** (2006) 133, `hep-ph/0508135`.

[107] J. Dai, H. Dykstra, R. G. Leigh, S. Paban, and D. Dicus, "CP VIOLATION FROM THREE GLUON OPERATORS IN THE SUPERSYMMETRIC STANDARD MODEL," *Phys. Lett.* **B237** (1990) 216.

[108] P. Kumar, "Neutrino Masses, Baryon Asymmetry, Dark Matter and the Moduli Problem - A Complete Framework," `0809.2610`.

[109] G. D. Coughlan, W. Fischler, E. W. Kolb, S. Raby, and G. G. Ross, "Cosmological Problems for the Polonyi Potential," *Phys. Lett.* **B131** (1983) 59.

[110] J. R. Ellis, D. V. Nanopoulos, and M. Quiros, "On the Axion, Dilaton, Polonyi, Gravitino and Shadow Matter Problems in Supergravity and Superstring Models," *Phys. Lett.* **B174** (1986) 176.

[111] B. de Carlos, J. A. Casas, F. Quevedo, and E. Roulet, "Model independent properties and cosmological implications of the dilaton and moduli sectors of 4-d strings," *Phys. Lett.* **B318** (1993) 447–456, `hep-ph/9308325`.

[112] T. Banks, D. B. Kaplan, and A. E. Nelson, "Cosmological Implications of Dynamical Supersymmetry Breaking," *Phys. Rev.* **D49** (1994) 779–787, `hep-ph/9308292`.

[113] S. Nakamura and M. Yamaguchi, "A Note on Polonyi Problem," *Phys. Lett.* **B655** (2007) 167–171, 0707.4538.

[114] M. Y. Khlopov and A. D. Linde, "Is It Easy to Save the Gravitino?," *Phys. Lett.* **B138** (1984) 265–268.

[115] M. Dine, R. Kitano, A. Morisse, and Y. Shirman, "Moduli decays and gravitinos," *Phys. Rev.* **D73** (2006) 123518, hep-ph/0604140.

[116] M. Endo, M. Kawasaki, F. Takahashi, and T. T. Yanagida, "Inflaton decay through supergravity effects," *Phys. Lett.* **B642** (2006) 518–524, hep-ph/0607170.

[117] M. Kawasaki, F. Takahashi, and T. T. Yanagida, "The gravitino overproduction problem in inflationary universe," *Phys. Rev.* **D74** (2006) 043519, hep-ph/0605297.

[118] S. Nakamura and M. Yamaguchi, "Gravitino production from heavy moduli decay and cosmological moduli problem revived," *Phys. Lett.* **B638** (2006) 389–395, hep-ph/0602081.

[119] T. Asaka, S. Nakamura, and M. Yamaguchi, "Gravitinos from heavy scalar decay," *Phys. Rev.* **D74** (2006) 023520, hep-ph/0604132.

[120] M. Endo, K. Hamaguchi, and F. Takahashi, "Moduli-induced gravitino problem," *Phys. Rev. Lett.* **96** (2006) 211301, hep-ph/0602061.

[121] V. S. Rychkov and A. Strumia, "Thermal production of gravitinos," *Phys. Rev.* **D75** (2007) 075011, hep-ph/0701104.

[122] M. Endo, K. Hamaguchi, and F. Takahashi, "Moduli / inflaton mixing with supersymmetry breaking field," *Phys. Rev.* **D74** (2006) 023531, hep-ph/0605091.

[123] M. Endo, F. Takahashi, and T. T. Yanagida, "Inflaton Decay in Supergravity," *Phys. Rev.* **D76** (2007) 083509, 0706.0986.

[124] M. Endo, F. Takahashi, and T. T. Yanagida, "Anomaly-Induced Inflaton Decay and Gravitino- Overproduction Problem," *Phys. Lett.* **B658** (2008) 236, hep-ph/0701042.

[125] K. Ichikawa, M. Kawasaki, and F. Takahashi, "The oscillation effects on thermalization of the neutrinos in the universe with low reheating temperature," *Phys. Rev.* **D72** (2005) 043522, astro-ph/0505395.

[126] M. Nagai and K. Nakayama, "Nonthermal dark matter in mirage mediation," *Phys. Rev.* **D76** (2007) 123501, 0709.3918.

[127] M. Kawasaki and K. Nakayama, "Baryon Asymmetry in Heavy Moduli Scenario," *Phys. Rev.* **D76** (2007) 043502, 0705.0079.

[128] M. Endo and F. Takahashi, "Non-thermal production of dark matter from late-decaying scalar field at intermediate scale," *Phys. Rev.* **D74** (2006) 063502, hep-ph/0606075.

[129] M. P. Hertzberg, M. Tegmark, S. Kachru, J. Shelton, and O. Ozcan, "Searching for Inflation in Simple String Theory Models: An Astrophysical Perspective," *Phys. Rev.* **D76** (2007) 103521, 0709.0002.

[130] L. McAllister and E. Silverstein, "String Cosmology: A Review," *Gen. Rel. Grav.* **40** (2008) 565–605, 0710.2951.

[131] T. Moroi and L. Randall, "Wino cold dark matter from anomaly-mediated SUSY breaking," *Nucl. Phys.* **B570** (2000) 455–472, hep-ph/9906527.

[132] M. Dine, L. Randall, and S. D. Thomas, "Baryogenesis from flat directions of the supersymmetric standard model," *Nucl. Phys.* **B458** (1996) 291–326, hep-ph/9507453.

[133] N. Kaloper and K. A. Olive, "Dilatons in string cosmology," *Astropart. Phys.* **1** (1993) 185–194.

[134] R. Brustein, S. P. de Alwis, and P. Martens, "Cosmological stabilization of moduli with steep potentials," *Phys. Rev.* **D70** (2004) 126012, hep-th/0408160.

[135] R. Brustein and R. Madden, "Classical corrections in string cosmology," *JHEP* **07** (1999) 006, hep-th/9901044.

[136] G. Huey, P. J. Steinhardt, B. A. Ovrut, and D. Waldram, "A cosmological mechanism for stabilizing moduli," *Phys. Lett.* **B476** (2000) 379–386, hep-th/0001112.

[137] N. Kaloper, J. Rahmfeld, and L. Sorbo, "Moduli entrapment with primordial black holes," *Phys. Lett.* **B606** (2005) 234–244, hep-th/0409226.

[138] L. Kofman *et. al.*, "Beauty is attractive: Moduli trapping at enhanced symmetry points," *JHEP* **05** (2004) 030, hep-th/0403001.

[139] S. Watson, "Moduli stabilization with the string Higgs effect," *Phys. Rev.* **D70** (2004) 066005, hep-th/0404177.

[140] T. Battefeld and S. Watson, "String gas cosmology," *Rev. Mod. Phys.* **78** (2006) 435–454, hep-th/0510022.

[141] S. Cremonini and S. Watson, "Dilaton dynamics from production of tensionless membranes," *Phys. Rev.* **D73** (2006) 086007, hep-th/0601082.

[142] B. Greene, S. Judes, J. Levin, S. Watson, and A. Weltman, "Cosmological Moduli Dynamics," *JHEP* **07** (2007) 060, hep-th/0702220.

[143] M. Dine, Y. Nir, and Y. Shadmi, "Enhanced symmetries and the ground state of string theory," *Phys. Lett.* **B438** (1998) 61–68, hep-th/9806124.

[144] C. Vafa, "The string landscape and the swampland," hep-th/0509212.

[145] R. Brustein and P. J. Steinhardt, "Challenges for superstring cosmology," *Phys. Lett.* **B302** (1993) 196–201, hep-th/9212049.

[146] M. Dine and N. Seiberg, "Is the Superstring Weakly Coupled?," *Phys. Lett.* **B162** (1985) 299.

[147] E. W. Kolb and M. S. Turner, "The Early universe," *Front. Phys.* **69** (1990) 1–547.

[148] M. Kawasaki, K. Kohri, and N. Sugiyama, "Cosmological Constraints on Late-time Entropy Production," *Phys. Rev. Lett.* **82** (1999) 4168, astro-ph/9811437.

[149] G. F. Giudice, E. W. Kolb, and A. Riotto, "Largest temperature of the radiation era and its cosmological implications," *Phys. Rev.* **D64** (2001) 023508, hep-ph/0005123.

[150] M. Kawasaki, K. Kohri, and N. Sugiyama, "MeV-scale reheating temperature and thermalization of neutrino background," *Phys. Rev.* **D62** (2000) 023506, astro-ph/0002127.

[151] S. Hannestad, "What is the lowest possible reheating temperature?," *Phys. Rev.* **D70** (2004) 043506, astro-ph/0403291.

[152] **WMAP** Collaboration, E. Komatsu *et. al.*, "Five-Year Wilkinson Microwave Anisotropy Probe (WMAP) Observations:Cosmological Interpretation," *Astrophys. J. Suppl.* **180** (2009) 330–376, 0803.0547.

[153] I. Affleck and M. Dine, "A New Mechanism for Baryogenesis," *Nucl. Phys.* **B249** (1985) 361.

[154] J. Simon, R. Jimenez, L. Verde, P. Berglund, and V. Balasubramanian, "Using cosmology to constrain the topology of hidden dimensions," astro-ph/0605371.

[155] V. Balasubramanian, P. Berglund, R. Jimenez, J. Simon, and L. Verde, "Topology from Cosmology," *JHEP* **06** (2008) 025, 0712.1815.

[156] N. Arkani-Hamed, G. L. Kane, J. Thaler, and L.-T. Wang, "Supersymmetry and the LHC inverse problem," *JHEP* **08** (2006) 070, hep-ph/0512190.

[157] J. L. Bourjaily, "Local Models in F-Theory and M-Theory with Three Generations," 0901.3785.

[158] J. L. Bourjaily and S. Espahbodi, "Geometrically Engineerable Chiral Matter in M-Theory," 0804.1132.

[159] J. L. Bourjaily, "Unfolding Geometric Unification in M-Theory," 0706.3364.

[160] J. L. Bourjaily, "Geometrically Engineering the Standard Model: Locally Unfolding Three Families out of E_8," *Phys. Rev.* **D76** (2007) 046004, 0704.0445.